



UNIVERSIDAD DE CHILE  
FACULTAD DE CIENCIAS FÍSICAS Y MATEMÁTICAS  
DEPARTAMENTO DE INGENIERÍA ELÉCTRICA

DESIGN OF A MEDIUM-ACCESS-CONTROL PROTOCOL FOR WIRELESS SENSOR  
NETWORKS CONSIDERING THE BATTERY STATE OF CHARGE AND STATE OF  
HEALTH

TESIS PARA OPTAR AL GRADO DE  
DOCTORA EN INGENIERÍA ELÉCTRICA

VANESSA LISBETH QUINTERO CEDEÑO

PROFESOR GUÍA:  
DR. CLAUDIO ESTÉVEZ MONTERO

PROFESOR CO-GUÍA:  
DR. MARCOS ORCHARD CONCHA

MIEMBROS DE LA COMISIÓN:  
DR. CESAR AZURDIA MEZA  
DR. CHRISTIAN OBERLI GRAF  
DR. JIA YUAN YU

SANTIAGO DE CHILE  
2019

RESUMEN DE LA MEMORIA PARA OPTAR  
AL GRADO DE DOCTORA EN INGENIERÍA ELÉCTRICA  
POR: VANESSA LISBETH QUINTERO CEDEÑO  
FECHA: 2019  
PROF. GUÍA: DR. CLAUDIO ESTÉVEZ MONTERO

## DESIGN OF A MEDIUM-ACCESS-CONTROL PROTOCOL FOR WIRELESS SENSOR NETWORKS CONSIDERING THE BATTERY STATE OF CHARGE AND STATE OF HEALTH

La disponibilidad de energía es una de las limitaciones que presentan las Redes de Sensores Inalámbricas (WSN, Wireless Sensor Network). Tradicionalmente, las baterías han sido utilizadas para proveer energía a los nodos de sensores y al tener una vida útil limitada afectan el tiempo de vida de la red. Soluciones como el uso de baterías de gran tamaño o el reemplazo de ellas no son viables, debido al gran número de sensores que componen la red y a que pueden ser desplegados en zonas de difícil acceso. Esta situación ha motivado que las soluciones para la conservación de la energía en las WSNs se enfoquen en el desarrollo de técnicas que actúen a nivel de las capas física y de enlace de datos, como es el caso de los protocolos de Control de Acceso al Medio (MAC, Medium Access Control).

Los protocolos MAC son una de las soluciones ampliamente estudiadas y utilizadas porque permiten un equilibrio entre la conservación de energía y otros parámetros críticos de la red, como el rendimiento, latencia, reducción de colisiones y mensajes de control. También tienen la facilidad de adaptarse a las nuevas aristas de trabajo que surgen al incorporar nuevas tecnologías como lo son los Dispositivos de Recolección de Energía (EHD, Energy Harvesting Device). Otro aspecto que está siendo considerado y estudiado en el diseño de los protocolos MAC es la información que se puede extraer de la batería, ya que al estimar la capacidad disponible de la misma, el mecanismo del Duty Cycling (DuC) puede ser ajustado con el propósito de aumentar la eficiencia energética y por lo tanto, extender la vida útil de la red.

Es necesario desarrollar técnicas que incorporen un mecanismo de conservación de energía que integre información de la batería a través de indicadores como el Estado de Carga (SOC, State of Charge) y Estado de Salud (SOH, State of Health) para mejorar la eficiencia energética en WSN. La idea de incorporar información de la batería se debe a que la capa MAC está a cargo de controlar los modos de operación del nodo sensor, lo que está directamente relacionado con la cantidad de corriente exigida a la batería. Conocidos los perfiles de uso de la batería es posible estimar los indicadores SOC y SOH que se han utilizado ampliamente en diversas aplicaciones para conocer la cantidad de energía disponible en la batería y la degradación que ha sufrido la misma.

En este trabajo se propuso el desarrollo de un protocolo que actúa en la subcapa MAC y que considera la información de la batería para tomar decisiones con respecto al tiempo activo y de reposo del nodo de sensor, con la finalidad de promover el uso eficiente de la energía y extender la vida útil de la red. Los resultados obtenidos validan esta nueva propuesta de algoritmo y establecer pautas para guiar el diseño de protocolos MAC que se centren en minimizar el consumo de energía teniendo en cuenta los dispositivos de recolección de energía y la información de la batería.

SUMMARY OF THE THESIS TO OBTAIN THE  
DEGREE OF DOCTOR IN ELECTRICAL ENGINEERING  
BY: VANESSA LISBETH QUINTERO CEDEÑO  
DATE: 2019  
ACADEMIC ADVISOR: DR. CLAUDIO ESTÉVEZ MONTERO

DESIGN OF A MEDIUM-ACCESS-CONTROL PROTOCOL FOR WIRELESS SENSOR  
NETWORKS CONSIDERING THE BATTERY STATE OF CHARGE AND STATE OF  
HEALTH

Energy unavailability is one of the limitations of Wireless Sensor Networks (WSNs). Traditionally, batteries have been used to provide power to the sensor nodes and having a limited lifetime affect the operation time of the network. Solutions such as the use of larger batteries or the replacement of them are usually not viable due to the total amount of sensor nodes and the possible deployment in difficult access areas. This situation has motivated that the solutions for the maximization of the available energy in a WSNs focus on the development of techniques that act at the physical and data-link layers; such is the case of the Medium Access Control protocols (MAC).

The MAC protocols are one of the solutions widely studied and used because their capability to balance between energy conservation and critical network parameters such as throughput, latency, collision reduction, and control messages. They also have the ability to adapt to new working conditions when incorporating new technologies such as Energy Harvesting Devices (EHD). Another aspect that is being considered and studied in the design of MAC protocols is the information that can be obtained from the battery, since when estimating the available capacity of the battery the mechanism of the Duty Cycling (DuC) can be adjusted with the purpose of increasing energy efficiency and therefore extending the network lifetime.

It is necessary to develop techniques that incorporate an energy conservation mechanism that integrates battery information through indicators such as the State of Charge (SOC) and the State of Health (SOH) to improve energy efficiency in WSN. These indicators have been widely used in various applications to know the amount of energy available in the battery and the degradation that it has suffered. The idea of incorporating battery information in MAC protocols resides on how the MAC sub-layer is responsible for controlling the operating modes of the sensor node, which are directly related to the amount of current required by the battery. Since the usage profiles of the battery are known, it is possible to estimate both the SOC and SOH.

In this work, the development of a protocol that acts in the MAC sub-layer and that considers battery information for making decisions regarding the sleeping and activation times of the sensors node is proposed. The main objective is to promote the use of efficient energy and extending the network lifetime. The results obtained validate this new proposal and establish guidelines for the design of MAC protocols that focus on minimizing energy consumption considering the EHD, as well as battery information.

*Con mucho cariño a toda mi familia y amigos,  
en especial a mis padres Miriam y Maximino,  
a mi hermana Laura y a mis sobrinos Emma y Max .*

# Acknowledgements

Quiero agradecer en primer lugar a mi familia, por su apoyo incondicional. A mis padres Miriam y Maximino por su amor, por sus consejos y su paciencia. A mi hermana Laura por su cariño, consejos y ser mi soporte. A mi sobrina Emma por regalarme divertidos momentos que a pesar de la distancia me daban fuerza para continuar. A Yirina por su apoyo y amistad. A mi abuelo Abilio por ser mi segundo papá y no reparar en cariño y atenciones. A mi abuela Veja por quererme y cuidar a mi abuelo. A mis tíos, tías, primos y primas por su cariño y respaldo.

En segundo lugar quiero incluir a mis profesores guías Dr. Claudio Estévez y Dr. Marcos Orchard. Gracias por la oportunidad y confianza de desarrollar este tema de investigación, por cada una de las horas dedicadas a mi persona a través de conocimientos, consejos y sobre todo por la calidad humana que poseen, aspecto clave en este largo camino. De igual forma quiero agradecer a Dr. Cesar Azurdia, Dr. Christian Oberli y Dr. Jia Yuan Yu, miembros de la comisión evaluadora, por su tiempo y comentarios que contribuyeron a mejorar el trabajo presentado.

En tercer lugar quiero agradecer a cada uno de los amigos que Chile me brindó y sin los cuales este camino hubiese sido insoportable. Ros, mi parce, mi hermanita de la vida, mil gracias por estar allí, por darme ánimos, por regalarme un abrazo cuando hacia falta, por escucharme y por tu cariño sincero. Leo, mi yulipsito, por tu valioso consejo en el momento más crítico de mis estudios, por tus bromas y tu cariño. Aramis, amiguís, por sus consejos, por su disponibilidad y su apoyo incondicional. Francisco, Panchito, por tu calidad de persona, por abrirme las puertas de tu casa y dejarme ser parte de tu familia. Carlos, rulitos, por los abrazos, el cariño, las pláticas y las serenatas. Juan Sebastian, Sebas, por tu comprensión y cariño. Jacquie y Diego, mi pareja favorita, simplemente gracias por todos los consejos y el cariño sincero. Luis, Luismi, gracias por cada una de las pausas activas y por siempre tener palabras de aliento. Elizabeth, mi hermana de la luz, gracias por ser tu y brindarme tu amistad sincera. Javiera, Javi, gracias por brindarme una amistad bonita, por tus palabras de aliento y el cariño brindado. Gonzalo, Gonza, llegaste al final de este proceso para brindarme palabras de aliento, regalarme sonrisas, tu cariño y darme ánimos para concretar esta meta.

A los chicos del laboratorio de Fallas y Control Avanzado 1 (Jorge, Pablo, Herald, Diego, Esteban, Felipe, Matías, Sebastián, David, Ismael) mil gracias por hacer que el trabajo fuera más divertido y por la buena disposición. A los chicos del laboratorio OWL (Boris, Diego y Lili) gracias por las pláticas y los buenos momentos. A Jorge y Victor del laboratorio

de Procesamiento de Voz mil gracias por toda la ayuda prestada durante el inicio de mis estudios doctorales.

Gracias a Faby, Cristy, Shalabi, Pablo, Elisa, Nico y Pepo, mis amigos de Panamá, por sus consejos, palabras de aliento y por hacer que la distancia desapareciera. Eliana y Carol por las gestiones y orientación que necesité de ustedes en los temas administrativos del departamento de Ingeniería Eléctrica. De igual forma quiero agradecer a Milena por su orientación en los temas administrativos de la escuela de postgrado y sobre todo por el cariño y amistad brindada. A los chicos y chicas del fútbol y del gym gracias por los ratos de esparcimiento que ayudaron a disipar el estrés.

Finalmente mis agradecimientos a la Universidad Tecnológica de Panamá, IFARHU y CONICYT, mediante la beca CONICYT-PCHA/Doctorado Nacional/2016-21161427, por ser el soporte de mis estudios doctorales.

# Table of contents

<b>1</b>	<b>Introduction</b>	<b>1</b>
1.1	General Context and Motivation . . . . .	1
1.2	Problem Definition . . . . .	3
1.3	Hypotheses . . . . .	4
1.4	Objectives . . . . .	5
	1.4.1 General Objective . . . . .	5
	1.4.2 Specific Objectives . . . . .	5
1.5	Contributions . . . . .	5
1.6	Document Structure . . . . .	6
<b>2</b>	<b>Theoretical Framework</b>	<b>7</b>
2.1	MAC Protocols General Aspect . . . . .	7
	2.1.1 Duty Cycling Technique . . . . .	8
	2.1.2 Synchronous MAC Protocols . . . . .	9
	2.1.3 Asynchronous MAC Protocols . . . . .	11
2.2	MAC Protocols with EHDs . . . . .	13
	2.2.1 General Characteristics . . . . .	13
	2.2.2 MAC Protocols Designed for EH-WSN . . . . .	14
2.3	Process-Stacking Multiplexing Access Protocol . . . . .	16
2.4	MAC Protocols and Battery Information . . . . .	17
	2.4.1 Battery Model Importance . . . . .	17
	2.4.2 Battery SOC and SOH Estimation . . . . .	20
	2.4.3 Methods to Estimate SOC . . . . .	20
	2.4.4 Methods to Estimate SOH . . . . .	23
<b>3</b>	<b>Energy Efficient MAC Protocol with Battery SOC and SOH Awareness</b>	<b>28</b>
3.1	Access Control Management Design . . . . .	28
	3.1.1 Access Control Design . . . . .	30
	3.1.2 Packet Management . . . . .	31
3.2	Packet to Frame Encapsulation . . . . .	32
3.3	Collision Avoidance Mechanism . . . . .	34
3.4	Energy Management . . . . .	35
3.5	Metrics for the Time Sleep adjustment . . . . .	36
<b>4</b>	<b>Battery-Status MAC Protocol Validation</b>	<b>39</b>
4.1	MAC Protocol Validation . . . . .	39

4.2	SOC and SOH Estimation Validation . . . . .	44
4.2.1	SOC Estimation . . . . .	46
4.2.2	Performance of Methodology based on Particle Filter . . . . .	47
4.2.3	SOC Prediction . . . . .	49
4.2.4	SOH Estimation . . . . .	52
4.3	Time Sleep adjustment . . . . .	53
4.3.1	Time Sleep Validation . . . . .	53
4.3.2	Adjustment of the sleeping time considering the SOC estimation . . .	55
4.3.3	Sleep Time adjustment considering SOH Estimation . . . . .	58
<b>5</b>	<b>Conclusions</b>	<b>60</b>
5.1	Future Work . . . . .	61
	<b>Appendices</b>	<b>62</b>
A1	Publications . . . . .	63
A1.1	Journal Publications . . . . .	63
A1.2	Conference Publications . . . . .	63
	<b>Bibliography</b>	<b>68</b>



# List of Figures

2.1	Multiplexing techniques . . . . .	8
2.2	Comparison between TDMA and PSMA . . . . .	16
2.3	Discharge open circuit voltage . . . . .	18
2.4	Concepts related to SOH . . . . .	24
2.5	Datasheet LIR2032 Battery - Appendix A1 . . . . .	25
3.1	Network information . . . . .	29
3.2	Base station and nodes interaction . . . . .	30
3.3	Base station processes . . . . .	30
3.4	Base station states . . . . .	31
3.5	Sensor node processes . . . . .	32
3.6	Node process state . . . . .	33
3.7	Frame format . . . . .	33
3.8	Queue internal States . . . . .	34
3.9	The internal structure of the encapsulation process . . . . .	34
3.10	Energy process state . . . . .	35
3.11	Algorithm to modify the transmission currents . . . . .	37
4.1	Interaction between <i>BS</i> and two <i>SNs</i> . . . . .	40
4.2	Interaction between <i>BS</i> and three <i>SNs</i> . . . . .	40
4.3	Interaction between <i>BS</i> and eight <i>SNs</i> . . . . .	41
4.4	Interaction between <i>BS</i> and eight <i>SNs</i> using a different schedule . . . . .	41
4.5	Example of node scheduling . . . . .	42
4.6	Collision Examples . . . . .	43
4.7	Different transmission time window assigned to each sensor node . . . . .	43
4.8	Battery remaining capacity . . . . .	44
4.9	Data used . . . . .	45
4.10	Usage profile . . . . .	45
4.11	Voltage and SOC estimation . . . . .	46
4.12	Definition of operation cycle . . . . .	47
4.13	Voltage and SOC estimation . . . . .	48
4.14	RMSE and processing time histogram . . . . .	49
4.15	RMSE and processing time histogram . . . . .	50
4.16	SOC prediction . . . . .	51
4.17	SOC percentage using different currents . . . . .	51
4.18	Battery information . . . . .	52

4.19	Algorithm to determine a cycle operation . . . . .	53
4.20	Relationship between $T_{sleep}$ and energy harvesting rate . . . . .	54
4.21	Relationship between $T_{sleep}$ and $T_{tx}$ . . . . .	55
4.22	Relationship between the SOC and the $T_{sleep}$ . . . . .	56
4.23	SOC prediction . . . . .	56
4.24	SOC prediction . . . . .	57
4.25	Battery discharge process using different currents . . . . .	58
4.26	Section of Figure 4.25 . . . . .	59
4.27	Adjustment of $T_{sleep}$ according to SOH . . . . .	59
A1	Datasheet LIR2032 . . . . .	67

# List of Tables

1	Acronym List . . . . .	xi
2.1	Protocols and DuC adjustments . . . . .	9
2.2	Characteristics of DuC MAC protocols . . . . .	13
2.3	MAC protocols with EHD . . . . .	15
2.4	Escalation factors for different degradation cases . . . . .	26
4.1	Currents characteristics - CC2500 . . . . .	46
4.2	Maximum and Minimum $T_{sleep}$ . . . . .	54
4.3	Maximum and Minimum SOC . . . . .	57
4.4	Maximum and Minimum $T_{sleep_{SOC}}$ - Case 1 . . . . .	57
4.5	Maximum and Minimum $T_{sleep_{SOC}}$ - Case 2 . . . . .	58
4.6	$T_{sleep_{SOH}}$ information . . . . .	59

Table 1: Acronym List

<b>Acronym</b>	<b>Meaning</b>
ACK	Acknowledgement
ADC	Analog-Digital Converter
AIMD	Additive-increase Multiplicative-decrease
ARQ	Automatic Repeat Query
CCA	Clear Channel Assessment
CL-PM	Close-loop Power Manager
CSMA	Carrier Sense Multiple Access
CTS	Clear to Send
DoD	Depth of Discharge
DSR	DuC Scheduling based Residual Energy
DSP	DuC Scheduling based on Prospective Increase in Residual energy
DuC	Duty Cycle/Cycling
EH	Energy Harvesting
EHD	Energy Harvesting Device
EIS	Electrochemical Impedance Spectroscopy
ENO	Energy Neutral Operation
ENAN	Estimate Number of Active Neighbors
ESD	Energy Storage Device
FRTS	Future Request to Send
KiBaM	Kinetic Battery Model
LCP	Low Complexity Policy
Li-Po	Lithium Polymer
LPL	Low Power Listen
MAC	Medium Access Control
MTS	More to Send
NAV	Network Allocation Vector
NIM	Neighbor Inform Message
NL	Network Lifetime
NQM	Neighbor Query Message
OCV	Open Circuit Voltage
PION	Pioneer Frame
PETF	Pattern Exchange Time Frame
PRFT	Pattern Repeat Time Frame
PSMA	Process-Stacking Multiplexing Access Protocol
RF	Radio Frequency
RLIS	Remaining Lifetime of Individual Sensor
RLSN	Remaining Lifetime of a Sensor Network
RTS	Request to Send
SCH	Scheduling Frame
SOC	State of Charge
SOH	State of Health
WSN	Wireless Sensor Network

# Chapter 1

## Introduction

### 1.1 General Context and Motivation

Technological advances in the area of wireless communications and electronics have significantly improved the performance of WSNs, increasing their usability in applications oriented to the monitoring of environmental events [1], industrial processes [2], healthcare [3], and others [4]. For example, in the highspeed-train industry, WSNs can provide information about the health of bridges, tracks, and train components, reducing maintenance costs and providing a greater safety [5]. In the healthcare area, the information retrieved by the sensors allows doctors to have early-warning information about the patient's condition, allowing faster and more efficient decisions concerning the type of treatment that needs to be carried out [6]. Another example is in the mining area where the WSNs are used to monitor various aspects (temperature, humidity, gas emanation, etc.) to guarantee the well-being of workers thereby minimizing the amount of accidents.

WSNs are pervasive, and the energy limitation is a critical factor in the operation of mobile nodes [7]. WSNs consist of a set of devices, usually small and inexpensive, commonly referred to as nodes which have low-power sensors that are deployed through an area to monitor a phenomenon of interest [8] [9]. Each node is equipped with the required resources for the acquisition, processing, and transfer of data. These resources need energy, and therefore the node must have a power source, which can be a battery [10], a supercapacitor [11], and/or an EHD [12]. Energy availability is essential for the continuous operation and reliability of WSNs. Historically, nodes have been powered exclusively by batteries, which greatly affects the NL [13]. Solutions such as using batteries with higher storage capacity or the periodical replacement of batteries are often not viable due to the massive number of nodes deployed, many in difficult areas to reach [14]. This situation has led to solutions for energy conservation focused on the development of cross-layer techniques operating at non-physical layers, as well as the incorporation of new technologies and battery information.

Diverse techniques have been proposed to minimize energy consumption in WSNs, for example: routing techniques [15], DuC, and clustering [16]. Routing techniques select a path that minimizes energy consumption and maximizes the network lifetime considering

the type of application where they will be implemented [15] [17]. On the other hand, DuC is a technique widely used at the level of MAC protocols, capable of saving energy by placing the sensor node in a sleeping state (which means turning off the radio), when it does not perform functions of acquisition or transmission of data [18]. DuC has presented variants that decrease latency and loss of network coverage [19]. Another technique is clustering where one of them, the main node (cluster head), coordinates the activities of the rest of the members of the group [9] [20]. The use of this technique reduces the number of devices that share the medium and the control information required in each transmission [16].

Another way to improve the energy efficiency of the WSN is the use of sensors with technology that harvest energy from external sources, either environmental or otherwise to transform it into electrical energy. These devices are called EHD and have been incorporated into the WSN to make the network work for longer periods of time [21]. In addition, this device allows balance with other features of the network such as throughput and latency [22]. The use of EHDs has generated new challenges, such as, to guarantee the operation within the Energy Neutral Operation (ENO) state and the prediction processes of the energy available in the system [11] [13] [22]. In literature, several proposals are presented to face the challenges described above, for example, authors in [21] state the importance of making predictions about the battery charging times and enunciate methods such as Exponentially Weighted Moving-Average (EWMA) to make such predictions. In [22] some algorithms designed to act in the MAC sub-layer of the WSN with EHD are listed.

Another approach used in WSNs to reduce energy consumption is to collect information about the battery state. Having battery information improves the decision made by the algorithms that work at the level of the MAC sub-layers. For example in [23] a model is proposed to predict the battery lifetime of each sensor node, using information from the operation modes of the sensor and characteristics of the battery. Having indicators that determine the battery state is of the utmost importance and in literature, the SOC and the SOH are listed as two of the most used indicators [24] [25]. The SOC allows us to know how much energy is available in the battery and the SOH denotes the degradation suffered by the battery [24]. These indicators are used to determine the battery life, a topic of interest not only in the WSN field but other applications involving robots, electric vehicles, satellites, and others [25].

According to the previous information, the search for mechanisms that contribute to improve energy consumption in WSNs is still an area of great interest. The existing techniques still fail to achieve energy efficiency without affecting critical network parameters such as performance and latency. On the other hand, the implementation of new technologies such as EHD has contributed significantly to address the energy constraints presented in the WSN. However, the use of these devices has created new paradigms. In addition, the use of indicators such as SOC and SOH incorporate significant improvements to the applications where they are implemented, although their use implies a high computational load. This situation leads to consider whether the energy expenditure, product of the execution of these algorithms, is based on the benefits provided to the network. That is why a viable solution to address the energy difficulties is to design a technique that allows to include an energy conservation mechanism that is compatible with the EHD and also incorporates information from the battery, since the combination of these three strategies would allow facing the

disadvantages that each one presents separately.

## 1.2 Problem Definition

The main limitation that WSNs have is the need of a constant source of energy. Batteries have traditionally been used to power the sensor nodes, which affects the network operating time. Solutions such as the use of larger batteries or the replacement of them are usually not viable due to the total amount of sensor nodes and the possible deployment in difficult access areas [13]. The solutions for the conservation of energy in a WSN focus on the development of techniques that act at physical and data-link layers. One example is the case of the MAC protocols algorithms that are implemented to the level of the MAC sub-layer to provide scalability, adaptability, and reliability to the network, in addition to promoting energy conservation.

The energy conservation is one of the main characteristics of the MAC protocols designed. In the available literature, various mechanisms developed to deal with this problem are referenced [20]. An example is presented in [13], where the authors classify MAC protocols into four large groups: asynchronous, synchronous, frame-slotted, and multi-channel. The protocols belonging to these groups have brought considerable improvements to the WSN, but still present challenges that must be solved, such as reducing costs and delays, minimizing collisions, and assigning the transmission channel. Another example is presented in [20] where the energy saving mechanisms applicable to the MAC sub-layer are listed. Within the mechanisms is DuC, which is the most used at the level of the MAC protocols. This mechanism presents challenges that must still be studied, such as the use of low power and the management of the times when the node must remain in a state. On the other hand, in [26] the authors make a study of the DuC mechanism where they enunciate the challenges that this tool must consider in its design, for example, the collision rate and the control information. In addition, the authors present a classification of synchronous and asynchronous DuC, where each group presents aspects to improve, for example, for the technique of strict synchronization, although it allows to reduce the listening time and collisions requires more equipment or control messages, or in the case of the programming-based scheme, energy is conserved at the expense of increased latency.

As noted, the MAC protocols are still under study because a solution must be proposed that allows the balance between energy conservation and critical network parameters such as performance, latency, collision reduction, and control messages. Also, the MAC protocols must face the new working edges that arise when incorporating new technologies such as the EHD. In [27] a review of the MAC protocols developed for WSN with EHD is presented; protocols such as EH-MAC (Probabilistic Polling for Multi-hop Energy Harvesting-WSN), ODMAC and LEB-MAC (Load and Energy Balancing MAC Protocol for Energy Harvesting Powered WSN) are enunciated.

Another aspect that is being considered and studied in the design of the MAC protocols is the information that can be extracted from the battery when estimating the available capacity of it; the DuC mechanism can be adjusted in the best way for increasing energy efficiency and

therefore extend the life of the network [28]. In [29] a methodology is presented to estimate the useful life of the battery considering the modes of operation of the nodes, for this a complete discharge of the battery is made, and a model of its behavior is obtained by approaching the curve resulting in a polynomial expression that allows evaluating the evolution of energy in the battery. Another example is presented in [23] where the authors enunciate a methodology to predict the time of life of a WSN based on the energy consumption of the different modes of operation of the node. Kerasiotis et al. introduces a factor that represents the proportion of time when Enables the current demand for energy, it is also considered a polynomial approach to adjust the discharge curve obtained from the AA alkaline battery. Although both works allow us to estimate the useful life of the network, a mechanism is not established about which decisions can be taken that favor the operation of the network. In both cases, the battery model has been simplified which awakens the interest to evaluate more complex models and to analyze if, when making the change, more precise results are obtained.

Detailed all these situations, as a possible solution, to try to improve the efficient use of energy in the WSN, is to develop a technique that incorporates an energy conservation mechanism that integrates information from the battery through indicators such as the SOC and the SOH. The idea of combining these tools in a single technique arises from the fact that the MAC sub-layer is responsible for controlling the operating modes of the sensor, which are directly related to the amount of current required by the battery. Well-known the usage profiles of the battery it is possible to estimate the SOC and SOH indicators which have been widely used in various applications to know the amount of energy available in the battery and the degradation that it has suffered. The development of an algorithm at the level of the MAC sub-layer is feasible due to the design characteristics of the protocols that act in that layer. In addition to the estimation and prognostic of the SOC and SOH that will allow the energy saving mechanism to make more efficient decisions in terms of rest and activation times of the sensors, managing to promote an efficient use of energy and extending the lifetime of the network.

### 1.3 Hypotheses

- Access control algorithms based on DuC and time-division multiplexing (TDM) reduce energy consumption by controlling sleep periods of the sensor nodes until they can restore their energy, also achieving consistency with other critical parameters of the WSN which means that the network becomes self-sustaining.
- The algorithms used for the estimation and prediction of the battery SOC and SOH with the incorporation of the DuC mechanism improve the energy network performance by providing information to aid the decision making process regarding the energy consumption of the network, and increasing the energy autonomy of the network.



## 1.4 Objectives

### 1.4.1 General Objective

Design a MAC protocol oriented to WSN that incorporates techniques for the estimation and prediction of the battery SOC and SOH, to obtain a balance between energy consumption and other parameters of the network such as throughput, and reduction of the collisions.

### 1.4.2 Specific Objectives

- Develop a MAC protocol that uses a TDM variant and the DuC mechanism to improve energy consumption in a WSN, avoiding a throughput reduction and increment of collisions.
- Implement a SOC and SOH estimation and prediction algorithm that supply information to the MAC protocol to assist the decision-making process of how the available energy in each node must be used.
- Validate, through simulations and using evaluation metrics such as throughput, and collision reduction, the correct operation of the MAC protocol when the information of the SOC and SOH is incorporated.

## 1.5 Contributions

During the development of this thesis, several conferences and journal articles were published (see A1.1) and the following contributions made in this thesis:

- Review of the existing literature regarding the techniques and methods proposed to minimize energy consumption in WSN that consider the introduction of EHD and battery information through indicators such as SOC and SOH. Within this review, the importance of the new MAC protocols for WSN considering these parameters is underlined. This contribution was published in the scientific journal *IEEE Communications Surveys and Tutorial*.
- Comparison of the proposed SOC estimation algorithm used in the MAC protocol with other methods proposed in the literature, that use a polynomial expression, to establish design parameters of the MAC protocols for WSN. This contribution was published in the magazine *IET Electronics Letters*.
- Design of a MAC protocol for WSN based on TDM and DuC that considers the information coming from the battery. The incorporation of battery information is achieved by modifying the sleep time equation of the sensor node by including the SOC and SOH indicators. This contribution is under writing for *IEEE Communications Magazine*.

- Development of guidelines on how the MAC protocols should adjust the sleep time of each sensor node based on indicators of the battery status, namely SOC and SOH, including how the algorithms used for estimation and prediction of SOC and SOH are established. This contribution was published in the Annual Conference of to the magazine *the Prognostic and Health Management Society 2018*.

## 1.6 Document Structure

The structure of this thesis is the following: Chapter 2 discusses the characteristics of current MAC protocols for WSN considering DuC MAC protocols, EHD devices, and battery information. In addition, it explains the theoretical concepts of the techniques and methods implemented in this work. Chapter 3 describes the main characteristics of the proposed protocol, its differences with respect to the previous versions and how it adjusts the sleep time of the sensor nodes considering the SOC and SOH of the battery. Chapter 4 shows the results obtained to validate the performance of the MAC protocol and how it incorporates battery information. Finally, Chapter 5 presents the conclusions and future work.

# Chapter 2

## Theoretical Framework

### 2.1 MAC Protocols General Aspect

The MAC sub-layer, which is responsible for providing support to the physical layer and for coordinating the way in which the sensor nodes can share the medium once transmissions start to share, is found at the level of the data-link layer. The channel defines how and when a node will attempt transmission [30]. The so-called MAC protocols act at the level of MAC sub-layer. The responsibilities of MAC protocols include the medium access management, frame delimiting, collision avoidance, and error protection [13] [31]. When discussing MAC protocols specifically designed for WSN, energy conservation becomes one of the most critical aspects of the design. Therefore, it must be designed to synergize with other attributes to reduce any impact caused by the energy management system itself [31].

The MAC protocols are responsible for managing the transmission and reception schedule of information, as well as the entry into the sleep mode of each node [32]. The traditional classification divides MAC protocols under two sets. The first set consists of the techniques based on contention, where a central node is not required. This means that all the nodes have access to the transmission medium at the same time. The second group of techniques are based on programming. This group requires the dedicated assignment of the transmission medium and access to it by defining an order [31]. Time Division Multiple Access (TDMA), Frequency Division Multiple Access (FDMA) and Code Division Multiple Access (CDMA) are programming-based techniques, while Multiple Access with Carrier Monitoring (CSMA) is recognized as a technique of containment, see Figure 2.1. All these techniques are used by the MAC protocols of traditional networks. In the case of WSN MAC protocols, variants of these techniques are required [33].

TDMA is a technique that assigns equal time intervals to all devices that are part of the network, which guarantees the total bandwidth for each device during the assigned transmission time. TDMA has the peculiarity of making inefficient use of bandwidth since not all devices require transmitting the same amount of information, for which they will occupy the medium during different time intervals. TDMA generates greater energy consumption by assigning transmission time to devices that do not require it. In FDMA, the available

spectrum is divided into channels that have different frequencies, and each channel is assigned to a device. For CDMA, all devices have access to the transmission medium at the same time using different coding schemes. CSMA is a contention-based media access technique in which nodes only detect the channel when they must send information, and it is available [2]. Several research studies have shown that MAC protocols designed with TDMA variants are functional in the WSN since they correct the problem of energy expenditure and less complexity of implementation if it is compared with FDMA and CDMA [13] [20]. In the WSN the vast majority of the MAC protocols designed is based on TDMA and CSMA. In [2] it is indicated that according to the application one technique can be more efficient than the other.

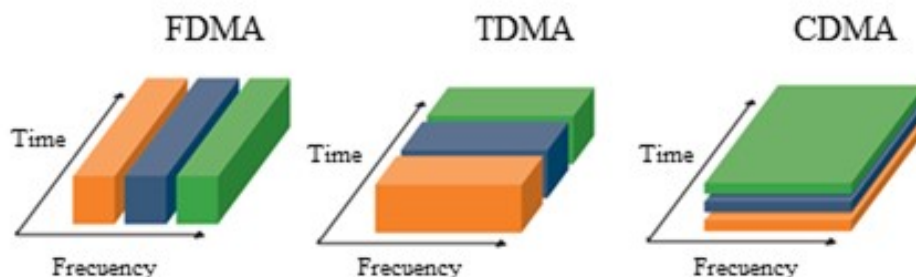


Figure 2.1: Multiplexing techniques

### 2.1.1 Duty Cycling Technique

A large part of MAC protocols that propose to minimize energy consumption in WSNs are used to control the operation activity (physical layer aspects) of the node, using techniques such as DuC [13] [20]. DuC is a technique capable of reducing energy consumption by toggling the sleep modes (implies turning off the radio) and active modes of the node [34]. The active periods of the sensor node can be defined as those in which different activities for the transmission and reception of information are performed, while the sleep periods are defined as those time lapses in which the sensor node is not found transmitting or receiving information, nor establishing communication with a base station [35] [36]. The use of DuC reduces energy consumption by decreasing the listening time of the nodes, and it has been evolving according to the requirements of the WSN and can be classified according to the mechanism to wake-up the sensor node.

DuC, in its original version, has the same duration of time for its listening and sleep periods in every sensor node. Over the years, different adjustments to DuC have been proposed. The first change made to DuC was to modify the duration of time of the sleep period to obtain a trade-off between energy savings and latency. Subsequently, the proposed modifications considered other aspects. In some cases, DuC is adjusted according to the energy harvested from the environment. For example, the techniques called Duty-cycle Scheduling based on

Residual energy (DSR) and Duty-cycle Scheduling based on Prospective increase residual energy (DSP) are designed considering this feature [37]. Another way to adjust the DuC uses information from the node sensor battery [38]. Table 2.1 shows how the DuC is defined for technique such as CL-PM and DSP.

Table 2.1: Protocols and DuC adjustments

Technique	Definition	Description
CL-PM	$T_{wi} = \frac{Q+Q_{pm}/\eta}{\beta+K_{leak}}$	<p>The wake-up period (<math>T_{wi}</math>) is define according to the total charge consumption (<math>Q</math>), the charge consumed by the power manager (<math>Q_{pm}</math>) at time <math>\eta</math> and the leakage current (<math>K_{leak}</math>).</p>
DSP	$I_{dc}^i = I_{dc}^{max} - \left[ I_{dc}^{max} \left( \frac{E_{r(c+T)}^i - E_{th}}{E_{max} - E_{th}} \right) \right]$	<p><math>E_{r(c+T)}^i</math> is the sum of the current residual energy <math>E_{r(c)}^i</math> and the increase residual energy <math>R_{surplus}^i</math>.</p>

DuC has undergone several changes that address other problems such as increased latency and loss of network coverage through the years [26] [39]. Traditionally DuC has been classified into two groups: synchronous and asynchronous. Synchronous DuC uses specific times in which each node can exit the sleep mode, while asynchronous DuC use other ways to wake up the nodes, e.g., sending pre-information called preamble frames [13]. The following subsections analyze the characteristics of these two groups and the mechanisms implemented by the MAC protocols that compose both group respectively.

### 2.1.2 Synchronous MAC Protocols

MAC protocols with synchronous DuC synchronize the wake-up of their nodes. Among the synchronous DuC MAC protocols there are two strategies that can be used to classify this group: One strategy is *rendezvous*, where all nodes wake up and return to sleep mode at the same time; in other words, it uses a global synchronization. Another strategy is *skewed/staggered*. In this case the synchronization occurs in step wise chronology according to a previously established pattern [26] [40]. There have been several MAC protocols designed for WSN that employ synchronous DuC, as in the case of S-MAC [35], T-MAC [41], D-MAC [42], PMAC [43], RMAC [44], DW-MAC [45] and TAS-MAC [46].

S-MAC was the first protocol designed specifically for WSN that implemented a duty cycle technique to improve the energy efficiency, so it is used as a reference in the design

of the newer MAC protocols. S-MAC prioritizes the energy conservation and it uses DuC, virtual clusters, and message passing techniques to achieve this purpose. T-MAC is another protocol that has similarities with S-MAC, since it uses mechanisms such as Request to Send (RTS)/ Clear to Send (CTS) and virtual clusters. The main difference between T-MAC and S-MAC is the incorporation of a period of time that represents the minimum listening time. This means that if no events that activate the node occur during this time, then it will enter its sleep mode. D-MAC is designed to organize the topology of the WSN in data-gathering trees. It does this by first identifying the sources and the sink (usually only one) and, second, shifting the listening modes of every node in the path, from the source to the sink, such that as the previous node completes transmission, the current node initiates the next transmission. This is referred as Staggered Wake-up Schedule.

P-MAC implements an adaptive sleep schedule. This technique is based on the node's traffic and the traffic pattern of its neighboring nodes. P-MAC uses specific rules to determine its sleep and wake-up schedules. These rules are formulated considering the sleep/wake-up pattern (tentative node schedule) and the sleep/wake-up schedule (current node schedule). The sleep sequence starts with no sleep scheduled. If there is no data to transmit then a sleep interval is inserted, which will have the same time duration as the listen interval, defined as  $T_R$  in [43]. R-MAC is a protocol that incorporates the use of control frames called Pioneer Frames (PIONs) to request communication and confirm a request. PIONs replace the RTS/CTS used in S-MAC, but this frame includes the same fields that an RTS frame and adds cross-layer information (the final destination address and the number of hops traveled). The PIONs are transmitted in a time window where all nodes are awake. Each PION signal indicates to its respective node when to sleep and when to wake-up. DW-MAC introduces a new algorithm that allows nodes to quit the sleep mode on demand. To do this, DW-MAC replaces RTS/CTS with a special type of frame called the Scheduling Frame (SCH).

All synchronous MAC protocols have three main operating cycles: SYNC, DATA and SLEEP. Synchronization of the sensor nodes clocks is a critical aspect of these protocols and if it is not done properly it will cause a tremendous negative impact on the performance of the network. The SYNC interval is reserved for this purpose. Several techniques are used to synchronize the clocks in sensor nodes, for example, S-MAC, T-MAC and P-MAC use a virtual clustering technique [35] [41] [43] while D-MAC, R-MAC and DW-MAC use a broadcast synchronizations scheme [42] [44] [45]. The aforementioned protocols use different control signals. For instance, S-MAC, T-MAC and P-MAC use the Request to Send (RTS)/ Clear to Send (CTS) [35] [41] [43]. Moreover, R-MAC uses Pioneer Frame (PION), while DW-MAC employs Scheduling Frame (SCH) [44] [45]. The use of PION and SCH signals in R-MAC and DW-MAC, respectively, decreases the amount of control messages contributing to the energy-consumption reduction [44] [45]. Each of these mentioned protocols have introduced improvements that have allowed to reduce energy consumption, reduce the latency, and improve the overall performance. A noteworthy observation is that synchronous MAC protocols evolved from having a cluster/local synchronization to having a global synchronization; hence, improving the overall flow in the network.

An important point to consider from the design of synchronous MAC protocols is that these protocols should be kept as simple as possible. Synchronization-sensitive protocols might pay a high price if they get disorganized. Also, in practice, complex algorithms require

a computational overhead that takes time and consumes energy itself. If the system spends too much computing time to “save time” it is counter productive. In general, WSN have large quantities of nodes to generate a diverse and comprehensive representation of the gathered information. Because large quantities are usually desired, sensor nodes generally have low-processing power. With very few exceptions, sensor nodes are small single-board computers with limited resources (processing power, memory, disk space, energy supply, etc.). These factors should be considered when designing MAC protocols, particularly the synchronization scheme in the case of synchronous MAC protocols.

### 2.1.3 Asynchronous MAC Protocols

Synchronous protocols introduce control messages to achieve the synchronization requirements necessary to toggle between active and sleep modes [47]. Asynchronous protocols use other mechanisms to get the nodes out of their sleep state. These mechanisms are divided into two groups: sender-initiated (or preamble sampling) and receiver-initiated. The sender-initiated protocols use a preamble signal, before transmitting, to notify the receiving node that data is queued and ready to transmit. The preamble-sampling basic scheme has a fixed time for the notification signal (preamble) that is known by all the nodes of the network. This particular scheme has several disadvantages, such as high overhead, costly collisions, excessive overhearing and incompatibility with newer radios [30]. These problems have been solved through the division of the preamble into short pulses or packets, synchronization of the information, and adaptations of the DuC. For receiver-initiated protocols, a short frame, called beacon, is sent by the receiver to initiate the transmission [26] [30]. A few asynchronous protocols proposed in literature are: B-MAC [48], WiseMAC [49], X-MAC [50], RI-MAC [47], PW-MAC [40], SA-RI-MAC [51], WX-MAC [52], SW-MAC [53], AS-MAC [54], DS-MAC [55] and MCAS-MAC [56].

Asynchronous DuC MAC protocols do not adhere to a regular pattern. The transmissions start at a random or pseudo-random time. The linkage is obtained by means of preambles, in essence the receiver searches for the transmitters preamble signal by Low Power Listen (LPL) samples, hence the name preamble sampling. In general, for low traffic networks, asynchronous MAC protocols are more energy efficient, particularly when the LPL sample period is long and the buffer capacity is sufficient. There is no clear optimal technique, the target application will determine if synchronous or asynchronous is better suited. A noteworthy comment about the asynchronous protocols is that in some cases the preamble design contains complex information, such as the time to start transmitting data. If the preamble is transmitted in low power mode it is difficult to argue that it can carry data. If it carries data, it is no longer in low power mode because if it were, the data is prone to errors. This is the reason why the data packets must be in normal energy mode, so it can clearly distinguish and deduce the digital content. Preambles and beacons are mainly signals, rather than messages, frames, or packets. Nevertheless, we adhere to the terminology used in the documentation cited for better comprehension.

B-MAC is a CSMA protocol that uses preamble sampling to reduce the listening time. The preamble length is longer than receiver’s sleep period to guarantee linkage. Furthermore, B-MAC uses Clear Channel Assessment (CCA) and packet back-off for channel arbitration,

unlike S-MAC. Additionally, in B-MAC, CCA is used to determine if there is activity in the channel during the LPL interval [48]. WiseMAC is based on B-MAC and therefore it shares some similarities in its functionality; nevertheless, it has a crucial difference that makes it more energy efficient. A node running WiseMAC learns the cycle of its neighbors. When the transmitter needs to send queued data it does not turn on the preamble immediately but rather it waits until the target receiver is near its LPL mode. X-MAC is a protocol designed to improve the energy efficiency and to decrease the latency by addressing some weaknesses of B-MAC. X-MAC introduces the concept of a strobing preamble, which consists of short preambles with enough information to identify a receiver. These short preambles are separated by time lapses that allow the receiver to send a signal called an Early Acknowledgement (ACK).

RI-MAC is the first asynchronous receiver-initiated MAC protocol proposed that attempts to reduce the time by which each sender node and its receiver occupy the medium to exchange information. To achieve this goal, a RI-MAC receiver node uses beacons to notify the transmitter it is ready for the data transmission. Each beacon is used to confirm the data reception and to notify the transmitter, again, that it is ready to receive new information. PW-MAC is an enhanced version of RI-MAC that introduces a pseudo-random generator to control the awakening of nodes. This technique reduces the possibility of collisions when compared to fixed schemes. PW-MAC is complemented by the incorporation of a prediction-based frame relay and prediction error calculation [40]. Another variant of this scheme is presented in [57] where a summary function is used to determine the active programming mode of each node, allowing in this way to decrease the listening time. SA-RI-MAC is based on RI-MAC and its designed to improve the performance under dynamic-traffic load conditions. The improvement incorporated by SA-RI-MAC is the contention solution for the senders when competing for the medium access.

WX-MAC is another protocol which decreases the size of the preamble by using a strobed preamble. This technique defines its preamble as an RTS series. WX-MAC is a protocol that estimates the beginning of the preamble similar to WiseMAC. SW-MAC is an asynchronous protocol designed to decrease latency. It uses a sequence of packets called scout packets to wake up the node. In SW-MAC, the sending of the scout packets is initiated by the node that tries to transmit. Furthermore, SW-MAC defines its active time according to the length of the scout packets, the bandwidth of the wireless channel, the number of sending nodes, and the queue length. AS-MAC is a protocol that reduces power consumption, packet loss, and delays. AS-MAC helps to reduce the length of the preamble by storing its neighboring nodes wake-up schedule, allowing it to determine when they wake-up. DS-MAC is an asynchronous protocol that improves the performance and reduces the latency of the network. DS-MAC reduces the waiting times by predicting the next wake-up time of the nodes, similar to WiseMAC, but additionally it is able to adjust the sleep time according to the demand. [55]. A multichannel asynchronous scheduled MAC (MCAS-MAC) is proposed in [56]. The design of MCAS-MAC is based on AS-MAC and it introduces back-to-back packets transmissions and a multichannel to support high traffic. Table 2.2 shows a summary of DuC MAC protocols features.



Table 2.2: Characteristics of DuC MAC protocols

Protocols	Year	Type	Characteristics
S-MAC	2002	Synchronous	First DuC [35].
T-MAC	2003	Synchronous	Uses a minimum listening time [41].
D-MAC	2004	Synchronous	Used in data-gathering trees [42].
B-MAC	2004	Asynchronous	Introduces LPL [48].
Wise-MAC	2004	Asynchronous	Learns about its neighbors [49].
PMAC	2005	Synchronous	Uses Adaptive sleep schedule [43].
X-MAC	2006	Asynchronous	Introduces strobing preamble [50].
R-MAC	2006	Synchronous	introduces Pioneers Frame [44].
DW-MAC	2008	Synchronous	sleep based on demand [45].
RI-MAC	2008	Asynchronous	First receiver-initiated protocol [47].
PW-MAC	2011	Asynchronous	uses pseudo-random generator [40].
SA-RI-MAC	2011	Asynchronous	Based on RI-MAC [51].
WX-MAC	2013	Asynchronous	Uses two different control messages [52].
AS-MAC	2013	Asynchronous	Reduces preamble length [54].
SW-MAC	2014	Asynchronous	Uses scout packets [53].
DS-MAC	2015	Asynchronous	Predict the next wake-up time [55].

## 2.2 MAC Protocols with EHDs

MAC protocols designed for EH-WSN have great freedom with respect to the power requirements, but they must consider other features to achieve the network performance. These protocols must be capable of predicting the availability and consumption of energy in the sensor node to ensure that the node operates within the ENO state. Moreover, they must consider the behavior of the ESD (i.e., battery) [58]. These considerations allow MAC protocols for EH-WSN to adjust their DuC by doing a trade-off between the available energy and the performance parameters of the network.

### 2.2.1 General Characteristics

Previously, it was mentioned that MAC protocols for EH-WSN must be able of incorporating characteristics associated to the use of EH. These characteristics are explained further below. The first characteristic is the ability to predict the amount of energy available through EH.

The prediction of energy available to harvest will depend on the type of EHD used by the sensor node. In [59] and [60] different sources of energy harvesting, as well as their characteristics are studied. According to the type of EH used, a model is required to predict the energy availability. Currently, various models of energy prediction have been proposed, for example, Exponentially-Weighted Moving Average (EWMA), Accurate Solar Energy Allocation (ASEA), Weather-Conditioned Moving Average (WCMA), Profile Energy Prediction Model (Pro-Energy), and a Solar Energy Prediction Algorithm with Q-learning (QL-SEP) [61] [62].

The second characteristic takes into account is the ability to determine the amount of energy consumed by the sensor node over a period of time. This process is done to ensure that the sensor node operates in the ENO state, regardless of whether it uses the energy coming from the EHD or the ESD. The energy consumption is calculated using the amount of current required by the EHD or the ESD during a period of time. Specifically in WSN, the energy consumption is calculated in the wake-up period and the different current levels used (e.g. transmission, reception, idle) are considered by the sensor node. An example of this is found in the work presented in [63]. The third characteristic considers the incorporation of information about the ESD, e.g. battery model, in the MAC protocol for EH-WSN. Traditionally, the ESD used is a battery, therefore, understanding its operation is of the utmost importance for the MAC protocol decision making process. Section 2.4 discusses about the existing battery models, the different indicators used to obtain battery status information, and how MAC protocols process this information.

### 2.2.2 MAC Protocols Designed for EH-WSN

ODMAC [64], EA-MAC [65], EH-MAC [66], S-MAC-EH [67], ERI-MAC [68], EL-MAC [69], LEB-MAC [70] and RF-MAC [71] are MAC protocols designed specifically for EH-WSN. On-Demand Medium Access Control (ODMAC) is a protocol designed to maximize the network performance and to achieve that each node operates near ENO-max status. ODMAC incorporates two types of DuC: static and dynamic. Energy Adaptive-MAC (EA-MAC) is a protocol designed to transfer energy through radio frequency (RF) using master nodes and slave nodes. This protocol implements a DuC and an adapted media containment window. For the adapted DuC, a threshold that allows the transition between the active and sleep mode is established. The threshold is determined so that the energy is sufficient to transmit a packet.

S-MAC based on energy harvesting modifies the traditionally S-MAC protocol allowing it to be used with EHDs. One of the proposed modifications is the incorporation of a throughput model that considers the relationship between the active period and the entire cycle time and the number of packets that they can be sent based on the level of energy available in the battery. The Energy Harvesting MAC Protocol (EH-MAC) is an asynchronous receiver-initiated protocol with a polling scheme. EH-MAC is designed for throughput maximization using the contention probability concept, which is the probability that the sender node transmits its data.

ERI-MAC is another asynchronous receiver-initiated protocol. This protocol implements

the same collision detection and retransmission used by RI-MAC. Moreover, ERI-MAC uses packet concatenation to reduce latency and a queuing mechanism to improve the ENO. Energy Level MAC (EL-MAC) is a protocol that considers primary and secondary users, i.e., a hierarchical topology. EL-MAC employs the energy level to determine the access probability and the window contention size for secondary users. Load and Energy Balancing MAC (LEB-MAC) is another asynchronous receiver-initiated DuC protocol. LEB-MAC is a protocol focused on improving the adjustment to DuC mechanism. RF-MAC is a protocol for EH-WSN that uses RF energy transfer. This protocol is designed considering two important aspects with respect to the energy available. The first aspect is related to the adaptive charging threshold, where each sensor node must calculate its maximum charging threshold. This threshold is calculated based on the communication activity of each sensor node. The second aspect is related to the prioritization of energy over exchange of information.

As mentioned before, the design of WSN with EHD has contributed significantly to improve the energy management of the network by allowing ESDs to be recharged. The design of MAC protocols for EH-WSN must include the time in which the EHD harvests energy, an aspect that directly influences the functions of the node. Considering all the protocols studied previously, it is observed that the existing protocols for EH-WSN focus on working in the ENO state, ensuring the extension of the network lifetime. Moreover, the protocols discussed demonstrate the importance of the ESD when making decisions regarding the operation of different techniques or parameters (i.e, DuC, window contention, access probability). Evaluating the existing protocols, it can be seen that these protocols focus on other parameters of the network, such as the maximization of the throughput, minimization of latency and end-to-end delay, among others. Despite the progress made in this area, there are still challenges to be solved. For instance, the proposal is open to find an optimal point between throughput and energy conservation considering the energy injected by the EHD. Another aspect that arouses interest is the introduction of parameters that allow the evaluation of the ESD condition and study their effect on the behavior of the EH-WSN. Table 2.3 shows a summary of MAC protocols with EHD.

Table 2.3: MAC protocols with EHD

Protocols	Year	Type	Characteristics
ODMAC	2011	Asynchronous	Uses static and dynamic DuC [64].
EA-MAC	2011	Asynchronous	Uses master and slave nodes [65].
EH-MAC	2012	Asynchronous	Uses polling scheme [66].
S-MAC/EH	2013	Synchronous	Introduces throughput model [67].
ERI-MAC	2014	Asynchronous	Receiver-initiated [68].
EL-MAC	2014	Asynchronous	Considers primary and secondary users [69].
LEB-MAC	2014	Asynchronous	Uses Fuzzy Logic [70].
RF-MAC	2014	Asynchronous	Has a priority in data transfer process [71].

## 2.3 Process-Stacking Multiplexing Access Protocol

The Process-Stacking Multiplexing Access Protocol (PSMA) protocol is oriented to Wireless Personal Area Networks (WPAN), and it operates based on TDMA. In this case, the scheduling processes have different temporal durations. PSMA distributes the time of use of the transmission medium, according to the need of each node, creating a major difference when compared to the TDMA protocol, in which the time division is constant. The allocation of the time slot depends firstly on the need for a process to be executed, and second, on the size of the process. PSMA is a protocol that adapts to the use of EHD and provides support for energy control by extending the transmission or suspension times of each sensor node. The condition of self-sustainability for each node will depend on whether the energy stored is greater than or equal to the energy consumed. The energy consumed by the node depends directly on the different operating modes. Figure 2.2 shows the comparison between traditional TDMA and PSMA. TDMA traditionally assigns fixed time slots to each node without considering that the nodes may require different transmission times, it could be more, or less. Through PSMA, the transmission of information can be scheduled more frequently since the base station only allocates the time required by each node to send its packets, speeding up the availability of the channel for the other network nodes .

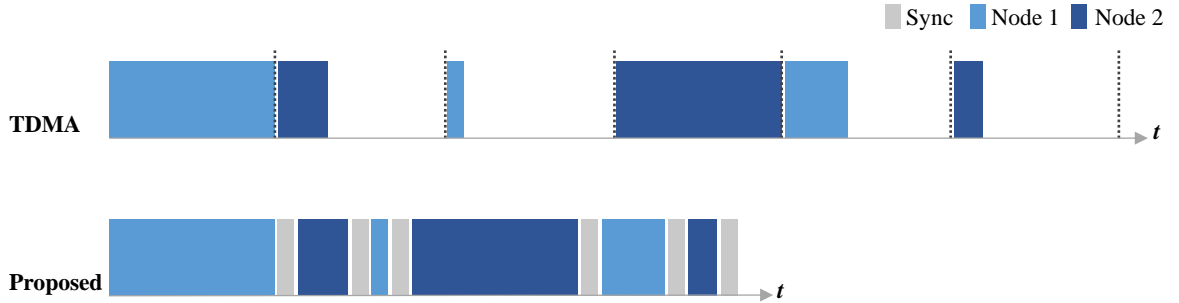


Figure 2.2: Comparison between TDMA and PSMA

PSMA operates in the ENO state and defines the sleep time as a function of the power consumed in each operation mode and is defined according to Equation 2.1 where  $(T^{\{sleep\}})$  is the sleep time,  $P^{\{t_x\}}$ ,  $P^{\{r_x\}}$ ,  $P^{\{idle\}}$  and  $P^{\{sleep\}}$  are the power consumed in the transmission, reception, idle and sleep mode of the sensor node in a specific time ( $T$ ). The power consumed when the sensor node harvests energy is  $P^{\{h\}}$ .

$$T^{\{sleep\}} = \frac{(P^{\{t_x\}} - P^{\{h\}}) \cdot T^{\{t_x\}} + (P^{\{r_x\}} - P^{\{h\}}) \cdot T^{\{r_x\}} + (P^{\{idle\}} - P^{\{h\}}) \cdot T^{\{idle\}}}{P^{\{h\}} - P^{\{sleep\}}}. \quad (2.1)$$

PSMA determines the node's activity and inactivity times through the operation of the antenna, making it possible to determine the energy consumption of each node in the different modes of operation. To calculate the energy consumption, PSMA uses Equations 2.2 and 2.3 where  $E_{battery}$  corresponds to the available energy in the battery in time  $k$ ,  $E_a$  is the available

energy in the battery in  $k - 1$ ,  $E_{harvesting}$  corresponds to the energy supplied by the EHD,  $E_{tx}$ ,  $E_{rx}$  and  $E_{SleepTime}$  are the energy consumption in the transmission, reception and sleep mode of the sensor node respectively.

$$E_{battery} = E_a + T(E_{harvesting} - E_{tx} - E_{rx}). \quad (2.2)$$

$$E_{battery} = E_a + T(E_{harvesting} - E_{SleepTime}). \quad (2.3)$$

In PSMA, the base station organizes the transmissions of the nodes using an internal memory that stores the start times of each transmitting process. These times are scheduled and transmitted immediately to the node that generated the process. The base station uses a global pointer that moves every time a process is scheduled. The relay master must be kept running at all times. When entering the network, a node sends to the access point, a broadcast containing the MAC address of the equipment and the size of the first process to be transmitted by the node. When the broadcast is received by the base station, it responds with a synchronization packet, which contains the MAC address of the relay master, and the transmission starts time for the first process sent by the node sensor. Once the synchronization packet is received by the sensor node, the connection to the WPAN can be established, and the transmission of packets begins, which are always answered by the base station with a synchronization packet to indicate the times in which they can transmit.

## 2.4 MAC Protocols and Battery Information

In the previous sections, it was stated that sensor nodes have been energized with ESDs, traditionally with batteries. It is known that batteries have a limited lifetime, therefore affecting the NL. With the introduction of EHD, this problem has been addressed by allowing sensor networks to extend their lifetime by operating in the ENO state. Regardless of the type of ESD used to power the network, it is necessary to understand its behavior and the information obtained from it. This aspect influences in the MAC protocol operation and network performance.

### 2.4.1 Battery Model Importance

The battery information is an important topic that has been studied for several years in WSN. They play a critical role in the network operation, as it has been established. The literature indicates that there are several proposed models that characterize the behavior of the battery. These battery models are used in the estimation of the remaining energy in the battery and the lifetime of the sensor nodes. Electrical, electrochemical or empirical models have been proposed to describe the behavior of the batteries [72]. The electric models represent the battery characteristics through an equivalent circuit. The Thévenin equivalent circuit is used in [73] to model a Li-ion battery. Another example is the one presented in [74]

where several equivalent circuits of a Li-ion battery are presented and evaluated. Electric models usually have a lower computational cost and are simpler than electrochemical models, although a great deal of effort must be made to parameterize them [75].

Electrochemical models characterize the battery behavior by considering its chemical properties and require accurate measurements and usually involve a considerable number of parameters [76]. An example of Electrochemical model is presented in [77], which includes the four basic equations that define the electrochemical behavior of lithium-ion batteries. Rakhmatov's model is another electrochemical model used to characterize the battery behavior [78] and is used to estimate the remaining energy capacity see Equation 2.4, where  $\sigma$  is the charge consumed by the node battery at time  $L_n$  (in terms of  $\Delta$ ).  $I_k$  is the constant current value during active state  $\delta_k$ , and  $k$  represents the state.  $I_n$  is the current at the time  $L_n$ ,  $\lambda = \xi_n(n)$  is the ratio between two functions that are dependent of the time and current. the state duration is defined by  $\delta_n$  and  $A$  is a function related to a current at any time  $L_n$  without the history information of the previous states.

$$\sigma(L_n) = \sum_{k=1}^n I_k \delta_k + \lambda \cdot \left( \sigma(L_{n-1}) - \sum_{k=1}^{n-1} I_k \delta_k \right) + 2 \cdot I_n \cdot A(L_n, L_{n-1} + \delta_k, L_{n-1}). \quad (2.4)$$

Empirical models have been used more frequently because of the flexibility they present and the simplification or reduction of parameters [24] [79]. An example of empirical model is presented in [24] and is used to characterize the battery behavior when discharging. This model uses the OCV curve to establish the measurement equation and is divided into three zone uses to define the open circuit voltage. Every zone has a parameter associated that characterize the behavior in this zone, see Figure 2.3.

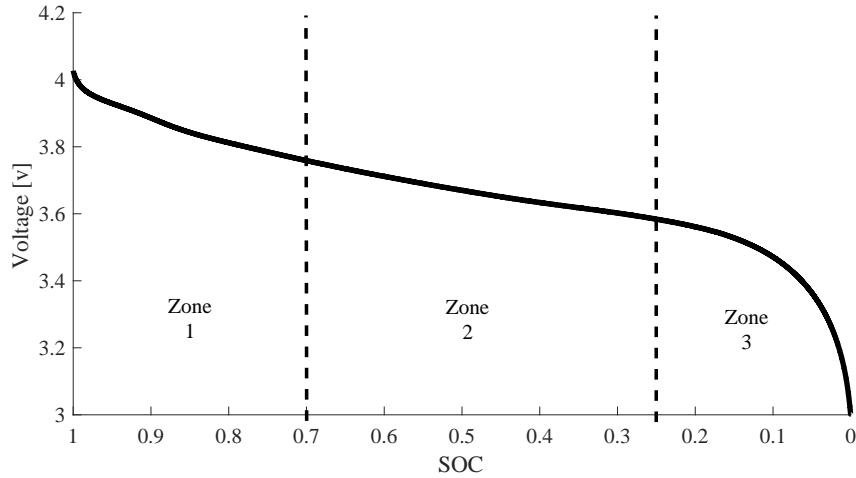


Figure 2.3: Discharge open circuit voltage

The phenomenological empirical model is defined according to (2.5), (2.6), and (2.7), where  $x_1(k)$  is an unknown parameter associated to internal impedance and it is estimated applying artificial evolution concept,  $x_2$  is the measure of SOC;  $i(k)$  and  $v(k)$  are the current

and voltage of the battery at time  $k$ ;  $\Delta t$  is the sample time;  $E_{crit}$  is the expected total energy delivered by the battery;  $\omega_1, \omega_2$  correspond to the process noises and  $\eta$  is the observation noise. The parameter  $v_0, v_l, \gamma, \alpha$  and  $\beta$  are model parameters and they are estimated off-line.  $v_0$  is the voltage when the battery is fully charged,  $v_l$  is the  $y$ -intercept of the extrapolation of the second zone and  $\gamma, \alpha, \beta$  are parameters associated to the three zones in which the OCV curve is divided [24].

**State transition equations:**

$$x_1(k+1) = x_1(k) + \omega_1(k) \quad (2.5)$$

$$x_2(k+1) = x_2(k) - v(k) \cdot i(k) \Delta t E_{crit}^{-1} + \omega_2(k) \quad (2.6)$$

**Measurement equation:**

$$v(k) = v_l + (v_o - v_l) e^{\gamma(x_2(k)-1)} + \alpha v_l (x_2(k) - 1) + (1 - \alpha) v_l (e^{-\beta} - e^{-\beta \sqrt{x_2(k)}}) - i(k) \cdot x_1 + n(k) \quad (2.7)$$

In [80], a second empirical model of battery-based voltage discharge curve is presented. To obtain the discharge voltage curves, a power consumption profile and Li-Po battery (3.7 V, 2000 mAh) are used. The power consumption profile considers three different modes: transmission, sleep, and parameters measurements. The resulting curves are modeled and approximated by a polynomial expression, which allows to determine the discharge of the battery for a duty cycle. The polynomial expression is defined in (2.8), where  $v(t)$  is the battery voltage at the time  $t$ .

$$v(t) = 9.559t^2 \cdot 10^{-10} - 4.275t \cdot 10^{-5} + 4.159. \quad (2.8)$$

A third example is an empirical model presented in [81], where the concept of C-rate is used. The C-rate is a measure of the rate at which a battery is charged or discharged concerning its nominal capacity. The model, defined in Equations 2.9 and 2.10 consists of a discrete state-space model that describes the process of battery degradation considering different discharge C-rate. In the model described, the  $x_1$  and  $x_2$  are related to the short and long-term contribution respectively. The coefficients  $a, b, c$  and  $d$  are parameters models.

$$\begin{cases} x_1(k+1) = e^b x_1(k) \\ x_2(k+1) = e^d x_2(k) \end{cases} \quad (2.9)$$

$$y(k) = ax_1(k) + cx_2(k) \quad (2.10)$$

Other examples of battery models are presented in [82] where three battery models are evaluated, the first one is the electrochemical model implemented in Battery Design Studio<sup>®</sup> software, where the characteristics of the CR2032 battery Lithium-Manganese Dioxide, 3 V,

and 230 mAh were used. The second model proposed is the Kinetic Battery Model (KiBaM), which describes the chemical processes of the battery through differential equations. Finally, the third model is a hybrid that combines the electrical circuit model and the KiBaM. In [83], the authors use the KiBaM to characterize the behavior of Ni-MH batteries. KiBaM describes two important aspects of the battery: rate capacity and recovery effect. A model that considers the battery-recovery effect is also proposed in [84]. It is important to understand the battery-recovery phenomenon because it can affect the battery lifetime, due to an increase of the available capacity.

## 2.4.2 Battery SOC and SOH Estimation

The battery state can be estimated through indicators such as the SOC and the SOH. These indicators provide information about the operating time, remaining energy and degradation of the battery of each node sensor [79] [85]. Since the SOC estimates the remaining energy of a battery at a given time instant, it is also possible to use this estimator to determine how much energy was used in an operation cycle. Furthermore, through the SOH, the number of battery operation cycles can be estimated. Due to the valuable information that can be extracted from these parameters, there is a growing interest to find new methods to estimate the SOC and SOH in WSN [86]. A recurring aspect in the models proposed for the estimation of the remaining energy and battery lifetime, is to consider the amount of energy consumed by the sensor node while it executes its different functions (transmission, reception, listening, sleep). In other words, the estimation of the remaining energy of the battery is made taking into account the DuC of the sensor node. An important point that should be disseminated, though it is fairly intuitive, is that it is not necessary for MAC protocols researchers to perform their own battery modeling research, but it is recommended to study the existing models and incorporate them in the study of the channel access and energy efficiency.

## 2.4.3 Methods to Estimate SOC

Over the years, various methods have been explored to estimate the SOC, such as the ampere-hour meter [87], open circuit voltage (OCV) measurement [88], electrochemical impedance spectroscopy (EIS) [89], and methods based on battery modeling [90, 91]. One Example is the SOC estimation model proposed in [92]. The authors use the sensitivity of OCV slope vs SOC to define the equation to estimate the SOC. First, the curve is divided into three zones and each zone is defined within an operating range associated to the SOC. The first zone, called  $H$ , defines the estimate of the SOC as shown in (2.11),

$$SOC_H = f^{-1}(V_{battery}) = a \cdot V_{battery} + b, \quad (2.11)$$

where  $V_{battery}$  is the voltage drop measured across battery terminals,  $a$  and  $b$  are the slope and the offset of the straight line that approximates the inverse function of the discharge profile in the region H. The second zone, called  $M$ , uses the ampere-hour method to estimate the SOC. The third zone, called  $L$ , is used as a threshold and the energy management system



should prevent the voltage from reaching this area (or these voltage levels) to prevent possible damage. The proposed model is defined according to (2.12). In this equation,  $SOC_H$  is the SOC estimation in region  $H$ ,  $Q_{task,i}$  is the charge provided by the battery for the execution in the  $i$ -th instant,  $N_{task,i}$  is the number of executions in region  $M$ , and  $Q_{battery}$  is the usable battery charge capacity.

$$SOC = SOC_H - \sum_i N_{task,i} \cdot \frac{Q_{task,i}}{Q_{battery}} \cdot 100. \quad (2.12)$$

Other example is LEB-MAC protocol that estimates the remaining energy in the battery using a fuzzy-logic controller. The controller defines the remaining energy of the battery in terms of low, medium, or high energy level. With this definition the membership function (trapezoidal and triangular) is obtained. In the case of LEB-MAC, the prediction of available energy that can be harvested from the environment is done using a solar EH and a first-order stationary Markovian model. The fuzzy-logic controller output is used to determine the DuC adjustment. In [93] the authors propose a method to estimate the SOC of the battery based on particle filtering. For this estimation, a state-space model is used. This model has input variables such as the current and voltage, where the voltage data is obtained from discharge tests performed on a Li-Ion coin cell LIR2032 using different current profiles. The proposed method allows accurate information about SOC, which improves the decision making, regarding the use that should be given to the battery. Another example is the use of the information obtained in the SOC estimation and prediction to determine the transmission current and therefore define guidelines that incorporate this indicator to assist the design of MAC algorithms [94]. In [95], the authors present the comparison of two different methods for SOC estimation, indicating that the selected method will depend on the sensor node characteristics and the type of application where the sensor nodes are used.

## Particle Filter

Particle filter is a Bayesian technique used for SOC estimation [96]. This Bayesian filtering tools require a prediction stage in which a state space model is used to perform the estimation, as well as an update stage where the observations are considered to obtain a more accurate estimate [97] [98]. Particle filter allow the estimation and prediction of the SOC online, being this the reason that has increased its use in applications of monitoring the state of the battery. Particle filter is usually used in the case of non-linear systems, because it has a better characterization of the uncertainty although it is sensitive to the initial conditions [24] [99]. The SOC based on PF has become more frequent because it provides relevant information for the operation of the application where it is implemented [100].

A particle filter is a sequential Monte Carlo method whose main idea is to represent the probability density function (pdf) through a set of random samples with associated weights [98] [101]. The particle filter considers to obtain samples from a target state probability distribution  $\pi_k(x_{0:k})$  and it is oriented to generate a set of  $N \gg 1$  particles with weights described by  $\left\{ w_k^{(i)}, x_{0:k}^{(i)} \right\}_{i=1 \dots N}$ ,  $w_k^{(i)} > 0, \forall k \geq 1$ , such that:

$$\sum_{i=1}^N w_k^{(i)} \phi_k(x_{0:k}^{(i)}) \xrightarrow{N \rightarrow \infty} \int \phi_k(x_{0:k}) \pi_k(x_{0:k}) dx_{0:k}, \quad (2.13)$$

where  $x_{0:k}^{(i)}$  for  $i = 1 \dots N$  is a set of support points,  $w_k^{(i)}$  is the associated weight,  $x_{0:k}$  corresponds to the state trajectory from time 0 to  $k$  and  $\phi_k$  is any integrable function  $\pi_k$ . The target distribution is chosen as  $\pi_k(x_{0:k}) = p(x_{0:k} | y_{1:k-1})$ , which is the a posteriori pdf state vector, conditioned by the noisy observations  $y_{1:k}$  [98]. As in any Bayesian process, the estimation process involves two main stages: prediction and update. In the prediction stage, the trajectories of the state vector are extended using a distribution of arbitrary importance  $q(\tilde{x}_{0:k} | x_{1:k-1})$ , where  $\tilde{x}_{0:k(i)} = (x_{0:k-1}, \tilde{x}_k)$ . In the update stage, the new weights  $w_k^{(i)}$  are evaluated by the measurement of probability using Equation 2.14, where  $\sum_{i=1}^N w_k^{(i)} = 1$  [24].

$$w_k^{(i)} \propto w_{k-1}^{(i)} \cdot \frac{p(y_k | \tilde{x}_{0:k}) \cdot p(\tilde{x}_k | x_{0:k-1})}{q(\tilde{x}_{0:k} | x_{0:k-1}, y_k)}. \quad (2.14)$$

The efficiency of this process is improved if the variance of the weights of the particles is minimized [98]. A common problem with the sequential importance sampling is the phenomenon of degeneration, where a few particles begin to have higher weights, while others appear with decreasing weights. The latter case requires a significant computational cost that is engaged in updating particles whose contribution to the a posteriori pdf is negligible. A technique to see if this phenomenon occurs, is to calculate the index:

$$N_{eff} = \frac{1}{\sum_{i=1}^N (w_k^i)^2}, \quad (2.15)$$

where  $w_k^i$  is the normalized particle weight.  $N_{eff}$  is a value between 0 and  $N$ , where the degeneration is considered to occur when the value  $N_{eff}$  is less than  $0.85N$  [102]. The sequence of instructions followed by the particle filter are described in the algorithm 1.

## Markov Chains

To predict the SOC of the battery is necessary to characterize the future usage profiles. One way to do it is through Markov chains. Using this technique the required current can be statistically characterized, and also different usage profiles can be obtained. To complete this task, the amount of states with their corresponding transition probability has to be determined. A method has been shown that demonstrated that belonging to a Markov chain can be defined using k-means, assuming a predetermined number of centroids [103]. It is expected that the greater the number of states, the better the chain represents a current profiles. However, as the number of states increases, the number of observations per state decreases, thus affecting the quality of the estimation of transition probabilities. To verify that the quality of the estimation two bounds are presented for the probability that the estimator  $\hat{p}_{i,j}$  differs from  $p_{i,j}$  in  $c$ , where  $p_{i,j}$  is the transition probabilities from state  $i$  to  $j$ .

---

**Algorithm 1** Generic Particle Filter

---

**Require:**  $[(x_{k-1}^i, \omega_{k-1}^i)_{i=1}^{N_s}, y_k]$ **Ensure:**  $[(x_k^i, \omega_k^i)]_{i=1}^{N_s}$ **for**  $i = 1 : N_s$  **do**    Draw  $x_k^i \sim q(x_k | x_{k-1}^i, y_k)$     Assign the particle a weight,  $\omega_k^i$ , according to 2.14**end for**Calculate total weight:  $t = \sum_{i=1}^{N_s} \omega_k^i$ **for**  $i = 1 : N_s$  **do**    Normalize:  $\omega_k^i = \frac{\omega_k^i}{t}$ **end for**Calculate  $\hat{N}_{eff}$  using 2.15**if**  $\hat{N}_{eff} < N_T$  **then**    Resample:  $[(x_k^i, \omega_k^i)]_{i=1}^{N_s} = RESAMPLE[(x_{k-1}^i, \omega_{k-1}^i)]_{i=1}^{N_s}$ **end if**

---

$$P\{|\hat{p}_{i,j} - p_{i,j}| > t\} \leq \frac{1}{4nt^2}. \quad (2.16)$$

$$P\{|\hat{p}_{i,j} - p_{i,j}| > t\} \leq 2exp(-2nt^2). \quad (2.17)$$

Where  $\hat{p}_{i,j}$  corresponds to the maximum likelihood estimator for  $p_{i,j}$  and it is defined as:

$$\hat{p}_{i,j} = \frac{n_{i,j}}{\sum_{j=1}^N n_{i,j}}. \quad (2.18)$$

Equations 2.16 and 2.17 represent the bounds for the probability that estimator  $p_{i,j}$  is different from its real value by a value greater than or equal to  $t$ . The maximum number of states for the Markov chain is determined by choosing a value of  $t \in (0, 1)$  with a scalar  $p^* \in (0, 1)$ , which corresponds to design parameters. These parameters are related by the inequality shown in Equation 2.19, where  $p^*$  represents the maximum probability that the user is willing to accept so that the estimator  $\hat{p}_{i,j}$  differs from its real value  $p_{i,j}$  within a higher value or equal to  $t$ .

$$P\{|\hat{p}_{i,j} - p_{i,j}| > t\} \leq p^*. \quad (2.19)$$

#### 2.4.4 Methods to Estimate SOH

The SOH, just like the SOC, have been recently incorporated as indicators to know the battery state in WSN. For example, in [104], the authors propose a stochastic model to describe

the degradation suffered by the battery. The model considers parameters like Depth of Discharge (DoD) or SOC to estimate the SOH. In addition, the model considers information extrapolated from the data-sheet manufacturer and from a realistic deterministic model proposed in the literature. It emphasizes optimization policies to maximize the battery lifetime considering the degradation suffered by the battery. Another case is presented in [105], which proposes a stochastic model that incorporates the aging of the battery as a metric to determine the performance of the network. SOH is defined as a function of the average SOC, the standard deviation of the SOC, and the effective number of cycles. The experimental tests guarantees that at a low rate of SOH degradation the battery life is prolonged, increasing the system reliability, although this incurs in higher delays, resulting in a trade-off between the network performance and the degradation of the battery.

The SOH estimation can be carried out through methods that account for the degradation suffered by the battery considering measurable parameters of the battery such as changes in internal impedance, temperature and discharge currents. The SOH is affected by the degradation suffered by the battery, in other words, the loss of capacity due to its use and age. A battery is considered degraded when the SOH is between 80 or 70% [106]. Some concepts related to the SOH are shown in Figure 2.4. There are different methods to estimate the degradation of a battery, one of them uses the Coulomb efficiency. It is defined as a measure of how much usable energy is expected to be delivered for the discharge in progress relative to the capacity exhibited during the previous cycle [86].

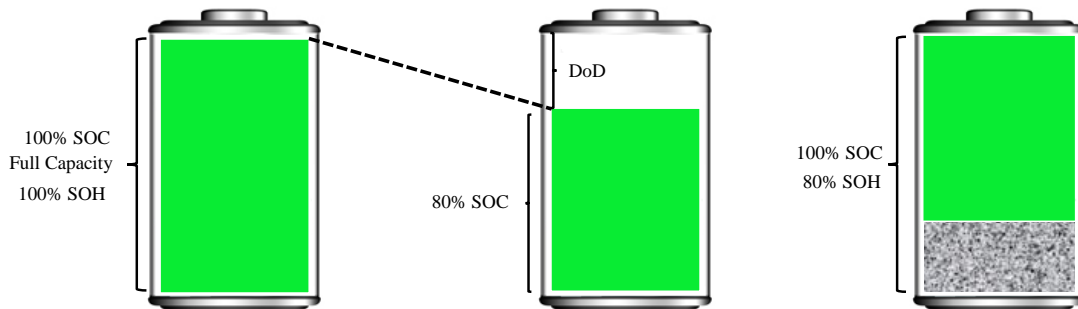


Figure 2.4: Concepts related to SOH

The Coulomb efficiency depends on different variables such as temperature, depth of discharges, the current intensity for both charge and discharge processes and others [86]. The concept of Coulombic efficiency is used to determine the percentage of degradation suffered by the battery in each cycle, grouping various effects and simplifying its estimation. The Coulombic efficiency is defined according to

$$\bar{\eta} = (\%Degradation)^{\frac{1}{\#cycles}} . \quad (2.20)$$

The determination of the Coulombic efficiency requires information supplied by the manufacturer such as the number of cycles and the percentage of degradation. For example,

Figure 2.5 shows the information from the datasheet of the LIR2032 battery. In this case, we have that for 500 operating cycles of the LIR2032 battery, a degradation percentage of 80% is reached.

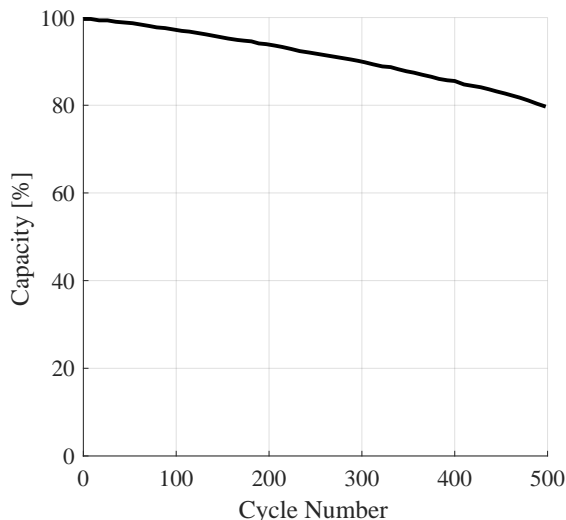


Figure 2.5: Datasheet LIR2032 Battery - Appendix A1

The information provided by the manufacturer does not allow to determine all the values of the Coulombic efficiency according to the SOC swing. Therefore the proposed methodology uses a combination of Similarity-Based Model (SBM) and K-nearest neighbors to determine all possible values. SOC swing is used to define the SOC range comprised between its initial and final value in a cycle. The swing range (SR) is the range where the SOC act [107]. This concept is important since you can have a SOC swing equal for different SR. Table 2.4 presents the values estimated by this methodology [86].

### Similarity-Based Model (SBM)

SBM is a non-parametric technique that estimate the output of a system through historical data and compare it with the actual and measured output [108]. It is frequently used in the detection of faults of various systems [109]. A system is described using 2.21, where  $x$  is the input of the system,  $y$  is the output, and  $f(\cdot)$  represents an unknown function.

$$y = f(x), \quad x \in \mathbb{R}^m, \quad y \in \mathbb{R}^p \quad (2.21)$$

The input and output values, obtained from the database, are separated in two different matrices. Equation 2.22a represents all the known inputs and Equation 2.22b is the

Table 2.4: Escalation factors for different degradation cases

SR	0.7	0.8	0.85
100-0	1.000000	1.00000000	1.00000000
100-25	1.000003	1.00000266	1.00000193
75-0	1.000024	1.00001860	1.00001354
100-50	0.999989	0.99999203	0.99999420
75-25	1.000019	1.00001521	1.00001108
50-0	1.000037	1.00002874	1.00002093
100-75	1.000027	1.00002146	1.00001563
75-50	1.000011	1.00000881	1.00000642
62.5-37.5	1.000008	1.00000620	1.00000451
50-25	1.000043	1.00003347	1.00002438
25-0	1.000054	1.00004184	1.00003047

corresponding output.

$$D_i = [x_1 \ x_2 \ \dots \ x_n] \in \mathbb{R}^{m \times n} \quad (2.22a)$$

$$D_o = [y_1 \ y_2 \ \dots \ y_n] \in \mathbb{R}^{p \times n} \quad (2.22b)$$

According to [108], in SBM for any given set of inputs  $x^*$ , the output  $y^*$  can be estimated through a linear combination of matrix  $D_o$  and a weighing vector denoted  $w$ . In other words, the estimated output  $\hat{y}^*$  is equal to the product between  $D_o$  and  $w$ , hence  $\hat{y}^* = D_o w$ . Equations 2.23 and 2.24 show how to calculate  $w$ .  $\Delta$  is the similarity operator.

$$\hat{w} = (D_i^T \Delta D_i)^{-1} (D_i^T \Delta x^*). \quad (2.23)$$

$$w = \frac{\hat{w}}{\mathbf{1}^T \cdot \hat{w}}. \quad (2.24)$$

As stated, the SOC and SOH are two indicators widely used to evaluate the battery state. It is necessary to explore methods capable of estimating both indicators in WSN. The SOC and the SOH have become more relevant with the addition of EHDs in WSNs because they deliver information about the amount of remaining energy and the degradation suffered by the battery [110]. This information is very useful for MAC protocols when defining the DuC of the sensor node. Hence, the DuC can adjust the activity periods of the sensor node

according to the available energy in the battery [110]. Remember that currently there are several models and methods to estimate the SOC and SOH. In literature, there are simplified models that characterize the behavior of the battery but under well defined restrictions. Also, there are more complex models that do not require definition of restrictions but involve many more parameters. Similarly, methods of estimation could be variable, for instance some of them can include recursive methods, fuzzy logic, or Bayesian inference. The selection of the method will depend exclusively on the type of application and the hardware characteristics of the sensor node.

# Chapter 3

## Energy Efficient MAC Protocol with Battery SOC and SOH Awareness

In this chapter, the characteristics and methodology used to design the energy efficient MAC protocol with battery SOC and SOH awareness are discussed. As previously mentioned, this protocol is oriented to WSN, therefore the minimization of energy consumption is one of its main characteristics. Based on this premise, the proposed protocol is based on PSMA, an energy efficient protocol, and combines several techniques that allow the reduction of energy consumption. Furthermore, the proposed protocol uses a synchronous scheme based on a TDMA variant to reduce collisions, one of the problems of WSN that increases energy consumption. In addition, the proposed protocol implements a DuC technique that minimizes energy consumption by placing sensor nodes in sleep mode for a dynamically varying time intervals. The proposed protocol improves the adjustment of the active and sleep times of the node considering the recharge times required by the EHD and the energy level in the battery. The proposed protocol incorporates information about the battery state through the SOC and SOH indicators to improve the decision-making process.

### 3.1 Access Control Management Design

The proposed protocol is used in a centralized type of WSN, and one of its main objectives is to extend the NL by minimizing energy consumption considering that the sensor node depends on the energy supplied by the battery. Therefore, by reducing the amount of energy available in the battery the node reduces its communication and sensing functions. This behavior is called dead node and in case a certain number of nodes have these characteristics, the network can be considered non-operational [111].

As mentioned, the proposed protocol uses TDMA and DuC. First, the use of the TDMA variant minimizes the risk of collision, which represents an energy saving by not having to retransmit the information. On the other hand, the use of DuC guarantees that the radio is only turned on when the node needs to transmit, which represents a reduction in energy



consumption. In other words, the nodes do not invest time listening to the channel, allowing the use of EHD to recharge the batteries of the *Sensor Nodes (SNs)*. This feature is extremely important because it extends the useful life of the *SNs*, and the implementation is performed in a platform that allows the design of the network according to the required characteristics of the application. Figure 3.1 shows the configuration of the network and the parameters implemented in it. The designed network consists of the main node, namely *Base Station (BS)*, and several *SNs*. The internal structure, of both devices, is established through processes that are composed of states.

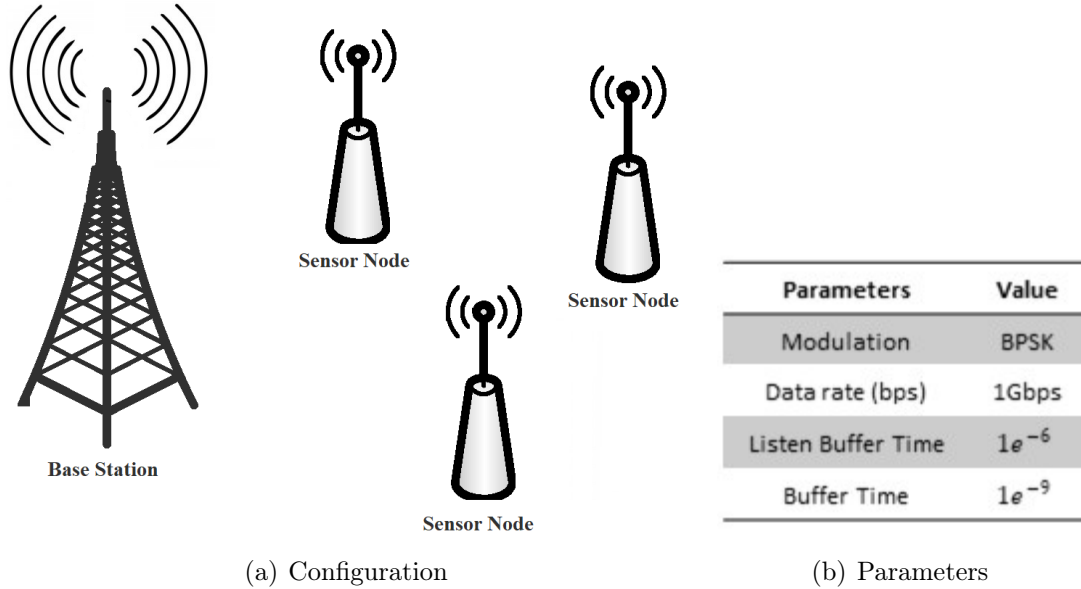


Figure 3.1: Network information

The proposed protocol, like PSMA, uses time division multiplexing with adjustable time slot depending on the size of the information that needs to be sent by each of the sensor nodes belonging to the network. To adjust the time slot of each node, the *BS* reads the field of the frame that indicates the size of information to be transmitted. As a result of this information, the *BS* is able to determine the time required by the node to transmit the information and it is capable to schedule the next active time of the node. The purpose of adjusting the time slot assigned to each sensor node is to make use of the channel more efficiently. Figure 3.2 shows the interaction between the *BS* and *SN* belonging to the network.

Another important characteristic of the proposed protocol is its ability to use the information about the available energy in the *SN* to adjust the transmission scheme. For this case, the *SN* calculates the amount of energy used in its different modes of operation and supplies this information to the *BS* so that it can make the corresponding adjustments. The energy availability in the *SN* is used by the *BS* to give transmission priority to them. An important difference between PSMA and the proposed protocol lies in the way of calculating the energy consumed by each *SN*.

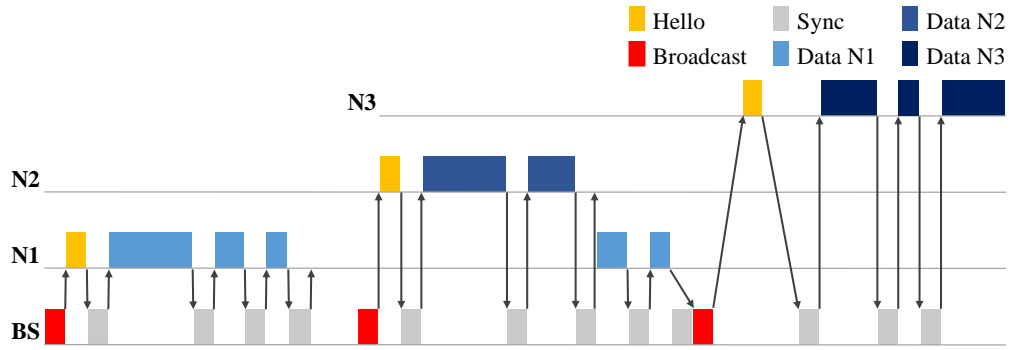


Figure 3.2: Base station and nodes interaction

### 3.1.1 Access Control Design

The *BS* is composed of three processes, two of which correspond to the transmission and reception antennas and the third is the main process called *Base Station (B\_S)*. Figure 3.3 shows the components that integrate the BS. *B\_S* process is responsible for the control management, and its internal structure has five states, see Figure 3.4, that allow the correct operation of the *BS*. The control functions are to compile the list of addresses where the order of transmission is indicated, as well as to determine the transmission time of each *SN*.

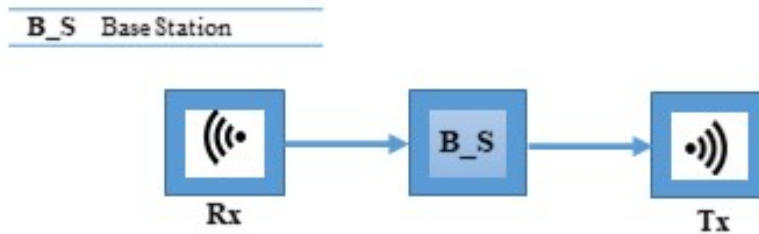


Figure 3.3: Base station processes

The *Start* state, for example, contains the initialization values of the variables used in this process. On the other hand, the *W\_H* state is responsible for creating the transmission schedule, updates the global pointer, and also performs functions that allow knowing the periods of energy collection if an EHD is used. The state *B\_T* is used to schedule the broadcasts, and the state *B* sends the broadcast. Finally, the state *E\_S* finalizes the process.

The proposed protocol executes specific functions at *BS* level. The protocol establishes minimum requirements that guarantees the correct operation of the protocol. In this case, the protocol must send the corresponding broadcast that will allow the integration of the different nodes to the transmission times schedule. The transmission schedule is generated from the information obtained from *Hello packet*, that is, the *BS* has knowledge about the reservation time that must be assigned to each node. Then, the *BS* updates the global pointer, ( $p[index]$  is defined according to 3.1), and sends the information to the *SN* indicating the times in which it must transmit.

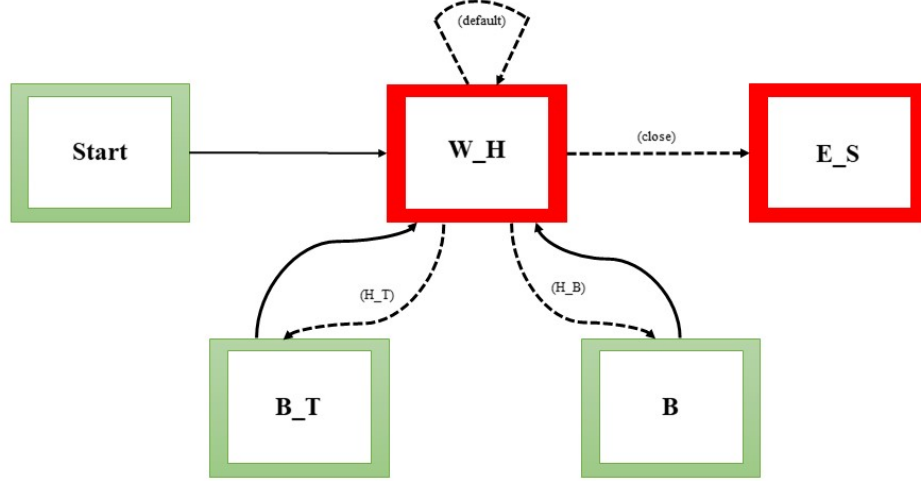


Figure 3.4: Base station states

$$p[index] = ap[index] + sleep_{time}[index] + t_{buffer} + t_{travel}. \quad (3.1)$$

In 3.1,  $ap[index]$  shows the individual pointer that is related to each  $SN$ , the  $sleep_{time}[index]$  is the sleep time,  $t_{travel}$  is the travel time, and  $t_{buffer}$  is a small time of buffer. The individual pointer is defined according to the previous value of  $p[index]$ , the travel time, the buffer time, and the time that indicates the time in which the sensor must transmit  $t_{reserve}$ , see Equation 3.2.

$$ap[index] = p[index] + t_{reserve} + t_{buffer} + t_{travel}. \quad (3.2)$$

The global pointer implements a function called *node schedule time* to verify that the global pointer does not schedule packets at times that have to be used by other nodes, this avoids packet collisions. The function verifies the list of active nodes; if it is the first node to be scheduled, the reservation time corresponds to the value contained in the global pointer variable. On the contrary, if there are several active nodes the function *node schedule time* checks the times assigned to each one of the  $SNs$  of the network and based on this information it establishes the minimum time for which the next sensor node will be scheduled. The structure of the function is shown in Appendix A - pseudocode 2.

### 3.1.2 Packet Management

In the  $SN$ , the protocol distinguishes the frames that contain control messages and those that contain the information for the transmission. Also, the protocol is responsible for managing the encapsulation of the information according to the established format and calculating the time required to transmit the frame. The proposed protocol interacts through three control messages and the frame that contains the information to be transmitted. The first control

message corresponds to the broadcast that is sent by the *BS* to scan the network and update the scheduled according to the nodes they wish to transmit. The second control message is the *Hello packet*, which is responsible for containing the information for transmission initiation by the node. The third message called *Sync* is responsible of confirming the correct receipt of the frame, see Figure 3.2.

The *SN* is composed of seven processes and two of which correspond to the transmission and reception antennas. The packet generator process (*P\_G*) is responsible for generating the information that will be transmitted and uses five variables (packet interval arrive, packet size, packet format, start time and stop time) that defines the form to generate the packets. For our proposal, the variable packet interval arrive takes two values. The first value corresponds to a constant value and the second corresponds to values generated with a Poisson distribution. The queue (*Q*) process is responsible for storing the packets until the node process authorizes the release of the packets and subsequent encasing in the encapsulating process (*E\_C*). Energy (*E*) and Node (*N*) processes are the most important because the energy process controls everything related to the availability of energy while the node process controls the information to be transmitted and the information received, see Figure 3.5.

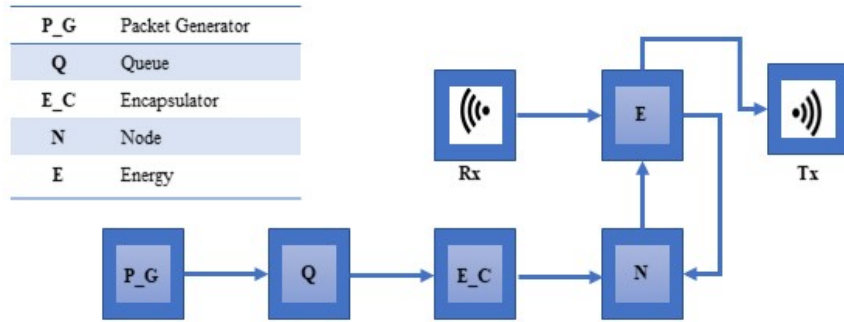


Figure 3.5: Sensor node processes

The node process is composed of nine states (see Figure 3.6), the *Start* state being the one that initializes the value of the variables that are used in this process, as well as determining the start of operation of each node belonging to the network. The *Turn-on* and *Queue* states are responsible for sending stored packets only when the node is powered on. The *Main* state distinguishes whether the information processed is from the node itself or if it is information sent by the BS. The *E\_P* state encapsulates the information to be transmitted to the *BS*, while the *B\_P* state obtains information sent by the *BS*. On the other hand, the *awake* state is used to inform the energy process (*E*) that the node is awake so that it can perform the calculations of energy consumption. The *Send* and *Close* states are used to send the frame and close the process respectively.

## 3.2 Packet to Frame Encapsulation

The frame format used by the proposed MAC protocol has five header fields and its structure is shown in Figure 3.7. The first field of the frame contains the source MAC address. The

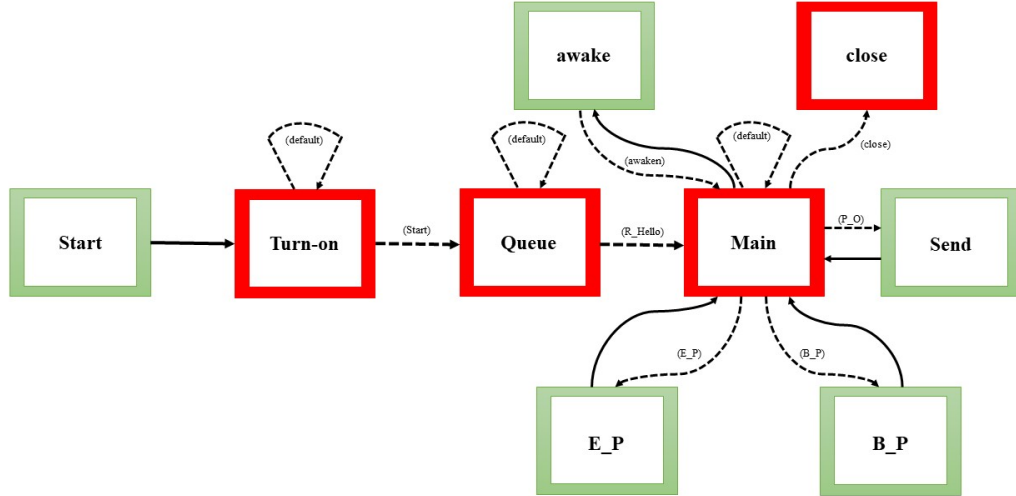


Figure 3.6: Node process state

second field provides the destination address. All MAC address are unique, i.e., no two nodes can have the same MAC address. The third field, called flags, contains the information that indicates which type of control message should be sent. The fourth field contains the time required to transmit, referred as the pointer. Finally, the fifth field contains information about the energy consumption of the battery of the  $SN$ .

Source (12 bits)	Destination (12 bits)	Flags (8 bits)	Pointer (16 bits)	Energy (16 bits)
Payload				

Figure 3.7: Frame format

The encapsulation of the data to be transmitted is done in the  $SN$ , and the  $Q$  and  $E_C$  processes play a fundamental role in this task, see Figure 3.6. The  $Q$  keeps the packets in order following a sequence of first in, first out (FIFO). As mentioned above, the  $Q$  process stores the packets to be transmitted until it receives the instruction to drop the packets that are encapsulated in the frame according to format. Once the data is encapsulated, the amount of time required to transmit the frame can be computed using the frame size and the transmission rate.

Figure 3.8 shows the internal structure of the  $Q$  process, where the  $S_H$  state counts the packets while the  $I_T$  state certifies the entry of a new packet. The  $Branch$  state is in charge of the flow of the operation of the process. Figure 3.9 illustrates the internal structure of the encapsulating process, where the  $fill$  state has the responsibility of placing the frame header and obtaining the size of the frame.

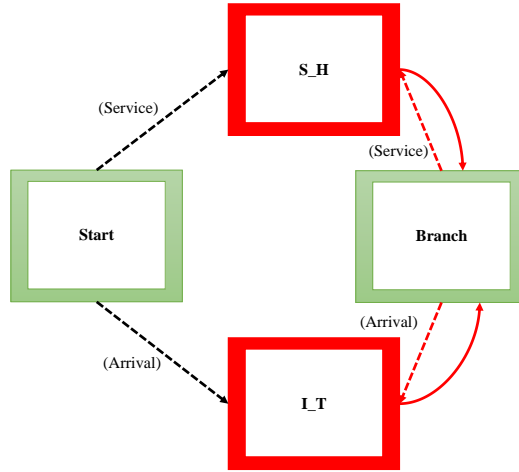


Figure 3.8: Queue internal States

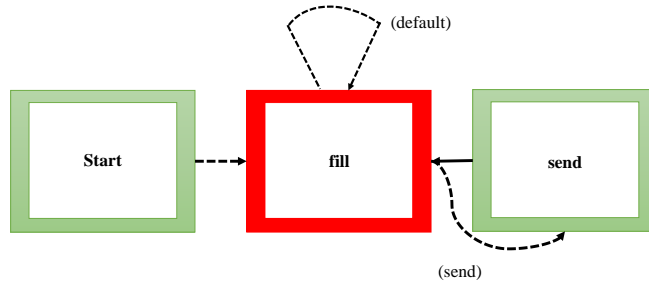


Figure 3.9: The internal structure of the encapsulation process

### 3.3 Collision Avoidance Mechanism

To minimize collisions that may occur in the network the proposed protocol is based on TDMA, which indicates that each node has a time allocated to transmit. The communication is initiated through the *BS*, which periodically sends a broadcast to determine if there are nodes that need to transmit. The broadcast sent by the *BS* is answered with a *Hello packet* by the nodes that need to transmit. Once the *BS* receives the *Hello packet* it responds with a *Sync packet*, that contains information about the time in which each node should initiate the transmission. This feature allows *SN* to make the changes between their various operating modes, thus contributing to lower energy consumption. Figure 3.2 also shows how the *BS* sends a broadcast each time period that allows the node that needs to transmit to make its request to be incorporated in the *BS* scheme. In the scheme it is observed that after each broadcast the *BS* receives a *Hello packet* from the node interested in transmitting. This *Hello packet* is answered with a *Sync packet* package that confirms the receipt of the previous packet and indicates the next transfer time. This sequence of messages between the *BS* and the *SN* allows the reduction of collisions by scheduling the times in which each node must transmit. To guarantee the reduction of collisions, the transmission time assigned to each node considers a buffer and travel time.

The sequence of messages described above that contributes to avoiding collisions fundamentally depends on the operation of the global pointer, which uses two verification processes to reduce the risk of scheduling a previously assigned time. The first process is related to the function *node schedule time* which was described in section 3.1.1, while the second process is related to the mechanism of scheduling the broadcasts, which also checks the times assigned to the nodes. This double verification contributes to improve the performance of the global pointer when assigning transmission times.

### 3.4 Energy Management

The *E* process is composed of three states, where the *Start* state defines the initialization variables of the process, specifically the currents required to the battery in each of the operating modes of the sensor node. The *Main* state contains all the instructions that distinguish the modes of operation of the node (Transmission, reception, listen, sleep), that is, the time and the current required to the battery is determined. The *Close* state closes the process. Figure 3.10 shows the structure of the Energy process.

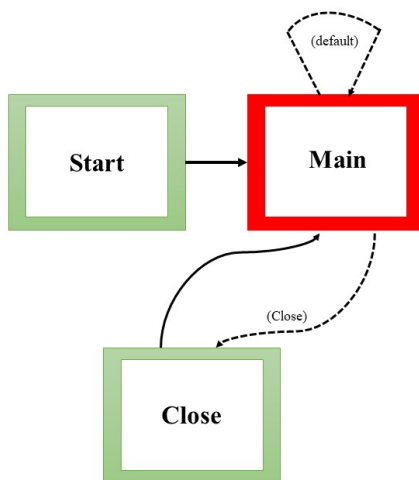


Figure 3.10: Energy process state

As mentioned above, an essential feature of the proposed protocol is use the provided battery information to improve decision making and adjust the sleep time of each *SN*. The required currents of the battery for the different modes of operation of the node is determined by the algorithm of the MAC protocol and this information is used to get an estimate of the amount of energy remaining in the *SN*. An improvement in the proposed protocol in comparison with other protocols is that considers the available energy in the battery as a restriction for the allocation of the time slot of each *SN*. For the proposed protocol, the current required by the battery in each operation mode of the node is considered. The energy process determines the remaining energy available in the battery. The *Main* state of the Energy process is programmed considering the following operation mode listen, sleep,

transmission and reception. The *Main* state has a block function that updates the battery information and put this information in the Energy field of the frame. The structure of the block function is shown in Appendix - pseudocode 3.

### 3.5 Metrics for the Time Sleep adjustment

In the previous section, the Equation 3.1 that defines the global pointer ( $p[index]$ ) includes the variable sleep time ( $T_{sleep}$ ) that adjust the rest times of each node according to their requirements and the network. The ( $T_{sleep}$ ) is defined based on the equation presented in 2.1, and in this section, the modifications of this equation are presented when considering the SOC and SOH estimations of the battery.

Based on Equation 2.1, the proposed protocol introduces metrics for the adjustment of the  $T_{sleep}$ , which are listed as follows:

- Determine the maximum  $T_{sleep}$  considering the minimum power that can be delivered by the EHD, in this case, a solar panel that can deliver energy between  $100\mu W$  to  $3 W$ .
- Determine the minimum  $T_{sleep}$  considering the following constraints:

$$T_{sleep} \geq T_{t_x} + T_{r_x} + T_{idle}$$

$$P_h > P_{sleep}$$

In [112], the authors define the  $T_{sleep}$  according to the equation described in 3.3 where the SOC indicator is introduced. This equation determines the  $T_{sleep}$  considering the percentage of remaining energy in the battery, where  $SOC_{max}$  is the maximum SOC and  $SOC_{min}$  is the minimum SOC or established threshold.

$$T_{sleep_{SOC}}(k) = T_{sleep} \cdot \frac{SOC_{max} - SOC(k)}{SOC_{max} - SOC_{min}}. \quad (3.3)$$

The Equation 3.3 requires some conditions that are defined as

$$SOC(k=0) = SOC_{max}$$

$$SOC_{min} < SOC_{max}$$

$$SOC_{min} \leq SOC(k) < SOC_{max}$$



Equation 2.1 supposes that the EHD continuously delivers energy, taking into account that if an EHD has periods in which it cannot supply enough energy, the sensor node will depend exclusively on the available amount of energy stored in the battery. In this case, the sleep periods would not be affected because the battery can not be charged until sunlight is available. For this particular case, the proposed adjustment is to modify the transmission currents of the sensor node to reduce energy consumption, an aspect discussed in section 4.2.3. Using the SOC prediction, it can be determined if the amount of energy present in the battery is sufficient to transmit all the information or if modify modification of the transmission current to increase the transmission time is required. Figure 3.11 shows the sequence followed by the algorithm to modify the transmission currents.

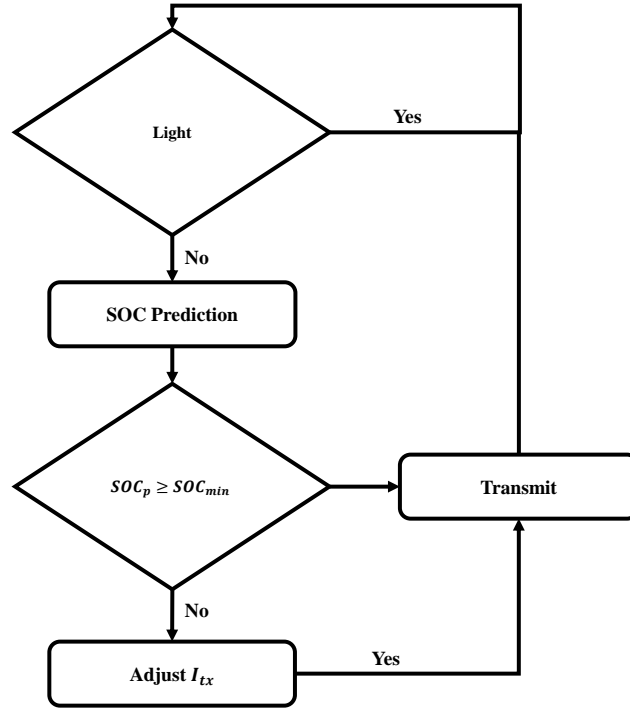


Figure 3.11: Algorithm to modify the transmission currents

The transmission current change allows to maintain the transmission rate but increasing the attenuation of the signal for the selected transceiver. Equation 3.4 allows us to determine the transmission time as a function of the SOC, while the equation of the  $T_{tx}$  is defined as a function of the extracted current from the battery for a period of time. Currents  $I_{tx}$ ,  $I_{rx}$ ,  $I_{idle}$  and  $I_{sleep}$  are constants.

$$T_{tx} = \frac{C_{nom} \cdot SOC(k) - (I_{rx} \cdot T_{rx} + I_{idle} \cdot T_{idle} + I_{sleep} \cdot T_{sleep})}{I_{tx}}. \quad (3.4)$$

In the other hand, with the inclusion of the SOH, Equation 3.3 is modified by introducing the Coulombic efficiency, according to 3.5, where  $F_{dp}$  is the degradation percentage. It is important to note that an established consideration is that this equation is executed and updated after each node has completed 100 cycles of operation.

$$T_{sleep_{SOH}} = T_{sleep} \cdot F_{dp} \cdot \frac{SOC_{max} - SOC(k)}{SOC_{max} - SOC_{min}}. \quad (3.5)$$

The SOC estimation and prediction is based on the particle filter. The selection of this algorithm is based on its ability to estimate the battery charge in real-time facilitating the acquisition of relevant information that may be considered by the MAC protocols for management control of the operating modes of the sensor. The implementation of the particle filter requires the use of a model that characterizes the behavior of the battery, see section 2.4.3. The SOH estimation is associated with the percentage of degradation suffered by the battery and the methodology described in section 2.4.4 is used to estimate the battery SOH.

# Chapter 4

## Battery-Status MAC Protocol Validation

This chapter presents the results obtained in the protocol performed and the battery SOC and SOH estimation algorithms. In the first section, the main characteristics of the protocol are validated, such as scheduling the transmission times, and minimizing collisions. In the second section, the results of the implementation of the battery SOC and SOH estimation algorithms are validated. In this section, we explain the experimental tests carried out to generate the data used in the execution of these algorithms. Finally, the third section presents the results obtained by incorporating the SOC and SOH indicators into the Equation 3.3 that defines the sleep time ( $T_{sleep}$ ). In this evaluation, the time windows assigned to the nodes are compared with the  $T_{sleep}$  in its original version and the sleep time containing both indicators ( $T_{sleep_{SOC}}, T_{sleep_{SOH}}$ ).

### 4.1 MAC Protocol Validation

After presenting the characteristics of the proposed protocol, the results of its operation are presented. The protocol operation is evaluated using various configurations and number of nodes in the network. The first scenario is composed of one **BS** and two **SNs**, it is shown in Figure 4.1(a). Figure 4.1(b) is an enlargement of Figure 4.1(a) where the entry of the second node is shown. A second scenario is designed to show the interaction of three **SNs** and the **BS**, see Figure 4.2. The third scenario considered consists in eight **SNs** and the **BS**, see Figure 4.3 and Figure 4.4. In both cases, the entry of the nodes is chosen randomly, which portrays the adaptability of the protocol. For all cases, it is shown how the protocol schedules the corresponding transmission times of each **SN** without a collision occurring when a new node is incorporated.

In the three cases described above, the input of each node is preceded by a **Hello** message in response to a **Broadcast** sent by the **BS**. The exchange of frames between the **BS** and the **SN** is corroborated as they are incorporated into the network. Figures 4.1(b) and 4.2(b) illustrate the interaction of control messages between **BS** and the **SN**. In Figure 4.1(b), the **Broadcasts** are identified with red rectangles, while the green rectangles refer to the **Sync** messages sent by the **BS**. The information transmitted by the **SN** is represented using cyan

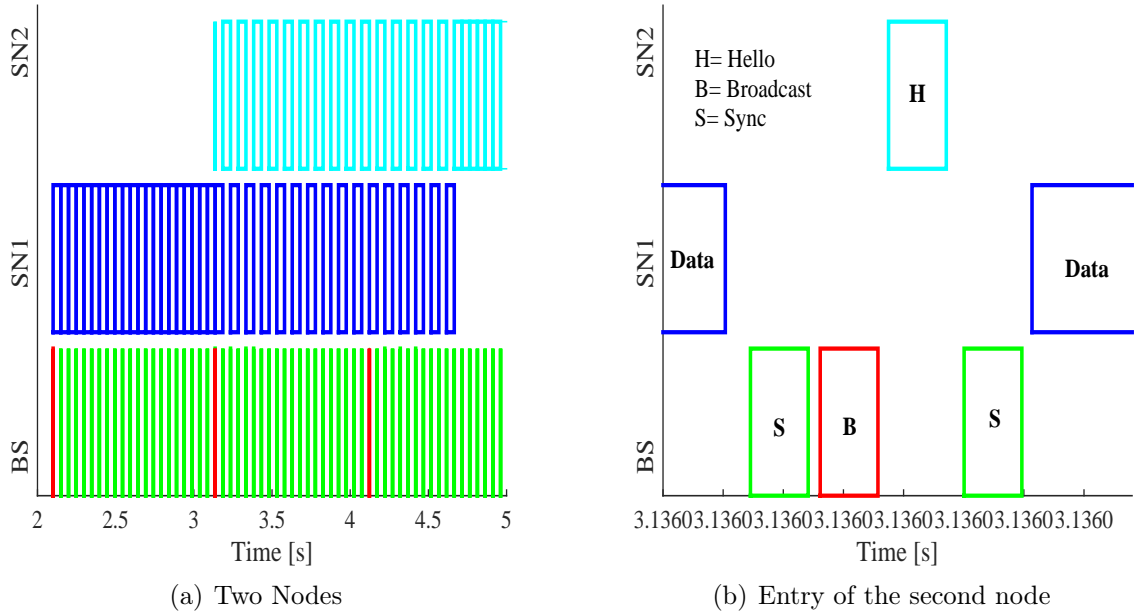


Figure 4.1: Interaction between  $BS$  and two  $SNs$

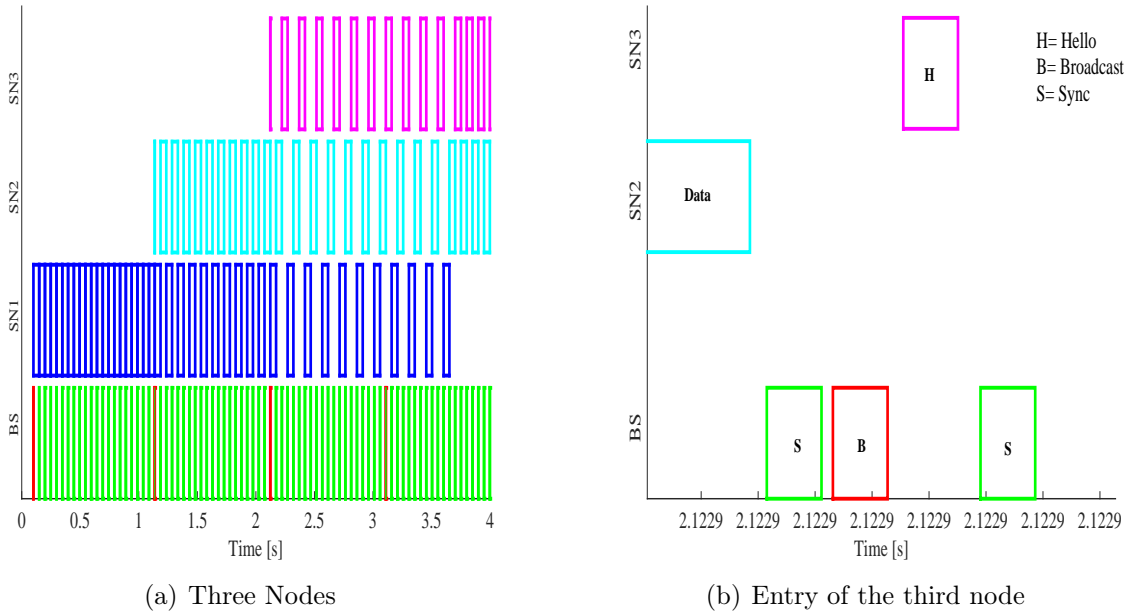


Figure 4.2: Interaction between  $BS$  and three  $SNs$

and blue. In Figure 4.2(b), the input of the third node is shown after the  $BS$  has sent a broadcast. The  $BS$  periodically sends a **Broadcast** to identify if there are new nodes that need to transmit. Figure 4.2(b) illustrates how the **Broadcast** is scheduled between two **Sync** messages, allowing a third node to respond with a **Hello** and it can be recorded in the scheduling scheme.

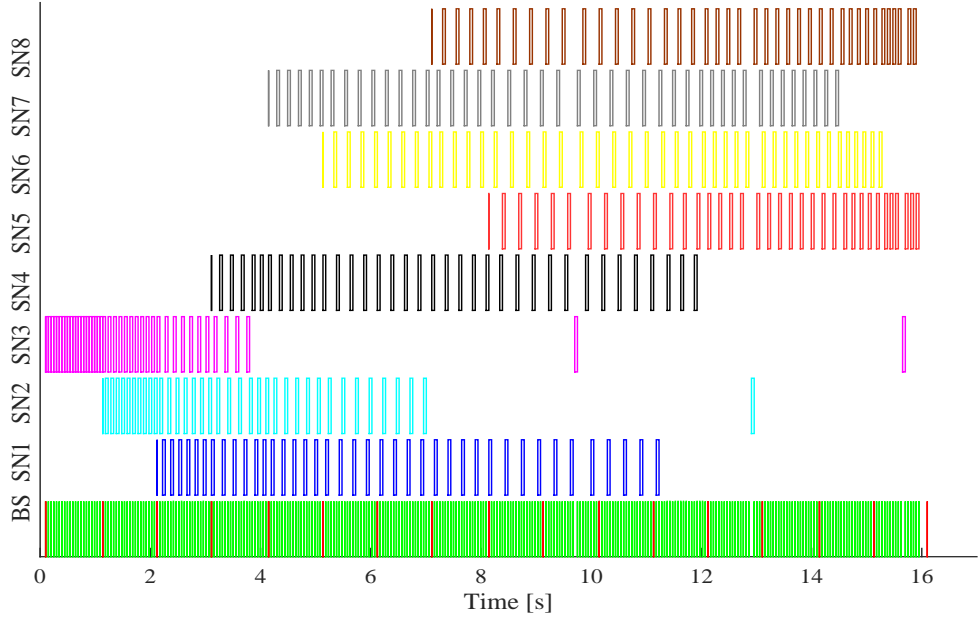


Figure 4.3: Interaction between *BS* and eight *SNs*

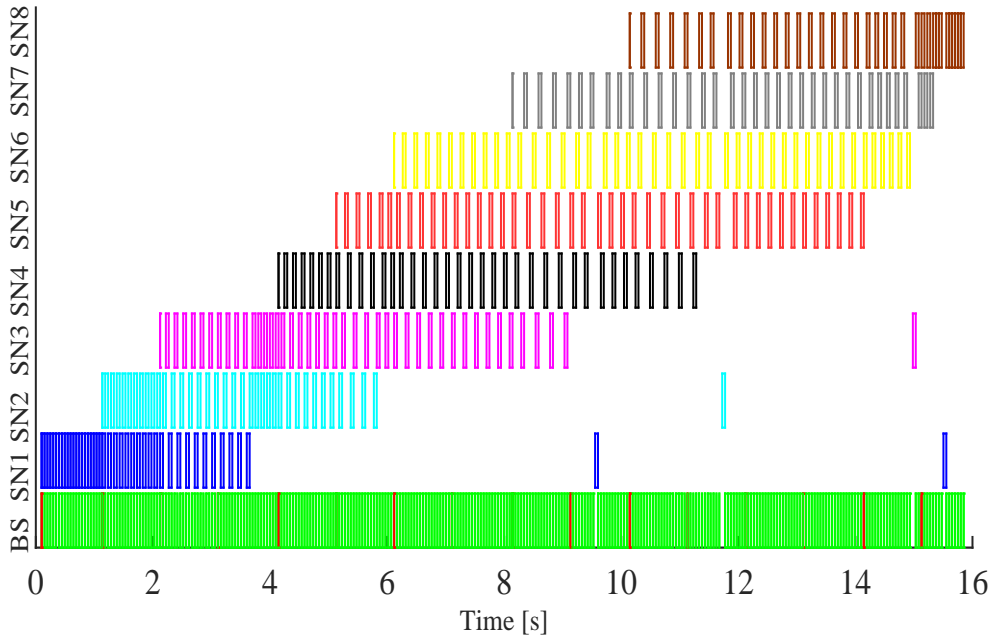


Figure 4.4: Interaction between *BS* and eight *SNs* using a different schedule

For the scenario shown in Figure 4.5, the first packet of *SN6* is scheduled immediately after the *BS* complies with the sequence of nodes already scheduled. The entry of *SN6*, identified with the yellow color, is observed after the *Broadcast* was sent, see Figure 4.5(b). In this case, *SN4* is represented with the color black, *SN1* is identified with the blue color, *SN2* is represented with the color cyan, and the *SN7* is identified with the color gray. When

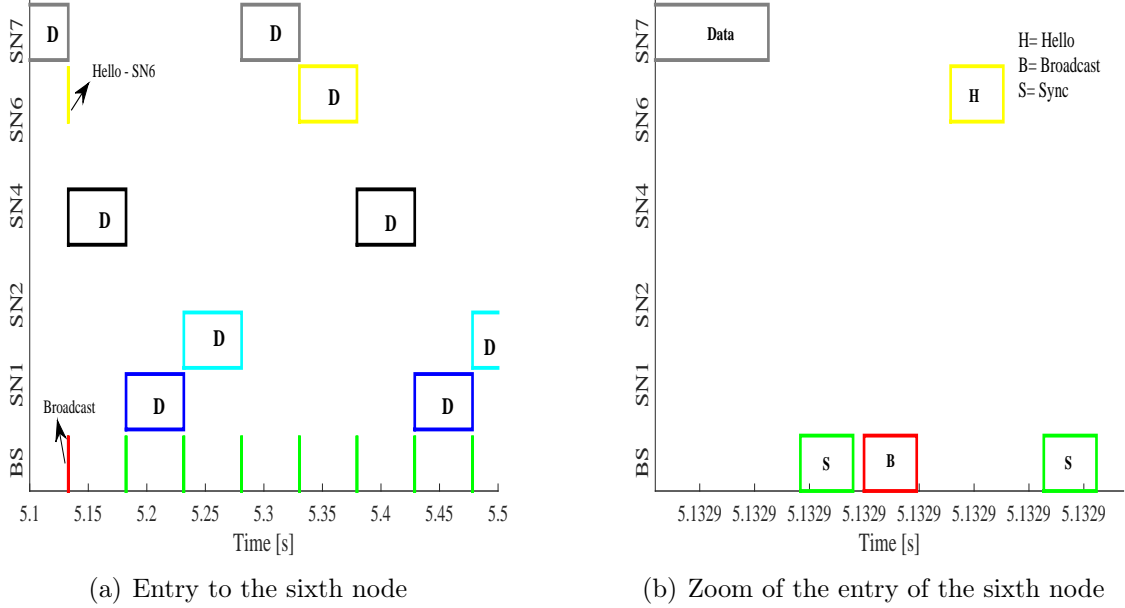


Figure 4.5: Example of node scheduling

analyzing Figures 4.1(b), 4.2(b) and 4.5, the correct operation of the global pointer is verified, a variable responsible for establishing transmission programming and, defined in Equation 3.1.

In every transmission system, there is the probability of packets colliding and our network configuration is not exempt of this problem, see Figure 4.6. The packet collision causes *SN5* to not be scheduled. This situation is seen in Figure 4.6(b), where the *Hello* sent by *SN5* collides with the *Hello* sent by *SN3*. This caused the *BS* to not receive the *Hello* sent by *SN5*. To avoid this situation, the proposed protocol uses the mechanism discussed in Section 3.3. The operation of the protocol using the collision mechanism is observed in Figure 4.3 and Figure 4.4.

One of the main characteristics of the proposed protocol is its ability to dynamically adjust the transmission time window assigned to each sensor node. Figure 4.7 illustrates this ability where the frames vary between 256 bits to 1024 bits. The assigned values are for demonstration purposes to evaluate the behavior of the protocol. It is emphasized that the time windows are determined through  $t_{reserve}$ . This feature distinguishes our protocol from the traditional TDMA, where the time windows are fixed. The adjustment made by the proposed protocol makes it possible to take advantage of the transmission channel more efficiently by only allocating the time required by each node and giving the opportunity for other sensor nodes to be integrated into the network and for it to transmit.

Another important characteristic of the proposed protocol is its ability to determine the remaining capacity in the battery through the *E* process. Figure 4.8 shows how the amount of energy is remaining in the sensor node's battery and it is updated according to the activities carried out. The proposed protocol has the characteristic of working in the ENO

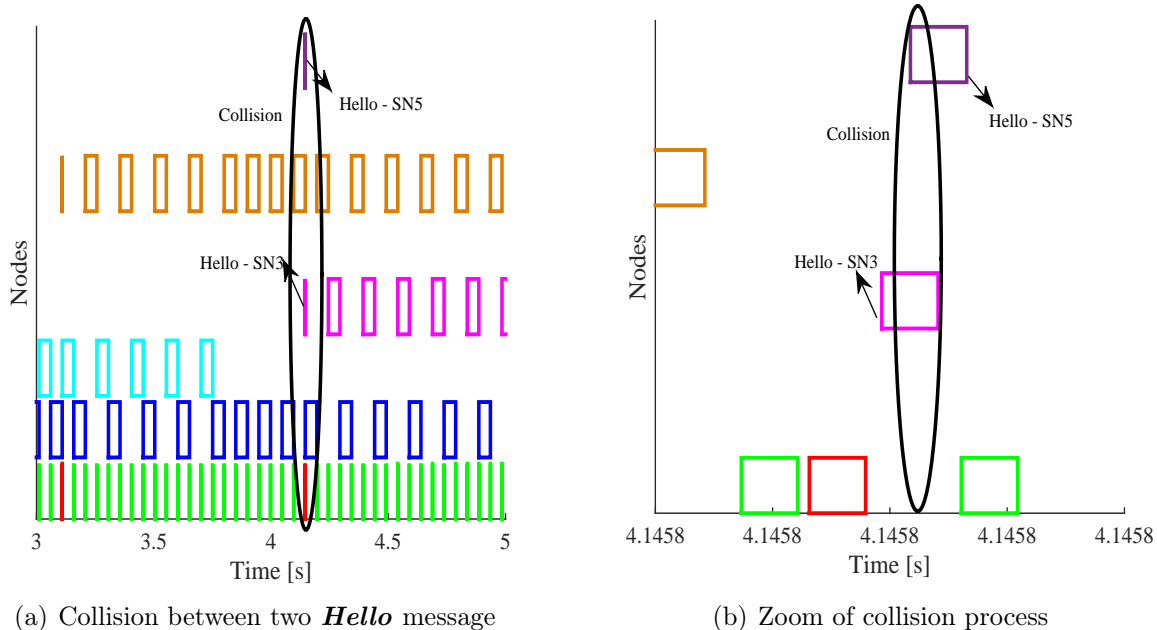


Figure 4.6: Collision Examples

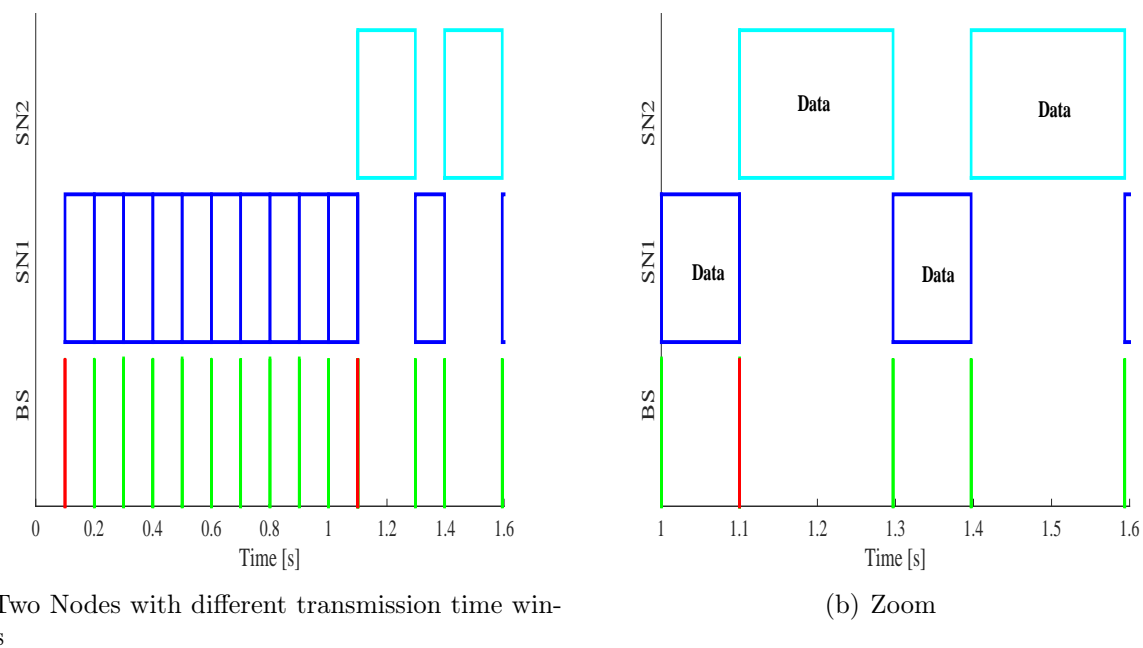


Figure 4.7: Different transmission time window assigned to each sensor node

state guaranteeing the self-sustainability of the nodes when using EHD. In Figure 4.8, this characteristic is reflected upon reaching 44% of the nominal capacity of the battery. This threshold is set to keep the battery within a safe range of operation.

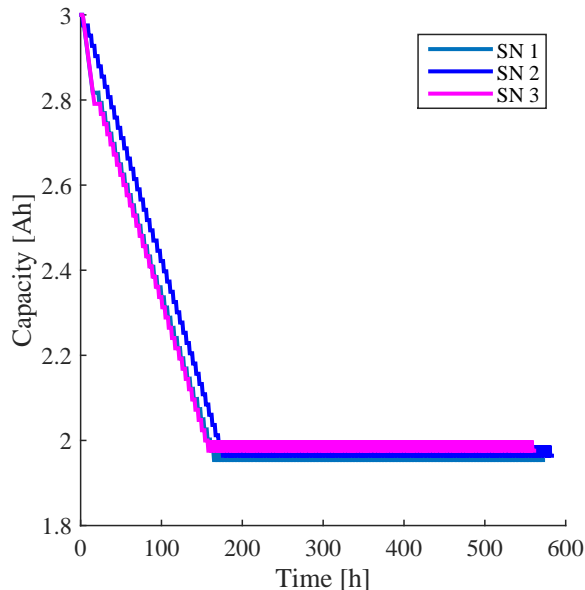


Figure 4.8: Battery remaining capacity

## 4.2 SOC and SOH Estimation Validation

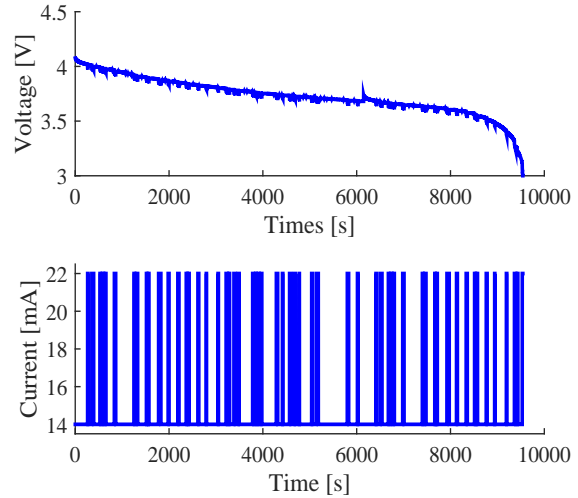
The methodology used to estimate the SOH and SOC is validated to guarantee that both indicators are used in the adjustment of the  $T_{sleep}$ . It is necessary to generate the database that will allow executing the SOC and SOH estimation algorithms explained in section 2.4 to validate the methodology. The data used was obtained by discharging a LIR2032 Li-ion battery (see Appendix - Datasheet A1) at constant ambient temperature using a B&K Precision 8500 Programmable DC Electronic Loads. The discharge process requires a current consumption profile, which indicates the amount of energy demanded by the sensor node at specific scheduled instances. The current profile used to discharge the battery is a combination of two current values, each of them describes two different operating modes: transmission mode (22 mA) and reception mode (14 mA) [93]. For our case study, the transmission and reception operation modes are selected since they are the modes that present higher energy consumption. Therefore, the characterization of the battery behavior depends on these modes. The current profile was obtained using the characteristics of the CC2500 transceiver, which has been designed for low-power wireless networks [113]. Table 4.9(a) shows relevant characteristics of this transceiver, including the currents used for different operating modes of the sensor node. The current and voltage values obtained from the discharge process are used to determine the parameters offline and to estimate the SOC by making adjustments to the particle filter-based algorithm. Figure 4.9(b) shows the voltage obtained during the discharge process with its corresponding current profile.

In addition, two usage profiles are generated to be used in the SOC prediction. This usage profiles are presented to evaluate the discharge time of the battery under different current profiles. The first profile is an aggressive type, meaning that the sensor node is constantly transmitting. The second profile is conservative, where the sensor node presents periods in



Operating Mode	Currents
Transmission	22 mA (0dBm output power)
Transmission	22 mA (0dBm output power)
Transmission	22 mA (0dBm output power)
Reception	14 mA
Idle	1,5 mA
Sleep	900 nA

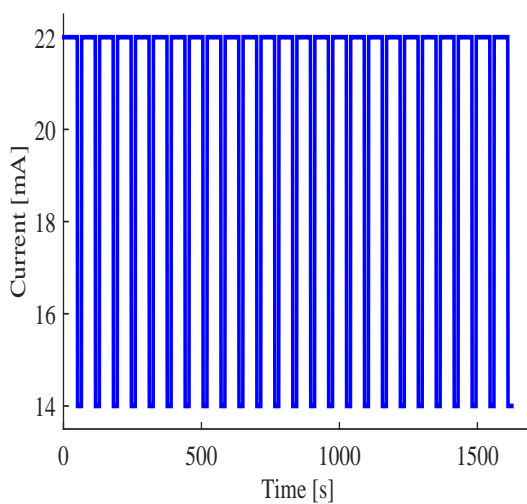
(a) CC2500 currents features [113]



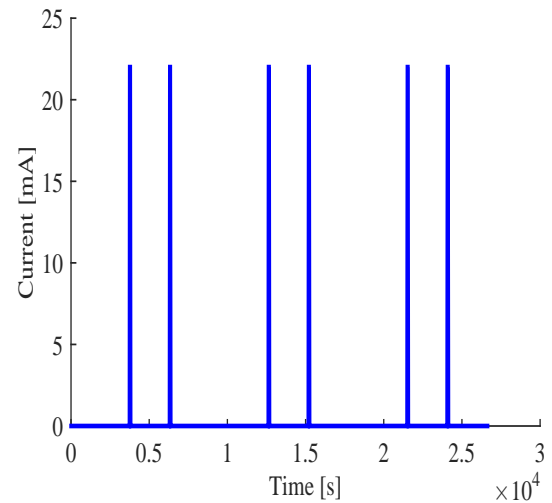
(b) Current and voltage discharge

Figure 4.9: Data used

which no activity is used to evaluate their impact on the discharge process. Both profiles use a random generated sequence that has electrical currents alternating between a transmission mode and reception mode, see Figures 4.10(a) and 4.10(b) [94].



(a) Aggressive profile



(b) Conservative profile

Figure 4.10: Usage profile

The model described in (2.5), (2.6), and (2.7) is simplified to eliminate the area where the OCV curve has an abrupt voltage drop. Removing this area ensures that the battery remains within its safety levels [95]. In this case, the OCV curve is defined between  $3.6 \leq V \leq 4.2$ , where 4.2 V is the maximum battery voltage. The measurement Equation 2.7 is simplified, and it is defined according to 4.1.

$$v(k) = v_l + (v_o - v_l)e^{\gamma[x_2(k)-1]} + \alpha v_l[x_2(k) - 1] - i(k)x_1 + n(k) \quad (4.1)$$

## 4.2.1 SOC Estimation

The data shown in Figure 4.9(b) is used to determine the parameter model presented in 2.7. These parameters are calculated offline using the Curve Fitting Tool from Matlab® and shown in Table 4.1. The noises associated with the model were calculated through the covariance matrix between the experimental and adjusted data, in addition of making empirical adjustments according to the particle filter performance. In addition, the filter parameters consist of 40 particles and 25 realizations according to the terms of [114].

Table 4.1: Currents characteristics - CC2500

Battery	$v_0$	$v_l$	$\alpha$	$\beta$	$\gamma$	$E_{crit}$
LIR2032	4.087	3.894	0.08023	16.87	9.95	534

With the model parameters defined in Table 4.1 and using the particle filter algorithm shown in pseudocode 1, the SOC can be estimated using a simulation time of 9542 seconds, which corresponds to the time it takes the battery to discharge until to the cutting point (3 V). Figures 4.11(a) and 4.11(b) show the voltage and SOC estimation based on particle filter using the data presented in 4.9(b).

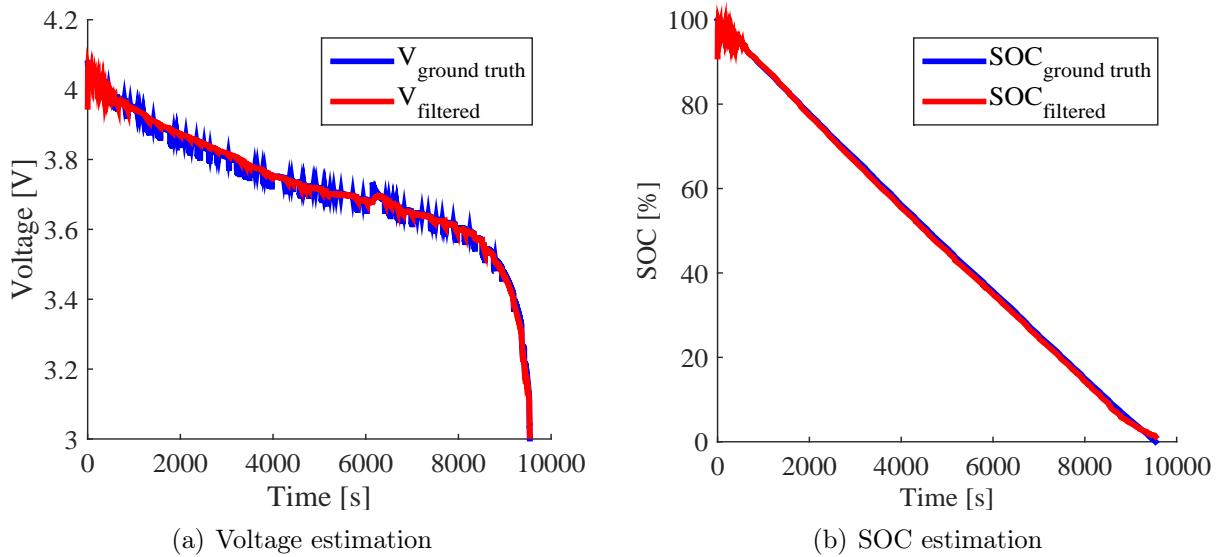


Figure 4.11: Voltage and SOC estimation

## 4.2.2 Performance of Methodology based on Particle Filter

The SOC estimation based on particle filter is validated through the comparison with the method proposed in [29]. The root-mean square error (RMSE) and the processing time to obtain the estimation are used to quantify the performance of both methodologies. For our case study, the methodology based on particle filter is namely  $M_1$  while the methodology presented in [29] is called  $M_2$ . The methodology  $M_2$  defines the voltage as a function of time using a polynomial expression according to 4.2. The amount of energy consumed in an operating cycle ( $E_{cycle}$ ) is define by 4.3, where  $P_{(t_x)}$  and  $P_{(r_x)}$  are the powers associated with the transmission and reception mode of the sensor node, respectively, and  $V(t)$  is the voltage measured in the corresponding time intervals.

$$V(t) = 4.446e^{-9}t^2 - 8.517e^{-9}t + 4.023. \quad (4.2)$$

$$E_{cycle} = \int_{t_0}^{t_1} \frac{P_{t_x}}{V(t)} dt + \int_{t_1}^{t_2} \frac{P_{r_x}}{V(t)} dt. \quad (4.3)$$

To estimate the SOC in  $M_2$ , it is necessary to determine the amount of energy consumed in an operating cycle. An operating cycle is defined when the current starts with the value of 14 mA switches to a current of 22 mA and returns to the initial value of 14 mA, see Figure 4.12.

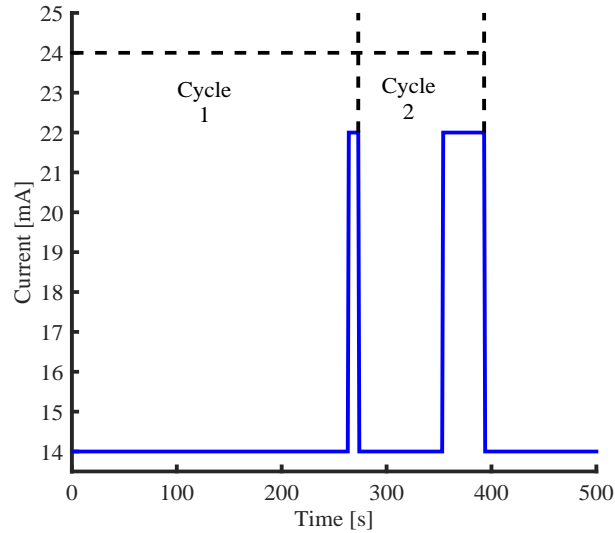


Figure 4.12: Definition of operation cycle

Both methodologies use the restriction  $V_{oc} \geq 3.65V$  because within this range, the battery is prevented from entering the abrupt zone of voltage drop while maintaining the safety level of the battery. The first results obtained correspond to the voltage and SOC estimation of the battery using both methodologies, see Figure 4.13(a) and Figure 4.13(b). In both figures, it is observed that the estimation in  $M_1$  achieves a better estimation of the voltage and SOC than  $M_2$ .

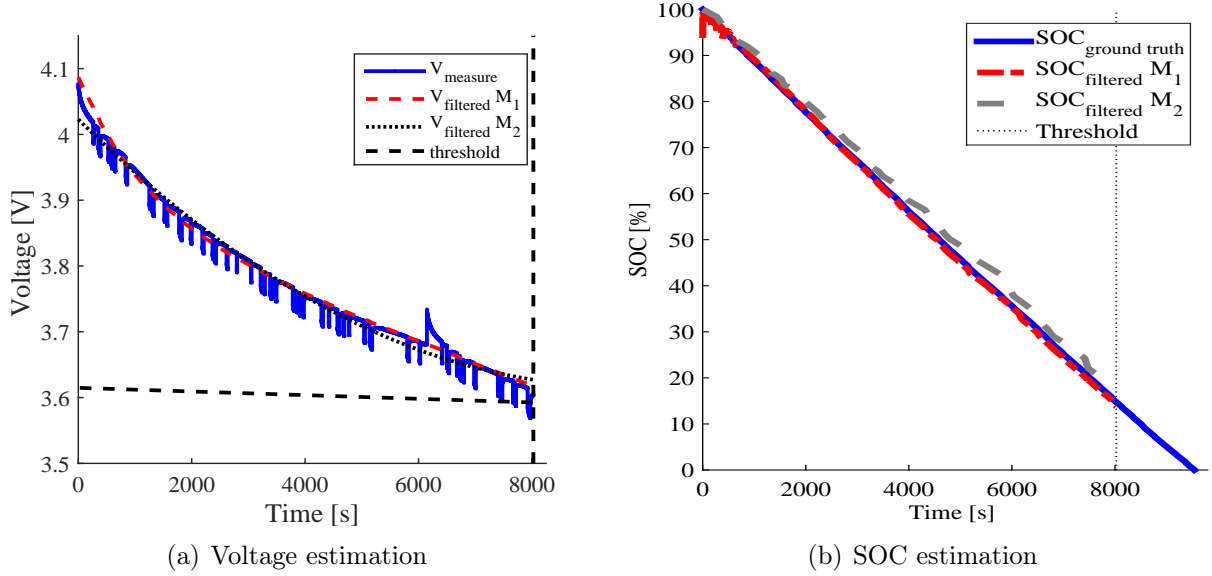


Figure 4.13: Voltage and SOC estimation

Figure 4.14 shows the RMSE and the processing time histogram obtained for 500 iterations of each methodology ( $M_1$ ,  $M_2$ ). When  $M_1$  is compared to  $M_2$ , it can be clearly noted that  $M_2$  has a faster processing time, see Figure 4.14 part (a) and (b). Regarding the accuracy,  $M_1$  presents a better performance than  $M_2$ . In most cases,  $M_1$  has RMSE lower than the value of 0.0153 presented by  $M_2$ . In Figure 4.14 part (c) is shown the histogram for the RMSE of  $M_1$ . Furthermore, after this 500 iterations of each methodology, results for  $M_1$  shows a mean value for the RMSE of 0.0086 and a standard deviation of 0.0045, while  $M_2$  shows the same RMSE. Note that the RMSE of  $M_2$  does not change and the variations in the processing time are minimal. In other words, the accuracy obtained is better when  $M_1$  are used even though the processing time remains approximately 7 times greater than the obtained with  $M_2$ .

The methodologies  $M_1$  and  $M_2$  are studied to observe their behavior when changing the battery usage profile. A Markov chain method is used to evaluate the battery usage profile change. In this case, two different current profiles are generated, see Figures 4.10(a) and 4.10(b). To create the two-state Markov chain, the methodology proposed in [103] and the current levels mentioned in Figure 4.9(b) are used. Also, the corresponding transition matrix ( $M_T$ ) is estimated through the maximum likelihood estimator [103], and it is defined as follows:

$$M_T = \begin{pmatrix} 0.9933 & 0.0320 \\ 0.0067 & 0.9680 \end{pmatrix} \quad (4.4)$$

The adaptability of both methods is studied by changing the usage profile. In this case,  $M_2$  has the same RMSE that the case before, while  $M_1$ , shows a mean value of the RMSE of 0.0099 and a standard deviation of 0.0056. Figure 4.15 shows the RMSE and the processing time histogram obtained when executing the algorithms with the current profiles obtained with the Markov chain method. Analyzing the RMSE obtained for each of the cases, it is

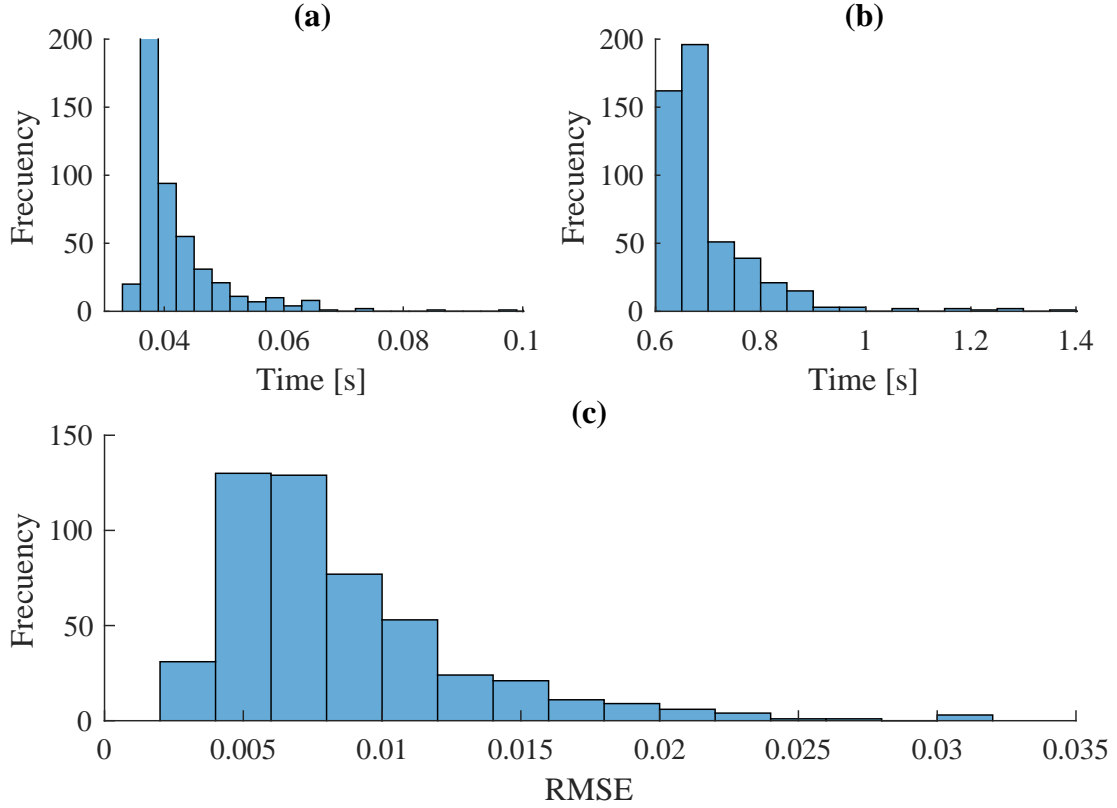


Figure 4.14: RMSE and processing time histogram

confirmed that  $M_2$ , cannot adjust to the changes in the current profile because the equation that defines the voltage is a function of time, so the model depends on the discharge current used. On the other hand, method  $M_1$  has the capability to adapt the future operation of the battery independently from the past.

From the results show in Figure 4.14 and Figure 4.15, several considerations can be made for the design of the MAC protocols. The selection of the SOC estimation method will depend on the type of application where the MAC protocol is used and the processing capacity of the network sensor nodes. For example, if the MAC protocol implemented in the WSN involves a large computational overhead, it is possible to opt for a lower processing SOC estimation algorithm like  $M_2$  considering the error margin. On the other hand, if the computational overhead contained in the sensor node is lower, it is possible to implement, within the MAC protocol, an algorithm for SOC estimation, for instance,  $M_1$ . A higher accuracy on the SOC estimation results in a better assessment of the amount of energy available in the battery.

### 4.2.3 SOC Prediction

SOC prediction is used to know the effect of using different transmission currents on the percentage of energy stored in the battery. In this case, the usage profiles presented in Figures 4.10(a) and 4.10(b) are used. These two profiles are generated in the same way for the

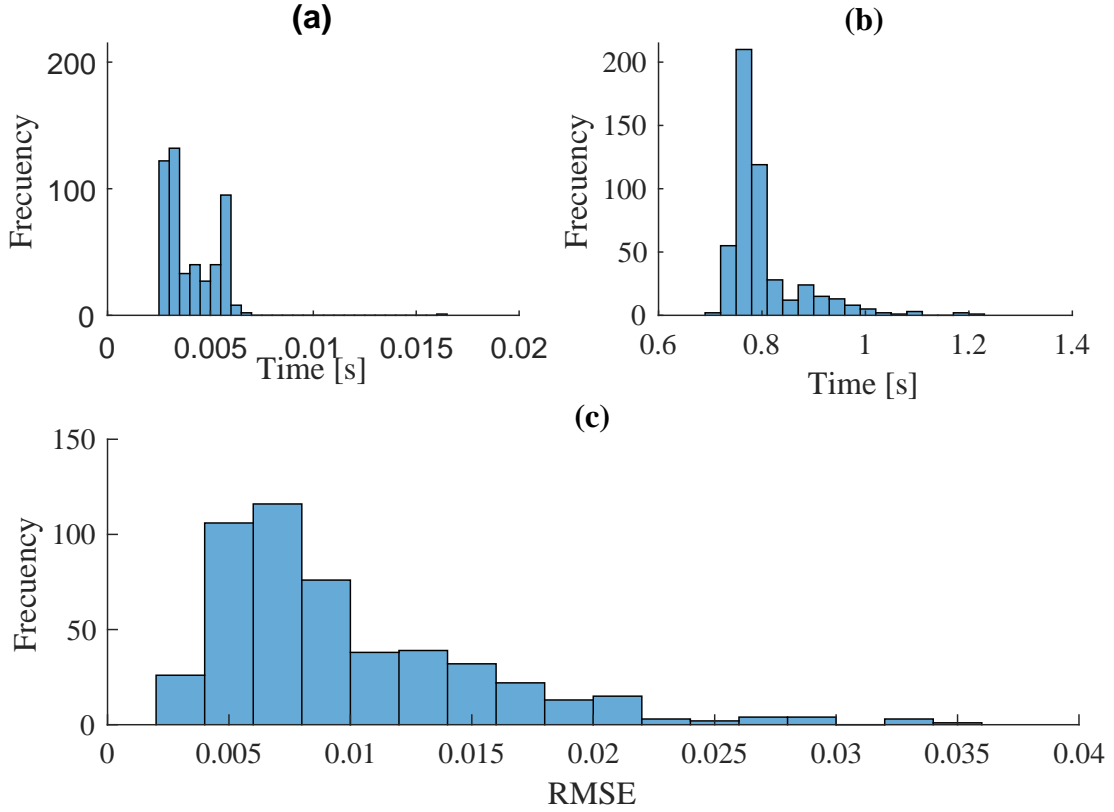


Figure 4.15: RMSE and processing time histogram

currents of  $11\text{ mA}$ , and  $15\text{ mA}$ , with the purpose of obtaining information about the discharge process of different currents. These currents are used for the CC2500 transceiver to transmit information with different power, see Figure 4.9(a). Additionally, the SOC prediction starts when its value reaches a threshold of approximately 80%. This condition is established through a random number generator. SOC prediction is used to design guidelines in MAC protocols design to adjust the DuC and select the best transmission current according to the requirements of the application.

The effect of employing various transmission currents is shown in Figure 4.16(a) and 4.16(b). In the first scenario, see Figure 4.16(a), the sensor node is continuously transmitting, without resting times. In this case, it can be seen that when the transmission current decreases, the transmission time increases by  $1/3$ . Under the second scenario, the sensor node includes resting times, which conserves energy, emulating a more realistic approach. Figure 4.16(b) shows that the SOC does not decay rapidly but remains constant for an instant of time, which coincides with the periods of inactivity of the sensor node. Under this scenario, the typical behavior of the OCV curve of the battery can be observed more clearly, having a 30% drop at the beginning and then entering the linear area defined by the  $0.25 \leq SOC \leq 0.70$ . This second scenario attempts to establish a guideline on how the sensor node should operate at night when it depends exclusively on the energy available in the battery.

Through the analysis of the results obtained in Figures 4.16(a) and 4.16(b), it is advisable

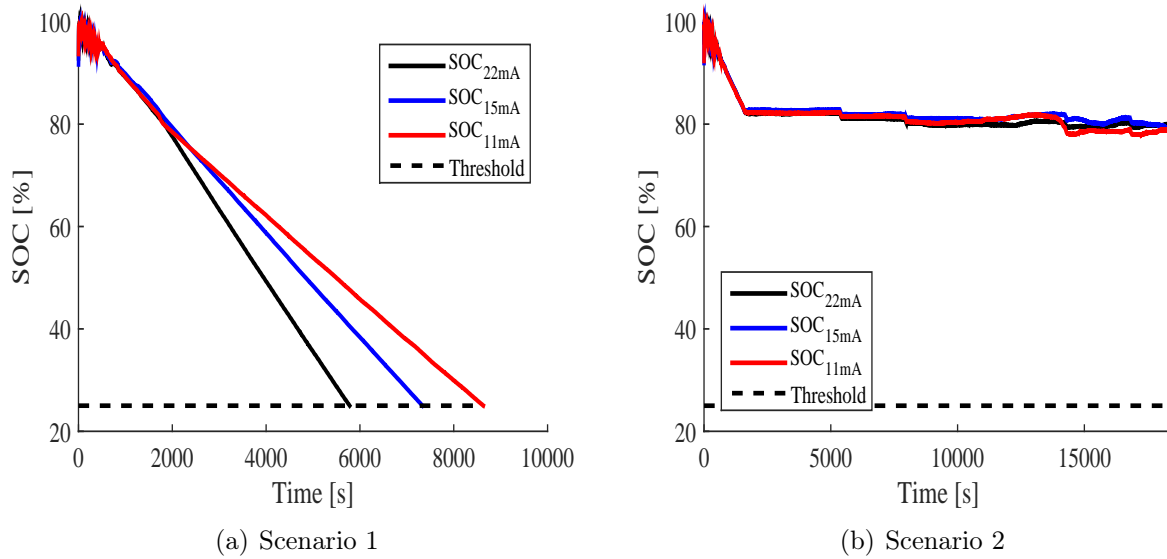


Figure 4.16: SOC prediction

to transmit to the minimum current allowed by the transceiver for aggressive profiles, while for profiles, such as the one in Figure 4.10(b), operating current ranges can be established. An example with different operating currents (11 mA, 15 mA, and 22 mA) according to the SOC of the battery is proposed and is shown in Figure 4.17. For the first transmission part, the current of 22 mA is used until 76% of the SOC of the battery is reached. After this point the transmission to a current of 15 mA or a 11 mA. In this case, we are using the current of 11 mA we goal the threshold with 4% more of energy that we use the current of 15 mA.

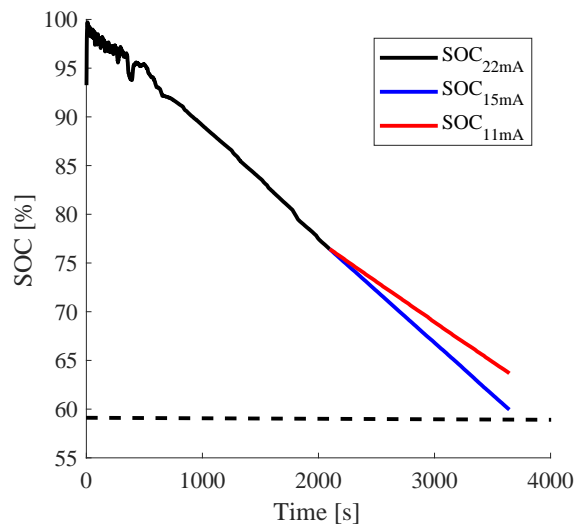


Figure 4.17: SOC percentage using different currents

## 4.2.4 SOH Estimation

Using the Coulomb efficiency methods the degradation suffered by the battery is obtained. For our case study, a cycle will be defined by the time period when the SOC starts at 100%, and the battery is discharged up to a SOC of 75%. The algorithm was executed 25 times to simulate several operating cycles of the sensor nodes. Figure 4.18 shows the histogram for the total working time of the sensor node required to complete an operating cycle when transmitting at 22 mA. Analyzing the histogram, it is observed that on average an operation cycle takes between 5 to 6 hours of operation. The sequence of instructions followed by the algorithm to determine the number of cycles is shown in Figure 4.19. The accounting of the number of cycles is of utmost importance in the calculation of the battery degradation.

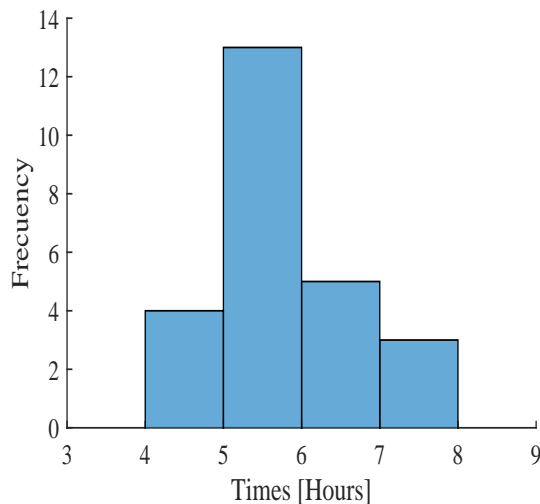


Figure 4.18: Battery information

The percentage of degradation suffered by the battery was obtained considering the number of the operating cycles simulated before and the information from the datasheet of the LIR2032 battery, see 2.5. With this information and using the Equation 2.20, we calculated  $\eta_k = 0.9995538$ . From this value and using the methodology proposed in [86] the Coulombic efficiency is determined using a SR (100 – 75%), being this  $\eta_k = 0.9995752629$ . Through the Coulombic efficiency, it is determined that after 25 operating cycles the capacity of the battery has degraded in 0.0017%. The methodology proposed in [86] allows the determination of an approximate percentage of degradation suffered by the battery, but it does not manage to distinguish when discharging the battery with currents other than 22 mA. Although an important issue to consider is that during the same amount of simulated time, the total cycles reached by the 11 mA profile was 23, meaning that the battery degraded less as expected. Furthermore, we can be aware of the maximum degradation that the battery can suffer, since using the current of 22 mA is transmitting at maximum power, which would be the worst case scenario regarding energy efficiency of the sensor node.



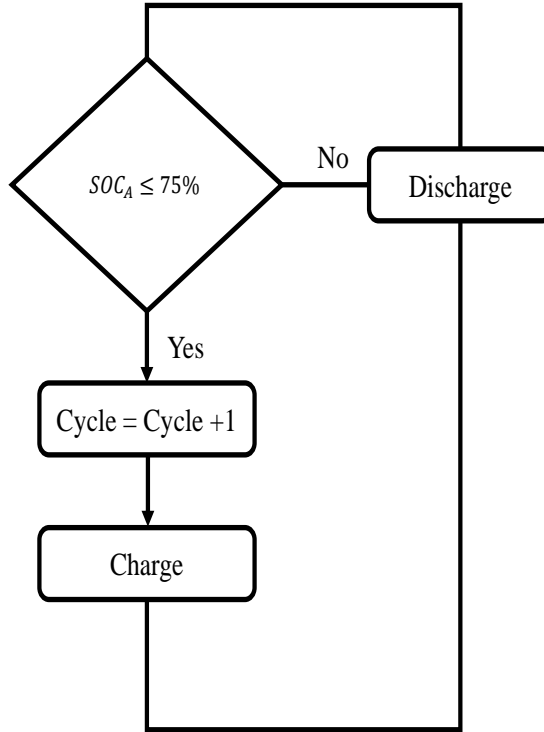


Figure 4.19: Algorithm to determine a cycle operation

### 4.3 Time Sleep adjustment

The verification of the adjustment of the  $T_{sleep}$  is done in two steps. In the first step, the metrics described in section 3.5 are validated, and in the second step, the SOC and SOH indicators are incorporated.

#### 4.3.1 Time Sleep Validation

The  $T_{sleep}$  given by 2.1 is used as a reference. The metrics are validated using two cases. In the first case, it is assumed that the node is constantly transmitting for two hours, i.e., 7200 s. Therefore, the expression in 2.1 is simplified because the sensor node does not spend time in other operation mode, so  $T_{rx}$  and  $T_{idle}$  are equal to 0. For the second case implemented, it is assumed that the node worked in the operating modes transmission, reception and idle, so the expression presented in 2.1 is used completely. For this second case, it is assumed that the transmission time is 1000 s corresponding to a single transmission period since the sensor node only spends a period of time in each operating mode. Using the information about the EHD, the maximum and minimum  $T_{sleep}$  are obtained and are shown in Table 4.2.

Table 4.2: Maximum and Minimum  $T_{sleep}$

Case	Parameter	Min	Max
1	$T_{sleep}$	7142	1764000
2	$T_{sleep}$	1638	355125

Using the  $T_{sleep}$  maximum and minimum values, the existing relationship between the duration of the  $T_{sleep}$  and the energy delivered by the EHD can be found and it is shown in 4.20. This relationship allows us to know the maximum sleep windows that the sensor node can have during the day when taking into account the variations in energy generation that EHD according to the availability of sunlight.

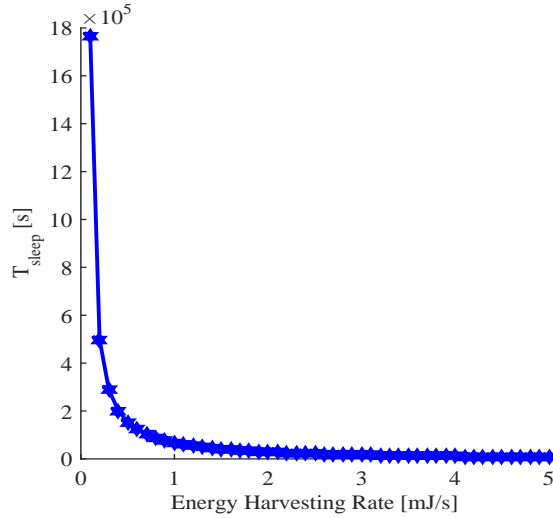


Figure 4.20: Relationship between  $T_{sleep}$  and energy harvesting rate

With the information of the maximum sleep window, the sensor node is able to make decisions about reducing or increasing the sleep time to prioritize the information transmission or the recharge of the battery. For example, during certain hours of the day when the EHD generates the highest amount of energy, the sensor node requires at least 7142 s to recharge the battery 100% according to the data of the first case. Under these parameters, the node can decide to charge the battery up to 80% and reduce the minimum  $T_{sleep}$  to a time of 5714 s allowing the node to be available to transmit half an hour before the established.

Figure 4.21 illustrates the relation between  $T_{sleep}$  and  $T_{tx}$  and it was obtained using 3.4. It is observed that the transmission time decreases when the sleep periods increases. This behavior reaffirms the aforementioned example whereby reducing the sleep period the node is available to transmit in advance what contributes to decrease the latency. With the determination of the adjustment interval of  $T_{sleep}$  the proposed protocol can make a trade-off between the required  $T_{sleep}$  and the network parameters (throughput, latency) required by the application. Other example, in the first case described, using a harvesting power of  $100\mu W$ , it is possible to reduce the  $T_{sleep}$  so that there is an increase factor of 3% for throughput.

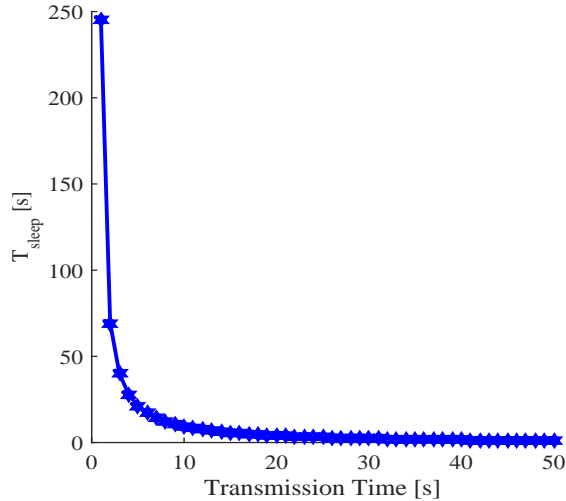


Figure 4.21: Relationship between  $T_{sleep}$  and  $T_{t_x}$

### 4.3.2 Adjustment of the sleeping time considering the SOC estimation

Using 3.3 and the SOC estimation the following results were obtained and are shown in Figure 4.22. This diagram shows the effect of considering the SOC on the duration of the sleep time. In the case shown,  $SOC_{max}$  is 100% and the  $SOC(k)$  is estimated until the condition of  $SOC_{min} = 0.25$ . In Figure 4.22 the sleeping time of the sensor node considering the SOC is reduced by approximately 40% compared to the traditional  $T_{sleep}$  described in 2.1. The adjustment achieved in the sleep time is meaningful, which allows the node to spend less time trying to recharge the battery when it is not required, guaranteeing that it can transmit more frequently.

SOC estimation and prediction are used in 3.4 to maximize transmission time. For our case study, the transmission currents of the CC2500 are used, see Table I. Figure 4.23 shows the effect of combining different transmission currents. The case shows in Figure 4.23, the node transmits using a current of 22 mA until reaching the value of  $SOC = 75\%$ . After this point, the effect of transmitting to a current of 15 mA or a current of 11 mA is evaluated. Switching to a lower current the battery can deliver energy for nearly 30 minutes more, when the sensor node is transmitting continuously. The advantage of having energy availability for 30 more minutes is that the sensor node will be able to continue transmitting for a longer time. Therefore, there is an increase in throughput and a decrease in latency.

Knowing the SOC of the battery contributes so the sensor node always have the amount of energy available to transmit. The way to use the obtained information from the SOC estimation will depend on the requirements of the application. For example, a threshold of 25% ( $SOC_{min} = 0.25$ ) is defined to force node to be recharged, but in other applications several thresholds could be used and for each of them to have an implemented, for example helping to minimize the latency when sending packages. A new scenario with three nodes is proposed to evaluate the effect of SOC estimation in sleep time. Figure 4.24 shows the

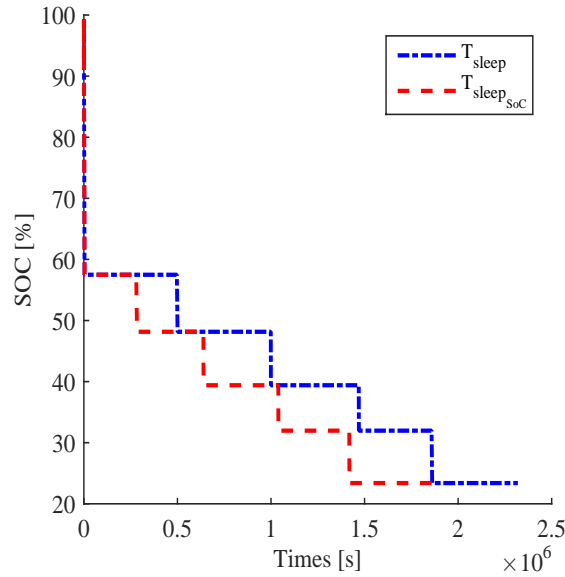


Figure 4.22: Relationship between the SOC and the  $T_{sleep}$

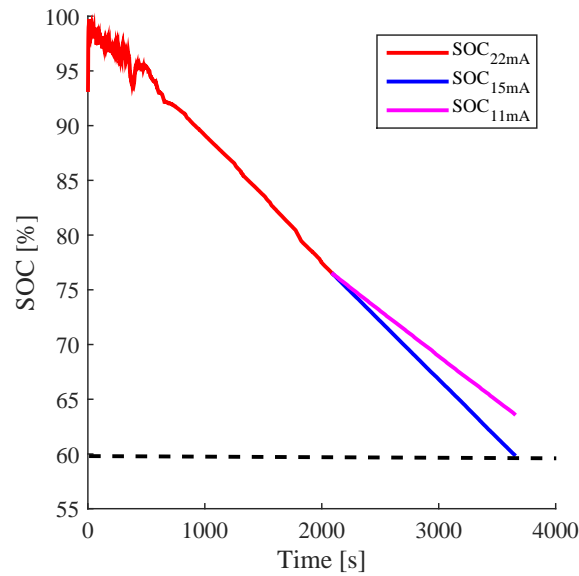


Figure 4.23: SOC prediction

remaining SOC percentage in the battery of each of the sensor nodes once the information has been transmitted. For this case, node one will have 52% SOC once it transmits all the scheduled information, while node two will have 61% and node three has 65%.

Figure 4.24 not only allows the user to know the current SOC percentage in the battery but also enables to see the used by each sensor node, see Table 4.3. With these data, the equation proposed in 3.3 can be updated and thus obtain the maximum and minimum time windows of each sensor node.

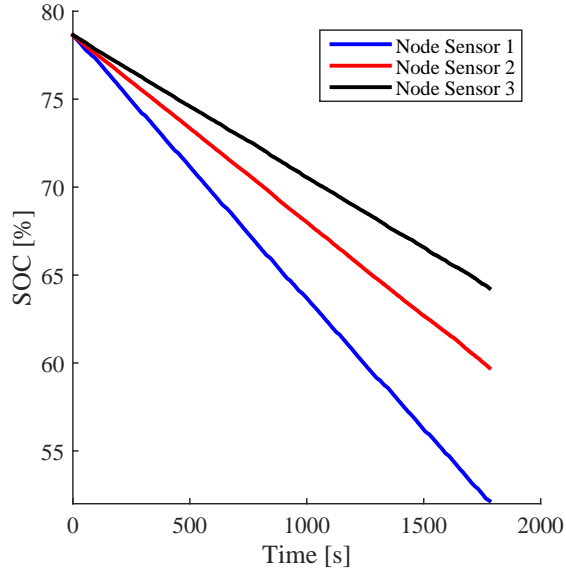


Figure 4.24: SOC prediction

Table 4.3: Maximum and Minimum SOC

Node	$SOC_{max}(\%)$	$SOC(k)(\%)$
1	79	52
2	79	61
3	79	65

Tables 4.4 and 4.5 show the adjustments made to the  $T_{sleepSOC}$  when considering the battery information through the SOC indicator. Using the cases presented in Table 4.2 and the information of Table 4.3, the  $T_{sleepSOC}$  is calculated for each of the three nodes presented in Figure 4.24. As it is observed the nodes that have less amount of available energy are those that extend their sleep windows to allow the recharge of the battery of the same ones.

Table 4.4: Maximum and Minimum  $T_{sleepSOC}$  - Case 1

Node	Parameter	Min	Max
1	$T_{sleepSOC}$	1857	458640
2	$T_{sleepSOC}$	2357	582120
3	$T_{sleepSOC}$	3571	882000

Table 4.5: Maximum and Minimum  $T_{sleep_{SOC}}$  - Case 2

Node	Parameter	Min	Max
1	$T_{sleep_{SOC}}$	426	92333
2	$T_{sleep_{SOC}}$	541	117191
3	$T_{sleep_{SOC}}$	819	177563

### 4.3.3 Sleep Time adjustment considering SOH Estimation

The adjustment of the sleep time is evaluated using the information from the SOH indicator. In this case, the information presented in 4.2.4 is used to find the battery degradation percentage. The Figure 4.25 shows the battery discharge process using different transmission currents. For our case study, a cycle will be defined by the time period when the SOC starts at 100%, and the battery is discharged up to a SOC of 75%. The Figure 4.26 shows that when using the transmission current of 22 mA, 5 operation cycles are reached in a time of 9000 s, while for the current of 15 mA and 11 mA, 4 and 3 cycles are obtained respectively.

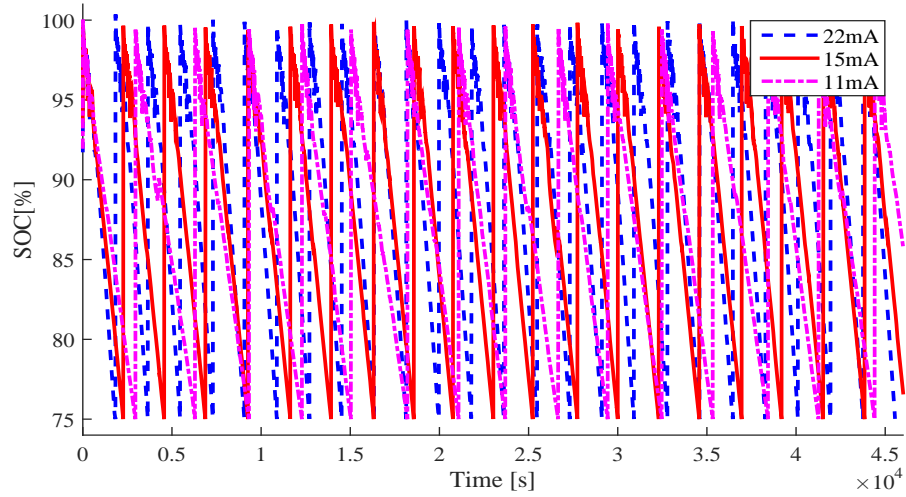


Figure 4.25: Battery discharge process using different currents

The data presented in Table 4.6 is obtained using information provided in 4.2.4 and the number of cycles obtained previously (see Figure 4.25). The sleep time and the degradation percentage are used to find the  $T_{sleep_{SOH}}$ . Figure 4.27 shows how the  $T_{sleep_{SOH}}$  is adjusted according to the transmission current.

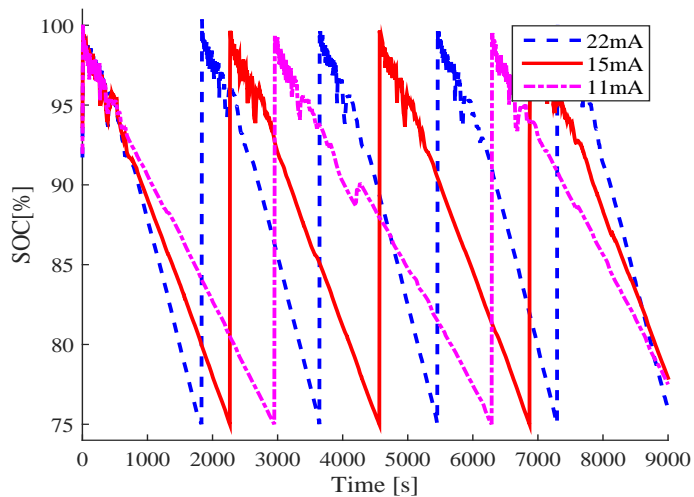


Figure 4.26: Section of Figure 4.25

Table 4.6:  $T_{sleep_{SOH}}$  information

Current [mA]	Number of Cycles	Degradation Percentage	$T_{sleep}$ [s]
22	25	1%	1830
15	20	0.84%	2266
11	16	0.65%	2949

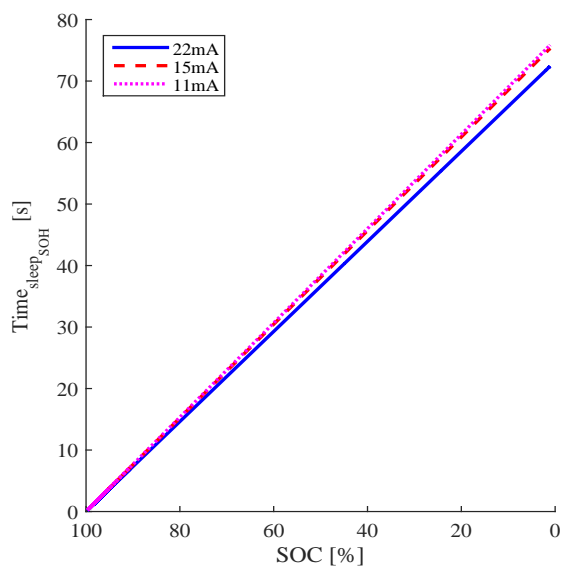


Figure 4.27: Adjustment of  $T_{sleep}$  according to SOH

# Chapter 5

## Conclusions

In this document, a new protocol for WSN based on TDM and DuC that considers the information is coming from the battery is proposed. The design of the protocol allowed for an update on the previous work, on how the adjustment of the DuC is influenced using the EHD, and the battery information through the SOC and SOH indicators. DuC has contributed significantly to the reduction of energy consumption in WSNs. This technique has gone through several modifications adapting to the network requirements, in short, it has evolved to be more dynamic, smarter, and with increased awareness.

The proposed MAC protocol defines the adjustment equations that includes both indicators. In the case of the SOC indicator, the estimation and prediction of it were done based on particle filter. The proposed methodology generates useful information to MAC protocols that allow it to improve the energy efficiency of the network as well as extend the life of the batteries, by preventing these from fully discharging. Moreover, SOC estimation helps to increase transmission times and presents the opportunity to select different current combinations to maximize the transmission time when high demand scenarios are present. In the other hand, the inclusion of the SOH is possible to quantify the degradation process, allowing the search for the best usage profile, that is, the one that causes less degradation in the battery and extends the lifespan of the battery. Through the simulated tests, it is found that the particle filter is able to adjust and deliver accurate and useful SOC estimations. Despite the implications of using particle-filter algorithms, such as computational overhead, the benefits regarding real-time estimation accuracy justify its implementation in battery-SOC estimation applications.

MAC-protocol designs should contemplate the inclusion of algorithms that allow online estimation of both indicators. The SOC estimation allows the nodes to know the amount of energy available in the battery, therefore the MAC protocol should be able to instruct the sensor nodes to enter sleep mode if the percentage of energy remaining in the battery is close to a predefined threshold. On the other hand, knowing the loss of capacity in the battery will contribute to the MAC Protocols awareness of which sensor nodes are more likely to fail and thus affect the performance and lifetime of the network. The estimation of the SOC and SOH allows the sensor nodes to carry out all their operations without involving excessive demands on the battery, which damage the battery.



## 5.1 Future Work

As future work, it is proposed to evaluate the protocol in various scenarios that present greater complexity to determine the performance of it. Also, the assessment of the effect of the computational load when introducing the proposed algorithms that provide information on the state of the battery shall be quantified. Moreover, the adjustment of the Time sleep is a fundamental part in the design of the MAC protocols for WSN since they contribute to minimize the energy consumption and therefore to extend the useful life of the network. That is why it is desired to develop experimental tests that validate the methodology used for the estimation of SOH. In addition the evaluation of other methodologies that consider changes in discharge current profiles and the analysis of how these changes influence the time sleep setting must be performed.

# Appendices

# A1 Publications

## A1.1 Journal Publications

**V Quintero**, C Estevez, M Orchard, and A Pérez. Improvements of Energy-Efficient Techniques in WSNs: A MAC-Protocol Approach. *IEEE Communications Survey and Tutorial*, Accepted: September 2018, DOI:10.1109/COMST.2018.2875810.

**V Quintero**, A Pérez, C Estevez, and M Orchard. State-of-Charge Estimation to improve Decision-making by MAC protocols used in WSNs. *Electronics Letters*, 55, 3, 10.1049 el.2018.7666., 2018.

A Pérez, **V Quintero**, F Jaramillo, H Rozas, D Jimenez, M Orchard, and R Moreno. Characterization of the Degradation Process of Lithium-ion Batteries when Discharged at Different Currents. *Proceedings of the Institution of Mechanical Engineers, Part I: Journal of Systems and Control Engineering*, 0(0):0959651818774481, 2018.

B Torres, **V Quintero**, C Estevez, M Orchard, and C azurdia. SoC control for improved battery life and throughput performance under VST-TDMA. *Electronics Letters*, 53, 3, 10.1049 el.2016.3659, 2017.

## A1.2 Conference Publications

**V Quintero**, A Pérez, C Estevez, and M Orchard. Sleep Time Adjustment through Performance Indicators of a Lithium-ion Battery. In *2019 Prognostics and System Health Management Conference (PHM 2019)*, Paris, France.

**V Quintero**, A Pérez, F Jaramillo, C Estevez, and M Orchard. Procedure for Selecting a Transmission Mode Dependent on the State-of-Charge and State-of-Health of a Lithium-ion Battery in Wireless Sensor Networks with Energy Harvesting Devices. In *Annual Conference of the Prognostics and Health Management Society 2018*, Philadelphia, PA, USA.

A Pérez, F Jaramillo, **V Quintero**, and M Orchard. Characterizing the degradation process of Lithium-Ion Batteries using a Similarity-Based-Modeling Approach. *Fourth European Conference of the Prognostics and Health Management Society 2108*, Utrecht, Netherlands.

**V Quintero**, Claudio Estevez. Frame Retransmission using a modified VST-TDMA access protocol in Picocell/WPAN, *IEEE Latin-American Conference on Communications, 2017*, Guatemala, Guatemala.

Aramis Pérez, **V Quintero**, Heraldo Rozas, Diego Jimenez, Francisco Jaramillo, and Marcos Orchard, Lithium-Ion battery pack arrays for lifespan enhancement, *CHILECON, 2017*, Pucon, Chile.

F Jaramillo, **V Quintero**, A Pérez, and M Orchard. Spatio-temporal probabilistic modeling

based on Gaussian mixture models and neural gas theory for prediction of criminal activity. In *Annual Conference of the Prognostics and Health Management Society 2017*, 2017, St. Petersburg, FL, USA.

S Seria, **V Quintero**, P Espinoza, A Pérez, F Jaramillo, M Benavides, and M Orchard. Electric Bicycle Energy Management Given an Elevation Traveling Profile. In *Annual Conference of the Prognostics and Health Management Society 2017*, 2017, St. Petersburg, FL, USA.

**V Quintero**, Claudio Estevez, and Marcos Orchard. State-of-Charge Estimation to Improve Energy Conservation and Extend Battery Life of Wireless Sensor Network Nodes, In *The Ninth International Conference on Ubiquitous and Future Networks*, 2017, Milan Italy.

A Pérez, **V Quintero**, H Rozas, F Jaramillo, R Moreno, and M Orchard. Modelling the degradation process of lithium-ion batteries when operating at erratic state-of-charge swing ranges. In *4th International Conference on Control, Decision and Information Technologies (CoDIT)*, pages 860-865, 2017, Barcelona, Spain.

D Pola, F Guajardo, E Jofré, **V Quintero**, A Pérez, D Acuña, and M Orchard. Particle-Filtering-Based State-of-Health Estimation and End-of-Life Prognosis for Lithium-Ion Batteries at Operation Temperature. In *Annual Conference of the PHM Society 2016*, 2016, Denver, Colorado, USA.

C Tampier, A Pérez, F Jaramillo, **V Quintero**, M Orchard, and J Silva. Lithium-Ion Battery End-of-Discharge Time Estimation and Prognosis based on Bayesian Algorithms and Outer Feedback Correction Loops: A Comparative Analysis. In *Annual Conference of the Prognostics and Health Management Society 2015*, 2015, San Diego, CA, USA.

---

**Algorithm 2** Node Schedule Time Function

---

**Require:**  $indx$ ,  $time\_pointer$ ,  $act\_nodes$ ,  $delta\_time$ ,  
 $start\_time$ ,  $end\_times$ ,  $buf\_times$ , and  $trvl\_times$

**Ensure:**  $reserve\_time = 36000$ ,  $sync\_time = 6.4e^{-8}$ ,  $fit = 1$ ;

```
for ( $x = 0$ ;  $x < act\_nodes$ ;  $x ++$ ) do
  if ( $indx! = x$ ) then
    if ( $time\_pointer > (start\_time[x] - delta\_time)$ ) then
       $fit = 0$ 
    end if
  end if
end for
if ( $fit == 1$ ) then
   $reserve\_time = time\_pointer$ 
else
  if ( $act\_nodes > 1$ ) then
     $reserve\_time = time\_pointer$ 
     $wait\_time = sync\_time + trvl\_time + buf\_time$ 
    for ( $y = 0$ ;  $y < act\_nodes$ ;  $y ++$ ) do
      for ( $x = 0$ ;  $x < act\_nodes$ ;  $x ++$ ) do
        if ( $indx! = x$ ) then
          if ( $reserve\_time > (start\_time[x] - delta\_time)$ ) and
            ( $reserve\_time < (end\_time[x] - wait\_time)$ ) then
            if ( $reserve\_time < end\_time[x] + wait\_time$ ) then
               $reserve\_time = end\_time[x] + wait\_time$ 
            end if
          end if
        end if
      else
         $reserve\_time = time\_pointer$ 
        WARNING!
      end if
    end for
  end for
end if
end if
```

---

---

**Algorithm 3** Update Battery Energy Function

---

**Require:** *input\_energy*, *harv\_curr*, *prv\_state*, *prv\_time*, *currs*

**Ensure:** *second2hour* = 3600

**Switch**(*prv\_state*) **do**

case LISTEN\_STATE

*output\_energy* = *input\_energy* - (*ost* - *prv\_time*) \* (*currs*[0] - *harv\_curr*) / *second2hour*

**if** *print\_energy\_info* == 1 **then**

    Previous state = Listen

**end if**

**break**

case SLEEP\_STATE

*output\_energy* = *input\_energy* - (*ost* - *prv\_time*) \* (*currs*[1] - *harv\_curr*) / *second2hour*

**if** *print\_energy\_info* == 1 **then**

    Previous state = Sleep

**end if**

**break**

case TX\_STATE

*output\_energy* = *input\_energy* - (*ost* - *prv\_time*) \* (*currs*[2] - *harv\_curr*) / *second2hour*

**if** *print\_energy\_info* == 1 **then**

    Previous state = TX

**end if**

**break**

case RX\_STATE

*output\_energy* = *input\_energy* - (*ost* - *prv\_time*) \* (*currs*[3] - *harv\_curr*) / *second2hour*

**if** *print\_energy\_info* == 1 **then**

    Previous state = RX

**end if**

**break**

**default**

"Warning ! State does no exist"

**if** *output\_energy* < *max\_battery\_charge* **then**

*output\_energy* = *max\_battery\_charge*

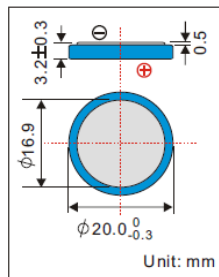
**end if**

---

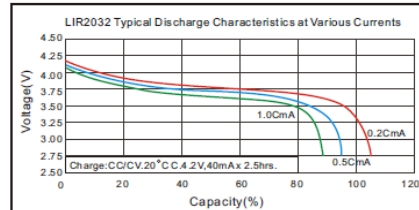
# LIR2032 *Brief datasheet*

## Lithium Ion Battery

### 1 Dimension



### 3 Electrical Characteristics



### 2 Basic Specification

Nominal Voltage	3.6V	
Nominal Capacity	Typical	45mAh
	Minimum	40mAh
Charge method	CC/CV (Constant Current-Constant Voltage) current: 0.5C Voltage: 4.2V End current: 0.02C	
Charging Voltage	4.20V	
Charging Std. Current	0.5C	
Max Current	Charge	1C
	Discharge	2C
Ambient Temperature	Std. Charge	-20°C to 45°C
	Discharge	-20°C to 60°C
	Storage	-20°C to 60°C
Discharge cut-off voltage	2.75V	
Internal Impedance	≤ 600 mΩ	
Cycle life	>500cycles (≥80% capacity)	
Nominal Weight	Approx. 3.1g	

\*1C = 1 Capacity

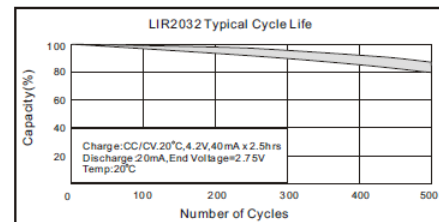
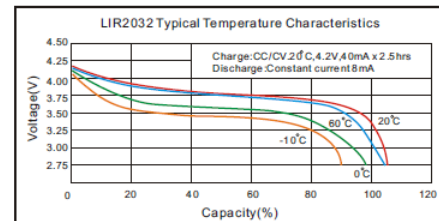


Figure A1: Datasheet LIR2032

# Bibliography

- [1] Dhanavanthan Balachander, Thipparaju Rama Rao, Prasad Mvsn, and Nishesh Tiwari. Ultra-high frequency near-ground short-range propagation measurements in forest and plantation environments for wireless sensor networks. *IET Wireless Sensor Systems*, 3(1):80–84, 2013.
- [2] A. Ajith Kumar S., Knut Ovsthus, and Lars M. Kristensen. An industrial perspective on wireless sensor networks-a survey of requirements, protocols, and challenges. *IEEE Communications Surveys and Tutorials*, 16(3):1391–1412, 2014.
- [3] JeongGil Ko, Chenyang Lu, Mani B Srivastava, John A Stankovic, Andreas Terzis, and Matt Welsh. Wireless sensor networks for healthcare. *Proceedings of the IEEE*, 98(11):1947–1960, 2010.
- [4] Charly Lersteau, André Rossi, and Marc Sevaux. Robust scheduling of wireless sensor networks for target tracking under uncertainty. *European Journal of Operational Research*, 252(2):407–417, 2016.
- [5] Victoria J Hodge, Simon O’Keefe, Michael Weeks, and Anthony Moulds. Wireless sensor networks for condition monitoring in the railway industry: A survey. *IEEE Transactions on Intelligent Transportation Systems*, 16(3):1088–1106, 2015.
- [6] Subhadeep Sarkar and Sudip Misra. From micro to nano: The evolution of wireless sensor-based health care. *IEEE pulse*, 7(1):21–25, 2016.
- [7] Jennifer Yick, Biswanath Mukherjee, and Dipak Ghosal. Wireless sensor network survey. *Computer networks*, 52(12):2292–2330, 2008.
- [8] Giuseppe Anastasi, Marco Conti, Mario Di Francesco, and Andrea Passarella. Energy conservation in wireless sensor networks: A survey. *Ad Hoc Networks*, 7(3):537–568, 2009.
- [9] Dilip Kumar. Performance analysis of energy efficient clustering protocols for maximising lifetime of wireless sensor networks. *IET Wireless Sensor Systems*, 4(1):9–16, 2013.
- [10] Jyoti Saraswat, Neha Rathi, and Partha Pratim Bhattacharya. Techniques to enhance lifetime of wireless sensor networks: A survey. *Global Journal of Computer Science*



and Technology, 2012.

- [11] Zhi Ang Eu, Hwee-Pink Tan, and Winston K.G. Seah. Design and performance analysis of MAC schemes for Wireless Sensor Networks Powered by Ambient Energy Harvesting. *Ad Hoc Networks*, 9(3):300–323, 2011.
- [12] He Yejun, Cheng Xudong, Peng Wei, G L Stuber, Yejun He, Xudong Cheng, Wei Peng, and Gordon L. Stüber. A Survey of Energy Harvesting Communications: Models and Offline Optimal Policies. *IEEE Communications Magazine*, 53(6):79–85, 2015.
- [13] Pei Huang, Li Xiao, Soroor Soltani, Matt W. Mutka, and Ning Xi. The Evolution of MAC Protocols in Wireless Sensor Networks: A Survey. *IEEE Communications Surveys & Tutorials*, 15(1):101–120, 2013.
- [14] Mehmood Abd, Sarab Majed, Brajendra Singh, Kemal Tepe, and Rachid Benlamri. Extending Wireless Sensor Network Lifetime with Global Energy Balance. *IEEE Sensors Journal*, 15(9):5053–5063, 2015.
- [15] Nikolaos A Pantazis, Stefanos A Nikolidakis, and Dimitrios D Vergados. Energy-efficient routing protocols in wireless sensor networks: A survey. *IEEE Communications surveys & tutorials*, 15(2):551–591, 2013.
- [16] Hesham Abusaimh and Shuang-Hua Yang. Energy-aware optimization of the number of clusters and cluster-heads in wsn. In *Innovations in information technology (IIT), 2012 international conference on*, pages 178–183. IEEE, 2012.
- [17] Shazana Md Zin, Nor Badrul Anuar, Miss Laiha Mat Kiah, and Al-Sakib Khan Pathan. Routing protocol design for secure wsn: Review and open research issues. *Journal of Network and Computer Applications*, 41:517–530, 2014.
- [18] Jie Hao, Baoxian Zhang, and Hussein T Mouftah. Routing protocols for duty cycled wireless sensor networks: A survey. *IEEE Communications Magazine*, 50(12), 2012.
- [19] Fayez Alfayez, Mohammad Hammoudeh, and Abdelrahman Abuarqoub. A survey on mac protocols for duty-cycled wireless sensor networks. *Procedia Computer Science*, 73:482–489, 2015.
- [20] Moshaddique Al Ameen, S. M Riazul Islam, and Kyungsup Kwak. Energy saving mechanisms for MAC protocols in wireless sensor networks. *International Journal of Distributed Sensor Networks*, 6(1):163413, 2010.
- [21] Sujesha Sudevalayam and Purushottam Kulkarni. Energy harvesting sensor nodes: Survey and implications. *IEEE Communications Surveys & Tutorials*, 13(3):443–461, 2011.
- [22] Parisa Ramezani and Mohammad Reza Pakravan. Overview of mac protocols for energy harvesting wireless sensor networks. In *Personal, Indoor, and Mobile Radio Communications (PIMRC), 2015 IEEE 26th Annual International Symposium on*, pages 2032–2037. IEEE, 2015.

- [23] Fotis Kerasiotis, Aggeliki Prayati, Christos Antonopoulos, Christos Koulamas, and George Papadopoulos. Battery lifetime prediction model for a wsn platform. In *Sensor Technologies and Applications (SENSORCOMM), 2010 Fourth International Conference on*, pages 525–530. IEEE, 2010.
- [24] Daniel A. Pola, Hugo F. Navarrete, Marcos E. Orchard, Ricardo S. Rabié, Matías A. Cerda, Benjamín E. Olivares, Jorge F. Silva, Pablo A. Espinoza, and Aramis Pérez. Particle-filtering-based discharge time prognosis for lithium-ion batteries with a statistical characterization of use profiles. *IEEE Transactions on Reliability*, 64(2):710–720, 2015.
- [25] Bharath Pattipati, Chaitanya Sankavaram, and Krishna Pattipati. System identification and estimation framework for pivotal automotive battery management system characteristics. *IEEE Transactions on Systems, Man, and Cybernetics, Part C (Applications and Reviews)*, 41(6):869–884, 2011.
- [26] Ricardo C. Carrano, Diego Passos, Luiz C S Magalhaes, and Celio V N Albuquerque. Survey and taxonomy of duty cycling mechanisms in wireless sensor networks. *IEEE Communications Surveys and Tutorials*, 16(1):181–194, 2014.
- [27] Reza Mohammad Ramezani, Parisa. Overview of MAC Protocols for Energy Harvesting Wireless Sensor Networks. *Personal, Indoor, and Mobile Radio Communications (PIMRC), 2015 IEEE 26th Annual International Symposium on*, pages 2032–2037, 2015.
- [28] Rafael J Lajara, Juan J Perez-solano, and José Pelegrí-sebastia. A Method for Modeling the Battery State of Charge in Wireless Sensor Networks. *IEEE Sensors Journal*, 15(2):1186–1197, 2015.
- [29] D Antolin, N Medrano, and B Calvo. Analysis of the operating life for battery-operated wireless sensor nodes. In *Industrial Electronics Society, IECON 2013-39th Annual Conference of the IEEE*, pages 3883–3886. IEEE, 2013.
- [30] Cristina Cano, Boris Bellalta, Anna Sfaïropoulou, and Miquel Oliver. Low energy operation in wsns: A survey of preamble sampling mac protocols. *Computer Networks*, 55(15):3351–3363, 2011.
- [31] Joseph Kabara and Maria Calle. MAC protocols used by wireless sensor networks and a general method of performance evaluation. *International Journal of Distributed Sensor Networks*, 8(1):834784, 2012.
- [32] Abdelmalik Bachir, Mischa Dohler, Thomas Watteyne, Ieee Member, and Ieee Senior Member. MAC Essentials for Wireless Sensor Networks. *IEEE Communications Surveys & Tutorials*, 12(2):222–248, 2010.
- [33] Supantha Das, Indrajit Banerjee, Mainak Chatterjee, and Tuhina Samanta. Performance analysis of tdma based data transmission in wsn. In *Intelligent Systems Design and Applications (ISDA), 2014 14th International Conference on*, pages 107–112. IEEE, 2014.

- [34] Jie Hao, Baoxian Zhang, and Hussein T Mouftah. Routing protocols for duty cycled wireless sensor networks: A survey. *IEEE Communications Magazine*, 50(12):116–123, 2012.
- [35] Wei Ye, John Heidemann, and Deborah Estrin. An energy-efficient mac protocol for wireless sensor networks. In *INFOCOM 2002. Twenty-First Annual Joint Conference of the IEEE Computer and Communications Societies. Proceedings. IEEE*, volume 3, pages 1567–1576. IEEE, 2002.
- [36] Pei Huang, Li Xiao, Soroor Soltani, Matt W Mutka, and Ning Xi. The evolution of mac protocols in wireless sensor networks: A survey. *IEEE communications surveys & tutorials*, 15(1):101–120, 2013.
- [37] Hongseok Yoo, Moonjoo Shim, and Dongkyun Kim. Dynamic duty-cycle scheduling schemes for energy-harvesting wireless sensor networks. *IEEE Communications Letters*, 16(2):202–204, 2012.
- [38] Andrea Castagnetti, Alain Pegatoquet, Cécile Belleudy, and Michel Auguin. A framework for modeling and simulating energy harvesting wsn nodes with efficient power management policies. *EURASIP Journal on Embedded Systems*, 2012(1):8, 2012.
- [39] Fayez Alfayez, Mohammad Hammoudeh, and Abdelrahman Abuarqoub. A survey on mac protocols for duty-cycled wireless sensor networks. *Procedia Computer Science*, 73:482–489, 2015.
- [40] Lei Tang, Yanjun Sun, Omer Gurewitz, and David B Johnson. Pw-mac: An energy-efficient predictive-wakeup mac protocol for wireless sensor networks. In *INFOCOM, 2011 Proceedings IEEE*, pages 1305–1313. IEEE, 2011.
- [41] Tijs Van Dam and Koen Langendoen. An adaptive energy-efficient mac protocol for wireless sensor networks. In *Proceedings of the 1st international conference on Embedded networked sensor systems*, pages 171–180. ACM, 2003.
- [42] G. Lu, B. Krishnamachari, and C. S. Raghavendra. An adaptive energy-efficient and low-latency mac for data gathering in wireless sensor networks. In *18th International Parallel and Distributed Processing Symposium, 2004. Proceedings.*, page 224, 2004.
- [43] Tao Zheng, Sridhar Radhakrishnan, and Venkatesh Sarangan. Pmac: an adaptive energy-efficient mac protocol for wireless sensor networks. In *Parallel and Distributed Processing Symposium, 2005. Proceedings. 19th IEEE International.* IEEE, 2005.
- [44] S. Du, A. K. Saha, and D. B. Johnson. RMAC: A Routing-Enhanced Duty-Cycle MAC Protocol for Wireless Sensor Networks. *IEEE INFOCOM 2007 - 26th IEEE International Conference on Computer Communications*, pages 1478–1486, 2007.
- [45] Yanjun Sun, S. Du, O. Gurewitz, and D.B. Johnson. DW-MAC: a low latency, energy efficient demand-wakeup MAC protocol for wireless sensor networks. *Proceedings of the 9th ACM international symposium on Mobile ad hoc networking and computing*, pages 53–62, 2008.

- [46] Chin-Jung Liu, Pei Huang, and Li Xiao. Tas-mac: A traffic-adaptive synchronous mac protocol for wireless sensor networks. *ACM Transactions on Sensor Networks (TOSN)*, 12(1):1, 2016.
- [47] Yanjun Sun, Omer Gurewitz, and David B Johnson. Ri-mac: a receiver-initiated asynchronous duty cycle mac protocol for dynamic traffic loads in wireless sensor networks. In *Proceedings of the 6th ACM conference on Embedded network sensor systems*, pages 1–14. ACM, 2008.
- [48] Joseph Polastre, Jason Hill, and David Culler. Versatile low power media access for wireless sensor networks. In *Proceedings of the 2nd international conference on Embedded networked sensor systems*, pages 95–107. ACM, 2004.
- [49] Amre El-Hoiydi and J-D Decotignie. Wisemac: an ultra low power mac protocol for the downlink of infrastructure wireless sensor networks. In *Computers and Communications, 2004. Proceedings. ISCC 2004. Ninth International Symposium on*, volume 1, pages 244–251. IEEE, 2004.
- [50] Michael Buettner, Gary V Yee, Eric Anderson, and Richard Han. X-mac: a short preamble mac protocol for duty-cycled wireless sensor networks. In *Proceedings of the 4th international conference on Embedded networked sensor systems*, pages 307–320. ACM, 2006.
- [51] Shagufta Henna. Sa-ri-mac: sender-assisted receiver-initiated asynchronous duty cycle mac protocol for dynamic traffic loads in wireless sensor networks. In *International Conference on Mobile Lightweight Wireless Systems*, pages 120–135. Springer, 2011.
- [52] Kai Han, Jun Luo, Yang Liu, and Athanasios V Vasilakos. Algorithm design for data communications in duty-cycled wireless sensor networks: A survey. *IEEE Communications Magazine*, 51(7):107–113, 2013.
- [53] Lulu Liang, Xiaonan Liu, Yongtao Wang, Weiduan Feng, and Guang Yang. SW-MAC: A low-latency MAC protocol with adaptive sleeping for wireless sensor networks. *Wireless Personal Communications*, 77(2):1191–1211, 2014.
- [54] Beakcheol Jang, Jun Bum Lim, and Mihail L. Sichitiu. An asynchronous scheduled MAC protocol for wireless sensor networks. *Computer Networks*, 57(1):85–98, 2013.
- [55] Guijuan Wang, Jiguo Yu, Dongxiao Yu, Haitao Yu, Li Feng, and Pan Liu. DS-MAC: An energy efficient demand sleep MAC protocol with low latency for wireless sensor networks. *Journal of Network and Computer Applications*, 58:155–164, 2015.
- [56] Jun Bum Lim, Beakcheol Jang, and Mihail L Sichitiu. Mcas-mac: A multichannel asynchronous scheduled mac protocol for wireless sensor networks. *Computer Communications*, 56(2):98–107, 2015.
- [57] Hanjin Lee, Jaeyoung Hong, Suho Yang, Ingoon Jang, and Hyunsoo Yoon. A pseudo-random asynchronous duty cycle MAC protocol in wireless sensor networks. *IEEE Communications Letters*, 14(2):136–138, 2010.

- [58] Andrea Castagnetti, Alain Pegatoquet, Trong Nhan Le, and Michel Auguin. A joint duty-cycle and transmission power management for energy harvesting wsn. *IEEE Transactions on Industrial Informatics*, 10:928–936, 2014.
- [59] Hafiz Husnain Raza Sherazi, Luigi Alfredo Grieco, and Gennaro Boggia. A comprehensive review on energy harvesting mac protocols in wsns: Challenges and tradeoffs. *Ad Hoc Networks*, 71:117–134, 2018.
- [60] Faisal Karim Shaikh and Sherali Zeadally. Energy harvesting in wireless sensor networks: A comprehensive review. *Renewable and Sustainable Energy Reviews*, 55:1041–1054, 2016.
- [61] Selahattin Kosunalp. A new energy prediction algorithm for energy-harvesting wireless sensor networks with q-learning. *IEEE Access*, 4:5755–5763, 2016.
- [62] Alessandro Cammarano, Chiara Petrioli, and Dora Spenza. Online energy harvesting prediction in environmentally powered wireless sensor networks. *IEEE Sensors Journal*, 16(17):6793–6804, 2016.
- [63] Andrea Castagnetti, Alain Pegatoquet, Cecile Belleudy, and Michel Auguin. An efficient state of charge prediction model for solar harvesting wsn platforms. In *Systems, Signals and Image Processing (IWSSIP), 2012 19th International Conference on*, pages 122–125, 2012.
- [64] Xenofon Fafoutis and Nicola Dragoni. ODMAC : An On-Demand MAC Protocol for Energy Harvesting - Wireless Sensor Networks. *Proceedings of the 8th ACM Symposium on Performance evaluation of wireless ad hoc, sensor, and ubiquitous networks*, pages 49–56, 2011.
- [65] Jaeho Kim and Jang-Won Lee. Energy adaptive mac protocol for wireless sensor networks with rf energy transfer. In *Ubiquitous and Future Networks (ICUFN), 2011 Third International Conference on*, pages 89–94, 2011.
- [66] Z A Eu and H P Tan. Probabilistic polling for multi-hop energy harvesting wireless sensor networks. *2012 IEEE International Conference on Communications (ICC)*, pages 271–275, 2012.
- [67] Navid Tadayon, Sasan Khoshroo, Elaheh Askari, Honggang Wang, and Howard Michel. Power management in SMAC-based energy-harvesting wireless sensor networks using queuing analysis. *Journal of Network and Computer Applications*, 36(3):1008–1017, 2013.
- [68] Kien Nguyen, Vu-Hoang Nguyen, Duy-Dinh Le, Yusheng Ji, Duc Anh Duong, and Shigeki Yamada. A receiver-initiated mac protocol for energy harvesting sensor networks. In *Ubiquitous Information Technologies and Applications*, pages 603–610. Springer, 2014.
- [69] Yunmin Kim, Chul Wan Park, and Tae-Jin Lee. Mac protocol for energy-harvesting users in cognitive radio networks. In *Proceedings of the 8th International Conference*

on *Ubiquitous Information Management and Communication*, page 59, 2014.

- [70] Huey-Ing Liu, Wen-Jing He, and Winston KG Seah. Leb-mac: Load and energy balancing mac protocol for energy harvesting powered wireless sensor networks. In *Parallel and Distributed Systems (ICPADS), 2014 20th IEEE International Conference on*, pages 584–591, 2014.
- [71] M. Yousof Naderi, Prusayon Nintanavongsa, and Kaushik Roy Chowdhury. RF-MAC: A Medium Access Control Protocol for Re-chargeable Sensor Networks Powered by Wireless Energy Harvesting. *IEEE Transactions on Wireless Communications*, 13(7):3926–3937, 2014.
- [72] R Ahmed, M El Sayed, I Arasaratnam, J Tjong, and S Habibi. Reduced-order electrochemical model parameters identification and soc estimation for healthy and aged li-ion batteries. part i: Parameterization model development for healthy batteryies. *IEEE Journal of Emerging and Selected Topics in Power Electronics*, 2(3):659–677, 2014.
- [73] Hongwen He, Rui Xiong, Xiaowei Zhang, Fengchun Sun, and JinXin Fan. State-of-charge estimation of the lithium-ion battery using an adaptive extended kalman filter based on an improved thevenin model. *IEEE Transactions on Vehicular Technology*, 60(4):1461–1469, 2011.
- [74] Hongwen He, Rui Xiong, and Jinxin Fan. Evaluation of lithium-ion battery equivalent circuit models for state of charge estimation by an experimental approach. *Energies*, 4(4):582–598, 2011.
- [75] Wenguan Wang, Henry Shu-Hung Chung, and Jun Zhang. Near-real-time parameter estimation of an electrical battery model with multiple time constants and soc-dependent capacitance. *IEEE Transactions on Power Electronics*, 29(11):5905–5920, 2014.
- [76] Alexander Bartlett, James Marcicki, Simona Onori, Giorgio Rizzoni, Xiao Guang Yang, and Ted Miller. Electrochemical model-based state of charge and capacity estimation for a composite electrode lithium-ion battery. *IEEE Transactions on Control Systems Technology*, 24(2):384–399, 2016.
- [77] M. F. Samadi, S. M Mahdi Alavi, and M. Saif. An electrochemical model-based particle filter approach for lithium-ion battery estimation. *Proceedings of the IEEE Conference on Decision and Control*, pages 3074–3079, 2012.
- [78] Daler Rakhmatov and Sarma Vrudhula. Energy management for battery-powered embedded systems. *ACM Transactions on Embedded Computing Systems (TECS)*, 2(3):277–324, 2003.
- [79] Carlos Tampier, Aramis Pérez, Francisco Jaramillo, Vanessa Quintero, Marcos E Orchard, and Jorge F Silva. Lithium-ion battery end-of-discharge time estimation and prognosis based on bayesian algorithms and outer feedback correction loops: A comparative analysis. In *Annual Conference of the PHM Society, PHM Society, San Diego, CA*, 2015.

- [80] D Antolin, N Medrano, and B Calvo. Analysis of the operating life for battery-operated wireless sensor nodes. In *Industrial Electronics Society, IECON 2013-39th Annual Conference of the IEEE*, pages 3883–3886, 2013.
- [81] Aramis Perez, Vanessa Quintero, Francisco Jaramillo, Heraldo Rozas, Diego Jimenez, Marcos Orchard, and Rodrigo Moreno. Characterization of the degradation process of lithium-ion batteries when discharged at different current rates. *Proceedings of the Institution of Mechanical Engineers, Part I: Journal of Systems and Control Engineering*, 232(8):1075–1089, 2018.
- [82] Christian Rohner, Laura Marie Feeney, and Per Gunningberg. Evaluating battery models in wireless sensor networks. In *International Conference on Wired/Wireless Internet Communication*, pages 29–42, 2013.
- [83] Leonardo M Rodrigues, Carlos Montez, Francisco Vasques, and Paulo Portugal. Experimental validation of a battery model for low-power nodes in wireless sensor networks. In *Factory Communication Systems (WFCS), 2016 IEEE World Conference on*, pages 1–4, 2016.
- [84] Chi-Kin Chau, Fei Qin, Samir Sayed, Muhammad Husni Wahab, and Yang Yang. Harnessing battery recovery effect in wireless sensor networks: Experiments and analysis. *IEEE Journal on Selected Areas in Communications*, 28(7):1222–1232, 2010.
- [85] Daniel Pola, Felipe Guajardo, Esteban Jofré, Vanessa Quintero, Aramis Pérez, David Acuna, and Marcos Orchard. Particle-filtering-based state-of-health estimation and end-of-life prognosis for lithium-ion batteries at operation temperature. In *Proceedings of the 2016 annual conference of the prognostics and health management society*, pages 137–146, 2016.
- [86] A Pérez, V Quintero, H Rozas, F Jaramillo, R Moreno, and M Orchard. Modelling the degradation process of lithium-ion batteries when operating at erratic state-of-charge swing ranges. In *2017 4th International Conference on Control, Decision and Information Technologies (CoDIT)*, pages 0860–0865. IEEE, 2017.
- [87] Kong Soon Ng, Chin Sien Moo, Yi Ping Chen, and Yao Ching Hsieh. Enhanced coulomb counting method for estimating state-of-charge and state-of-health of lithium-ion batteries. *Applied Energy*, 86(9):1506–1511, 2009.
- [88] Iryna Snihir, William Rey, Evgeny Verbitskiy, Afifa Belfadhel-Ayeb, and Peter H L Notten. Battery open-circuit voltage estimation by a method of statistical analysis. *Journal of Power Sources*, 159(2):1484–1487, 2006.
- [89] Li Ran, Wu Junfeng, and Li Gechen. Prediction of State of Charge of Lithium-ion Rechargeable Battery with Electrochemical Impedance Spectroscopy Theory. *2010 the 5th IEEE Conference on Industrial Electronics and Applications (ICIEA)*, pages 684–688, 2010.
- [90] Alvin J. Salkind, Craig Fennie, Pritpal Singh, Terrill Atwater, and David E. Reisner. Determination of state-of-charge and state-of-health of batteries by fuzzy logic

methodology. *Journal of Power Sources*, 80:293–300, 1999.

- [91] Mohammad Charkhgard and Mohammad Farrokhi. State-of-charge estimation for lithium-ion batteries using neural networks and EKF. *IEEE Transactions on Industrial Electronics*, 57(12):4178–4187, 2010.
- [92] G Giorgi, A Veronese, L Corradini, and L Scandola. A method for estimating state of charge in energy-aware wireless sensor nodes. In *Proc. 19th Symp. IMEKO TC 4*, pages 108–113, 2013.
- [93] Vanessa Quintero, Claudio Estevez, and Marcos Orchard. State-of-charge estimation to improve energy conservation and extend battery life of wireless sensor network nodes. In *Ubiquitous and Future Networks (ICUFN), 2017 Ninth International Conference on*, pages 153–158. IEEE, 2017.
- [94] V Quintero, A Perez, F Jaramillo, C Estevez, and M Orchard. Procedure for selecting a transmission mode dependent on the state-of-charge and state-of-health of a lithium-ion battery in wireless sensor networks with energy harvesting devices. In *Annual Conference of the PHM Society, Philadelphia, PA, USA*, 2018.
- [95] V Quintero, A Perez, C Estevez, and M Orchard. State-of-charge estimation to improve decision making by mac protocols used in wsns. *Electronics Letters*, 55(3):161–163, 2018.
- [96] Marcos E Orchard, Pablo Hevia-Koch, Bin Zhang, and Liang Tang. Risk measures for particle-filtering-based state-of-charge prognosis in lithium-ion batteries. *IEEE Transactions on Industrial Electronics*, 60(11):5260–5269, 2013.
- [97] Gary Bishop, Greg Welch, et al. An introduction to the kalman filter. *Proc of SIG-GRAPH, Course*, 8(27599-3175):59, 2001.
- [98] Marcos E Orchard and George J Vachtsevanos. A particle-filtering approach for on-line fault diagnosis and failure prognosis. *Transactions of the Institute of Measurement and Control*, 31(3-4):221–246, 2009.
- [99] M Berecibar, I Gandiaga, I Villarreal, N Omar, J Van Mierlo, and P Van den Bossche. Critical review of state of health estimation methods of li-ion batteries for real applications. *Renewable and Sustainable Energy Reviews*, 56:572–587, 2016.
- [100] Sebastian Seria, Vanessa Quintero, Pablo Espinoza, Aramis Pérez, Francisco Jaramillo, Matías Benavides, and Marcos Orchard. Electric bicycle energy management given an elevation traveling profile. In *Annual Conference of the PHM Society, St. Petersburg, FL*, 2017.
- [101] Du Jiani, Wang Youyi, and Wen Changyun. Li-ion battery soc estimation using particle filter based on an equivalent circuit model. In *2013 10th IEEE International Conference on Control and Automation (ICCA)*, pages 580–585. IEEE, 2013.
- [102] M Sanjeev Arulampalam, Simon Maskell, Neil Gordon, and Tim Clapp. A tutorial on



- particle filters for online nonlinear/non-gaussian bayesian tracking. *IEEE Transactions on signal processing*, 50(2):174–188, 2002.
- [103] H. Navarrete. Caracterización estadística del perfil de uso de baterías para el pronóstico del estado de carga. Master’s thesis, Facultad de Ciencias Físicas y Matemáticas, Universidad de Chile, Santiago, Chile, 2014.
- [104] Nicolò Michelusi, Leonardo Badia, Ruggero Carli, Luca Corradini, and Michele Zorzi. Energy management policies for harvesting-based wireless sensor devices with battery degradation. *IEEE Transactions on Communications*, 61(12):4934–4947, 2013.
- [105] Roberto Valentini, Nga Dang, Marco Levorato, and Eli Bozorgzadeh. Modeling and control battery aging in energy harvesting systems. In *2015 IEEE International Conference on Smart Grid Communications (SmartGridComm)*, pages 515–520. IEEE, 2015.
- [106] Long Lam and Pavol Bauer. Practical capacity fading model for li-ion battery cells in electric vehicles. *IEEE transactions on power electronics*, 28(12):5910–5918, 2013.
- [107] A Pérez, V Quintero, H Rozas, D Jimenez, F Jaramillo, and M Orchard. Lithium-ion battery pack arrays for lifespan enhancement. In *2017 CHILEAN Conference on electrical, electronics engineering, information and communication technologies (CHILECON)*. IEEE, pages 1–5, 2017.
- [108] Aramis Perez, Francisco Jaramillo, Vanessa Quintero, and Marcos Orchard. Characterizing the degradation process of lithium-ion batteries using a similarity-based-modeling approach. In *PHM Society European Conference*, volume 4, 2018.
- [109] Matheus A Marins, Felipe ML Ribeiro, Sergio L Netto, and Eduardo AB da Silva. Improved similarity-based modeling for the classification of rotating-machine failures. *Journal of the Franklin Institute*, 355(4):1913–1930, 2018.
- [110] Vanessa Quintero, Claudio Estevez, Marcos Orchard, and Aramis Pérez. Improvements of energy-efficient techniques in wsns: A mac-protocol approach. *IEEE Communications Surveys & Tutorials*, 2018.
- [111] Fatima Zahra Djiroun and Djamel Djenouri. Mac protocols with wake-up radio for wireless sensor networks: A review. *IEEE Communications Surveys & Tutorials*, 19(1):587–618, 2017.
- [112] Boris Torres, Vanessa Quintero, Claudio Estevez, Marcos Orchard, and César Azurdia. Soc control for improved battery life and throughput performance under vst-tdma. *Electronics Letters*, 53(3):183–185, 2016.
- [113] Texas Instruments. Cc2500 low-cost low-power 2.4 ghz rf transceiver datasheet, 2013.
- [114] Benjamín E Olivares, Matias A Cerda Munoz, Marcos E Orchard, and Jorge F Silva. Particle-filtering-based prognosis framework for energy storage devices with a statistical characterization of state-of-health regeneration phenomena. *IEEE Transactions on Instrumentation and Measurement*, 62(2):364–376, 2013.